Volume : 2, 2016

Annual Technical Volume of ELECTRICAL ENGINEERING DIVISION BOARD

The Institution of Engineers (India)

Electrical Engineering Division Board (2015-2016)

About the Division Board

The Institution of Engineers (India) has established Electrical Engineering Division in the year 1954. This Division consists of quite a large number of corporate members from Government, Public, Private sectors, Academia and R&D Organizations.

Various types of technical activities organized by the Electrical Engineering Division include All India Seminars, All India Workshops, Lectures, Panel Discussions etc., which are held at various State/Local Centres of the Institution. Apart from these, National Convention of Electrical Engineers, an Apex activity of this Division is also organized each year on a particular theme approved by the Council of the Institution. In the National Convention, several technical sessions are arranged on the basis of different sub-themes along with a Memorial Lecture in the memory of **"M S Thacker"**, former Director General, Council of Scientific & Industrial Research, Govt of India, New Delhi and eminent person in the field of Electrical Engineering, which is delivered by the experts in this field.

In order to promote the research and developmental work taking place in the field of electrical engineering, the Institution also publishes Electrical Engineering Division Journal quarterly in a year, where mainly the researches and its findings are focused. Due to multi-level activities related to this engineering discipline, this division covers different sub-areas such as:

- Provision of SCADA in Transmission and Distribution
- Special Focus on APDRD
- Upgradation of Skills in Power Sector
- Energy Conservation Building Code [ECPC 2006]
- Generation of Electricity from Hydrogen
- Alternative Energy – Solar and Solar PV
- Alternative Energy – Natural Gas, Bio-mass/Rice Husk
- Satellite Generation
- Recent Development in Cleaner Nuclear Technology
- Smart Grid in our villages, in context to Indian Scenario
- Sustainable Development and Renewable Energy
- Distributed Generation and Power Quality
- Reactive Power Control and Pricing
- FACTs Controller
- Integration of Communication Technology in Power Sector
- Energy Conservation

In order to promote the research and developmental work in the field of Electrical Engineering, the Institution also publishes Journal of The Institution of Engineers (India): Series B in collaboration with M/S Springer which is an internationally peer reviewed journal. The journal is published four times in a year and serves the national and international engineering community through dissemination of scientific knowledge on practical engineering and design methodologies pertaining to Electrical, Electronics & Telecommunication and Computer engineering.

Editorial

Electrical Engineering Division Board (ELDB) is pleased to release the Second Annual Technical Volume of ELDB today on November 11, 2016. The Annual Technical Volume of ELDB includes selected articles from All India Seminars and National Convention organized under the aegis of Electrical Engineering Division Board during the year 2015-2016. The tapping of renewable energy sources, distributed generation, micro grid, smart grid and retrofitting & refurbishment of existing equipment and systems have been the thrust area of All India Seminars during the current year.

The articles picked up from these seminars, reporting observations of field engineers, supplemented by factual data and working experience are covered in this Volume. The first three articles discuss the experience of retrofitting and refurbishment of substations, transmission lines and systems by incorporating modern monitoring, protection and control equipment to increase the reliability and power quality of the electrical systems.

The articles on operating experience of solar and wind generating plants, operation of micro grid, integration of DGs into grid will guide and help the power system engineers in taking up the challenges of tomorrow. The actual innovative experiments and pilot projects reported by TATA Power on solar, floating solar, and tailrace water energy recovery by mini hydro is the new area to be tapped. The use of solar tree is an innovative idea proposed for minimizing the land requirement of solar farms.

It is hoped that the sharing of knowledge and experience with other professional co-workers through this volume will build the confidence amongst power system engineers and speed up the implementation of innovative ideas in coming decade.

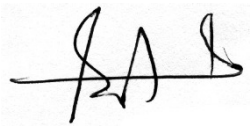

S B Dubey, FIE

Chairman

Electrical Engineering Division Board, IEI

Message from the Editor-in-Chief

It gives me immense pleasure to learn that the Electrical Engineering Division Board of the Institution is successfully bringing out its Volume 2 of Annual Technical Volume as per the decision of 126th CATE/682nd Council Meetings held at Pachmarhi, Madhya Pradesh during June, 2014.

I congratulate the Chairman and the Members of the Electrical Engineering Division Board and the Editorial Team of Technical Department for their sincere effort to bring out this Annual Technical Volume containing selected articles from All India Seminars and National Convention organized under the aegis of Electrical Engineering Division Board.

I believe that this compiled volume will be helpful for the academic, research as well as the industry professionals and will stimulate further research into these emerging fields of technology.

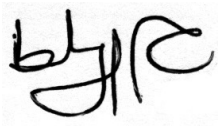

Prof (Dr) Nil Ratan Bandyopadhyay, FIE
Chairman, CATE, IEI

Annual Technical Volume of Electrical Engineering Division Board

Publisher

Maj Gen S Bhattacharya, VSM (Retd)
Secretary and Director General
The Institution of Engineers (India)
8 Gokhale Road, Kolkata 700020

Publication Office

The Institution of Engineers (India)
8 Gokhale Road, Kolkata 700020,
Ph : 2223-8311/14-16/33-34,
Fax : (033) 2223-8345,
e-mail : technical@ieindia.org,
website : www.ieindia.org

Contents

Retrofits and Upgrades in Power Transmission Systems using HVDC and FACTS Technologies

M. Arunachalam
Department of Electrical Engineering,
Raja Rajeswari College of Engineering,
Bangalore, Karnataka
E-mail : arunachalammlaiyandi @gmail.com;

Tayi Krishna Rao
Former Chief Engineer, Transmission Corporation of Andhra Pradesh Limited,
Hyderabad, Telengana
tayikrishnarao@gmail.com

Abstract

The demand for electrical power is increasing at a fast rate. The power transmission systems are becoming more and more complex and it is becoming difficult to construct the new transmission lines in a reasonable time frame as there are constraints like getting the Right of Way (RoW), arranging the funds etc. In this scenario, it is important that more and more existing transmission assets are utilized effectively by improving their system capabilities with much reduced investments.

In this respect, high voltage direct current and flexible ac transmission system technologies can be employed effectively in retrofitting and upgrading the existing assets of the transmission system with marginal investments.

In this paper, some sample projects on which the authors have worked and implemented like the up gradation by converting a 3-ϕ, 230 kV, double circuit ac line in to a dc link providing asynchronous link and also introducing new FACTS devices like controlled shunt reactor in a 400 kV line to replace fixed reactors are discussed.

Introduction

In the present day technological advancements and engineering maturity, the electrical and electronic control equipment are being designed and installed to give service to the owner for a life span of about 40 to 50 years. Whereas, the technological inventions and advancements are taking place at a fast rate. In this respect, the modern technologies like high voltage direct current (HVDC) and flexible ac transmission systems (FACTS) play important roles in making the present day power transmission system assets more and more effective and efficient by enhancing the capabilities and introducing the controllability. HVDC and FACTS are the enabling technologies in enhancing the capabilities of the existing transmission systems with comparatively much lesser investments and faster implementation.

The following approaches are used depending on the requirements.

Converting the existing 3-ϕ ac lines in to a dc bipolar line and thereby enhancing the power transfer capability to a maximum of about 3.5 times the existing capability with the additional benefits of capable of controlling the amount of power transfer at will, providing asynchronous tie,reduced losses and no additional demands for right of way (RoW).

The capabilities of the existing HVDC system can be enhanced by adding series or parallel HVDC substations. The investments are made in a pre-planned staged manner.

In case of power levels considered are of the order of 500 to 1000 MW, FACTS technology can be employed. The cases considered for discussion in this paper are:

a) Replacing the fixed shunt reactors in 400 kV substations with thyristor based controlled shunt reactor (CSR). CSR is a new FACTS device introduced by BHEL.

b) Introducing capacitors in series with the line. In the case of fixed capacitor, it is called as fixed series capacitors (FSC) and in the case of thyristor controlled variable capacitance, it is called as thyristor controlled series capacitors (TCSC).

c) In addition to improve the power transfer capability of the line as in the case of FSC, the power can also be ± locations in a power system to secure the stability of the system.

d) SVCs are also being introduced at the industrial substations to provide dynamic VAr compensation to tackle the rapidly changing VAr requirements of loads resulting in better voltage profile, enhancing the capability of drawing more power from utility at power factor close to unity and increasing the production and profit.

The cases, one for each of the above, on such systems the authors have worked are presented in this paper.

Conversion of Existing ac Lines into dc Lines

In this method of system upgradation, the existing ac line conductors and the insulators are proposed to be used.

Assuming that the effective ac current rating of the existing conductors and its dc current ratings are same and also that the peak value of the voltage rating of the existing ac line tower insulators provide the same dc rating, the line when converted in to dc can transmit nearly 1.5 times the power.

It is to be noted that, the additional befits are complete controllability, less losses and asynchronous tie.

The Indian National HVDC (NHVDC) in which the 230 kV double circuit line linking between lower Sileru and Barsur for power transfer between AP and MP was an asynchronous tie and through NHVDC project the link was converted in to a dc link of 200 kV, 200 MW mono-polar, implemented in two stages. In the first stage (phase 1), 100 kV 100 MW rating was realized in mono-polar mode. In the second stage (phase 2) the capability was further upgraded to 200 kV 200 MW. It was an experimental line with the key equipment like thyristor valves and controls were developed digenously. Though the project was conceived and executed as an R&D project with the aim of developing the technology capabilities in the country, today it gives an opportunity to extend the knowledge for upgradation of the system by converting the existing ac line in to a dc link. This aspect is discussed in [1],[2] including the design of the valve and control. The important features like the design of various type tests which were conducted for the new thyristor valve which are connected in series with the existing ones with the different type test capability are discussed below.

NHVDC is in monopolar mode with two 6 pulse converters connected in series, the bottom six pulse converter which is of standing structure and the upper six pulse converter is of the state-of-the art hanging structure. Figure 1 shows the connection schematic of these two converters. Both the converters are of double valve structures. They are shown in Figures 2 and 3.

It may be noted that in NHVDC phase1, 3.2kV, 1000 A, 55 mm thyristors, 96 numbers in series are used and in phase 2 , 7 kV, 1800 A, 100 mm, 48 numbers thyristors in series are used. In both the phases the state-of-the-art design, that is, air insulated, water cooled and fibre-optically triggered, is used. The valve losses are considerably less in phase 2 as there are only 48 thyristors and as these thyristors are of with larger wafer area the on state voltage drop is also less helping in resulting in less losses.

As it is noticed from Figures 2 and 3 that the bottom terminal of phase 1, valve 1 is at ground

potential and in phase 2 the bottom terminal of the valve is at 100 kV. Therefore, one has to simulate the impedance of phase 1 valve with proper impedance and connect it between bottom terminal of phase 2 valve and ground while conducting the dielectric type tests on phase 2 valves. This impedance has to be different for different type tests like ac withstand, dc withstand, switching, lightning and steep front impulse withstand tests. Through computer simulation were carried out with the suitable series impedances to verify whether the new valve is experiencing the required withstand test voltages.

The operational type tests were successfully carried out at Central Power Research Institute (CPRI) Bangalore. Figure 4 shows the picture of

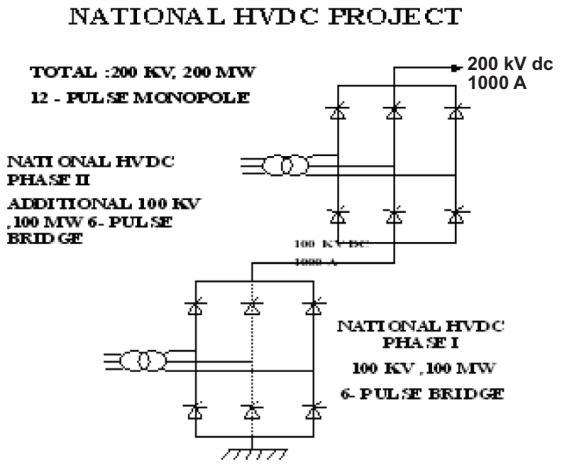

Figure 1 : Series connection schematic of NVDC phase 1 and phase 2 converters

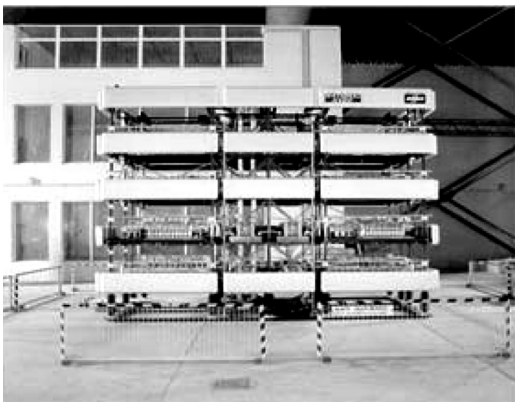

Figure 2 : Thyristor valve NHVDC phase I

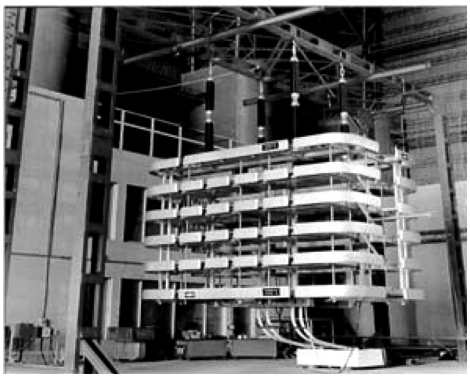

Figure 3 : Thyristor valve NHVDC phase II

OVER VIEW OF HVDC THYRISTOR VALVE

NHVDC PHASE I	NHVDC PHASE II
FLOOR MOUNTED TYPE	SUSPENDED VALVE
55mm DIA THYRISTOR	75 mm THYRISTOR
ANALOG THYRISTOR ELECTRONICS	HYBRID THYRISTOR ELECTRONICS
IMPORTED SATURABLE REACTOR	INDIGENOUS SATURABLE REACTOR
IMPORTED FINE WATER COOLING SYSTEM	INDIGENOUS FINE WATER COOLING SYSTEM
OPERATIONAL TYPE TEST AT GEC, UK	OPERATIONAL TYPE TEST AT CPRI

the phase 2 double valve structure erected at CPRI Bangalore for type tests.The test voltages were calculated as per IEC and the test were performed as per IEC [3].

Upgradation of HVDC Converter Station by Adding Series or Parallel Sub-stations

HVDC converter stations can be upgraded by introducing series or parallel HVDC sub-stations [4]. Figures 4 and 5 give the schematic of addition of series and parallel sub-stations, respectively for upgradation purposes.

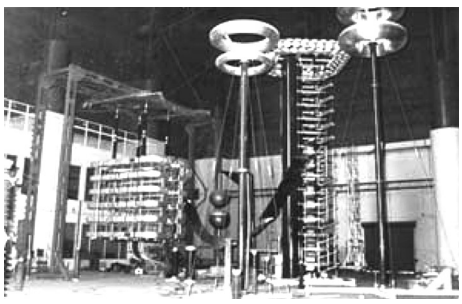

Figure 4 type test arrangements at CPRI Bangalore.

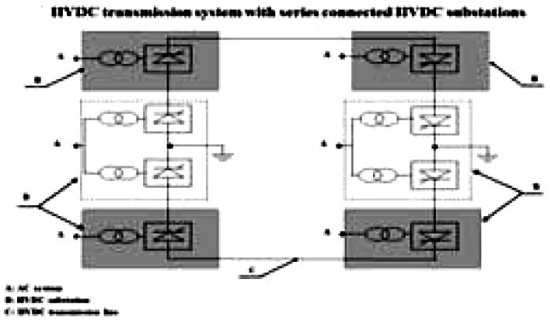

Figure 5 : Series connected HVDC substation

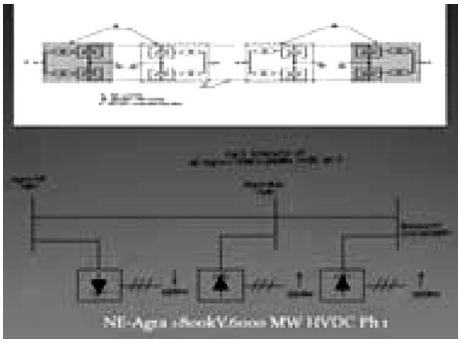

Figure 6 : Parallel connected HVDC substation

Figure 6 also shows the schematic of NE -Agra ±800 kV 6000 MW phase 1 being executed in the country. In phase 2 of the project parallel substations will be added as shown in Figure 7 to upgrade the rating from 6000 MW to 12000 MW. It is a multi-terminal UHVDC system being executed in the country with many first of the type in the world.

Upgradation of Transmission System using FACTS Technology

Like HVDC, FACTS is also an enabling technology to make the transmission system more valuable. Controlled shunt reactor (CSR) is a FACTS device introduced by BHEL [5]. It is used to replace the fixed shunt reactor in in 400 kV transmission line to improve the voltage profile, reduce the losses and improve the power transfer capability. Figure 8 shows the schematic of such a scheme.

FACTS devices like thyristor controlled series compensation (TCSC) are also used to upgrade the capability by introducing thyristor based variable capacitance in series with the line to improve the power transfer capability and the power transmitted is controllable. The upgradation in the case of the Kanpur- Ballabgargh system is carried out in stages [7]. First fixed capacitor was introduced and later a portion of the fixed (8%) is made variable by introducing thyristor controlled reactor (TCR) in parallel to the eight percent portion of the fixed capacitor making it variable up to 20% with a boost factor of 2.5. Figure 9 shows the schematic of the scheme. A number of lines in the country have been upgraded using FSC schemes improving the voltage profile, reducing the losses and upgrading the power transfer capabilities. Table 1 gives the details.

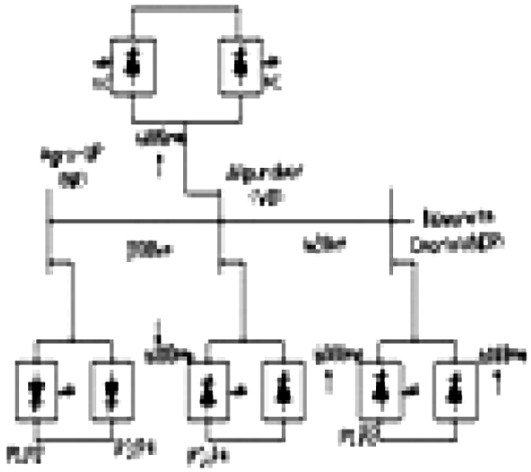

Figure 7 : Schematic of NE-Agra phase-2 upgrading to 12000 MW

Static VAr compensators (SVCs) are used to inject necessary reactive power in to the system to control the voltage profile of the utility and industrial busses. SVCs are thyristor based. Now turn off device based STATCOMs are more and more referred for their superiority in fast control and ability to supply rated reactive power at much reduced bus voltages. Table 2 gives some of the projects executed in the country and the befits realized.

TABLE – 1

BHARAT HEAVY ELECTRICALS LIMITED

REFERENCES FOR SERIES COMPENSATION

SL NO.	CUSTOMER/ LOCATION	VOLTAGE	DESCRIPTION OF THE FEEDER	CAPACITOR BANK RATING	IMPROVEMENTS ACHIEVED/ANTICIPATED
1.	KSEB KOZHIKODE	220kV	221 KM LONG LUDUKKI-KOZHIKODE	36 Ohm,650A, 23.4kV,45.75MVAr, 40% COMPENSATION	• INCREASE IN POWER TRANSFER CAPABILITY FROM 170MW TO 230 MW. VOTAGE FROM 0.8PU TO 0.9 PU •LOSS REDUCTION:38MW
2.	PDD J&K WANPOH	132kV	152 KM LONG UDHAMPUR-PAMPORE	43.3 OHM,400A,17.32kV, 2X20.28MVAr, 60% COMPENSATION	• INCREASE IN POWER TRANSFER CAPABILITY by70MW. VOTAGE FROM 0.85PU TO 0.92 PU AT PAMPORE •LOSS REDUCTION:1.4MW
3.	MPEB PICHHORE	220kV DOUPLE CIRCUIT LINE	240KM LONG GWALIOR TO BINA	34.8OHM,600A,20.88kV, 2X36.6MVAr, 45% COMPENSATION	• INCREASE IN POWER TRANSFER CAPABILITY by60MW. VOLTAGE FROM 0.84PU TO 0.9 PU AT GWALIOR
4.	MSEB MIRAJ	220kV	84.6KM LONG KARAD TO MIRAJ	24.2OHM,650A,14.8kV, 30.66MVAr, 70% COMPENSATION	• INCREASE IN POWER TRANSFER CAPABILITY by30MW. VOTAGE FROM 0.82PU TO 0.9 PU AT MIRAJ • LOSS REDUCTION:2.5 MW
5.	MPEB HANDIA	220kV DOUPLE CIRCUIT LINE	ITARSI - BARWAHA	34.8OHM,600A,20.88kV, 2X36.6MVAr , 45% COMPENSATION	• INCREASE IN POWER TRANSFER • VOLTAGE AND TRANSIENT STABILITY IMPROVEMENT
6.	MPEB BIJAWAR	132kV	210KM LONG DAMOH-BIJAWAR-PRITHVIPUR	50.0 OHM,350A,17.5kV, 18.4MVAr , 60% COMPENSATION	• INCREASE IN POWER TRANSFER CAPABILITY by6MW. VOTAGE FROM 0.82PU TO 0.9 PU AT BIJAWAR • LOSS REDUCTION:20MW
7.	MSEB AURANGABAD	220kV DOUPLE CIRCUIT LINE	80KM LONG BABLESHWAR-AURANGABAD	22.3OHM,650A,14.5kV, 2X28.2MVAr , 60% COMPENSATION	• VOTAGE FROM 0.85PU TO 0.92 PU AT AURANGABAD • LOSS REDUCTION:1.85 MW
8.	POWER GRID, KISHENPUR,J&K	220kV DOUPLE CIRCUIT LINE	174KM LONG KISHENPUR TO PAMPORE,J&K	30 OHM, 800A, 24.0kV, 3X19.2MVAr , 42.86% COMPENSATION	• INCREASE IN POWER TRANSFER CAPABILITY

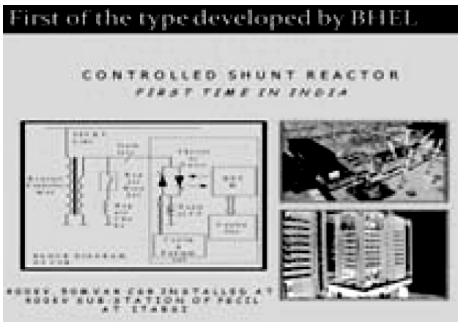

Figure 8 : Schematic of controlled shunt reactor

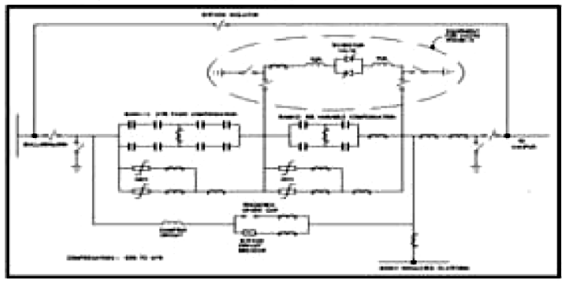

Figure 9 : Schematic of TCSC controlled shunt reactor

TABLE – 2

BHARAT HEAVY ELECTRICALS LIMITED

SVCs COMMISSIONED

SL NO.	CUSTOMER/ LOCATION	VOLTAGE	No. OF SETs	REMARKS
1.	BHEL, BHOPAL, GBX	11kV±3.75MVAr	1	REACTIVE POWER CONTROL
2.	MPEB, BARSOOR	12kV±30.0MVAr	1	VOLTAGE CONTROL OF 220kV LINE
3.	TNEB	11kV+15/-30 MVAr	3	---DO----
4.	SAIL, ALLOY STEEL PLANT, DURGAPUR	33kV 0-35MVAr	1	POWER FACTOR IMPROVEMENT OF SMS WITH ARC FURNACE
5.	SAIL, BSP, BHILAI	11kV 0-12.5MVAr	1	REACTIVE POWER CONTROL FOR RAIL AND STRUCTURAL MILL
6.	TISCO JAMSHEDPUR	33kV 0-50MVAr	1	REACTIVE POWER CONTROL FOR HOT STRIP MILL
7.	SAIL, RSP, ROURKELA	33kV 0-50MVAr	1	POWER FACTOR / VOLTAGE CONTROL OF TANDEM MILL
8.	SAIL, VSP, VIZAG	1.65kV±5.0MVAr	2	REACTIVE POWER CONTROL OF MEDIUM MERCHANT STRUCTURAL MILL
9.	HDC, MALANPUR	33kV±100MVAr	1	FLICKER CONTROL OF ARC FURNACE LOAD

Enhancing the Capabilities by Overcoming the Limitations Like Thermal, Dielectric and Stability

The systems capability can be both during summer and winter period through off line computations. The line will be able to deliver larger power during winter as the ambient temperature is likely to be low and hence the line current can be larger for the same sag.

Moreover, the thermal ratings of the lines are much larger. In order to utilize this capability, FACTS are used along with on-line monitoring and computational feature so that possible maximum capability of the line is utilized.

When the line is operating with enhanced power level, any load throw-off or any other forced trappings may result in over voltages of unacceptable level. FACTS devices based voltage suppressors can help in this regards.

The stability issues also come in the way of utilizing the potential capability of the asset. SVCs and STATCOMs play important roles in enhancing

the stability of the system and helps to reduce the margin provide for safe operation.

FACTS based power swing damping helps to reduce the oscillations fast and provide the system with better security and hence enable to transmit larger power.

Conclusion

HVDC and FACTS are the enabling technologies and used to upgrade the capabilities of power transmission systems. In this paper, upgradation of the system by converting the ac line in to dc link to improve the power transfer capability, increase the efficiency, introduce full controllability and also provides asynchronous tie. Series and parallel HVDC substations can be added in the existing HVDC converter stations for upgrading the capacity. FACTS technology also helps to improve the power transfer capability, improve the voltage profile and stability. A number of projects in which the authors have worked using the indigenously developed schemes have been discussed in this paper.

Acknowledgement

The authors are thankful to former Executive Director, Corporate R&D, Bharat Heavy Electricals Limited, Hyderabad for his encouragement in preparing and presenting this paper.

References

1. S. K. Raizada, M. Arunachalam, R. Rajan Babu and G. K. Agarwal, 'Design and Testing of Thyristor Valve for Indian National HVDC Experimental Line Project', Symposium of Specialists in Electric Operation and Expansion Planning, Brazil, August 21-25, 1989.

2. Ghamandi Lal, Devashees Das, G. V. Paradkar and M. Arunachalam, 'Thyristor Valves for National HVDC Project II-Design and Testing Aspects', BHEL Journal, vol. 24, no.1, January 2003.

3. 'IEC-60700-1 Testing of Semi-conductor Valves for High Voltage dc Power Transmission'.

4. 'IEC-60633 Terminology for High-voltage Direct Current Transmission'.

5. International Tutorial and Colloquium on HVDC and STATCOM under the aegis of CIGRE Study Committee B4 on HVDC and Power Electronics, Agra, September 21 -26 , 2015

6. S V N Jithin Sundar, S C Bhageria, M Arunachalam, etal, 'Design, Testing and Commissioning of First 420 kV, 50 MV AR Controlled Shunt Reactor in India,' Cigre Session 20.

7. M. Arunachalam and Ghamandilal Lal, Rajiv C. G., 'Performance Verification of TCSC Control and Protection Equipment using RTDS', 15th Power System Computation Conference (PSCC), Liege, Belgium, August 22- 26, 2005.

Experiences in Substation Retrofitting

S. Rao Cheepuri **E. Sreenivasulu** **B. Sarang**

Asa Bhanu Technical Services Limited,
Hyderabad, Telengana
E-mail : srao.cheepuri@asabhanu.com; sreenivase@asabhanu.com; bsarang@asabhanu.com

Introduction

There are two scenarios in general for improving the aging substations to perform again at its full potential and be in line with modern substations which have been designed.

The design criteria for modern substation are as given in Figure 1.

- Reliability
- Security
- Interoperability
- Re-configurability
- Controllability
- Maintainability
- Operational flexibility
- Economic cost
- Environmental impact

The two scenarios are,

• Replacing part of the existing primary/secondary sub-station equipments on account of their age or condition of the equipment or need of new technologies, etc known as sub-station retrofitting.

• Expanding the capacity, voltage or performance of the existing substation using new technologies and suitably rated equipment.

Figure 1 : Modern sub-station design criteria

In retrofit projects, the old and new parts must be compatible and the continuity of the substation's operation must be assured during the transition. Outages must be used only where no other possibility exists; and their duration must be as short as possible. The operation of the overall transmission network must be unaffected by the work. Project teams must therefore carefully analyze and gain a detailed understanding of the existing system.

Therefore, retrofit projects are, by their nature, more challenging than projects in which everything is built new from scratch.

Substations perform adequately during the retrofitting exercise provide service to the full designed potential (economical and technical) meeting the modern substation criterion leading to smart grid technologies.

In this paper, authors have described their experiences in retrofitting the various existing substations.

Need of Retrofitting in Substations

Retrofitting is a process by which the primary and secondary equipments in a substation are replaced by adequate plan without disrupting the service beyond the agreed minimum, fully considering safety, economy and speed.

Substations to begin with are installed as per the adopted and available technology and applicable standards and then age during their service. The primary electrical equipment like transformers, switchgear, cables etc. designed to have 30 to 35 years life and secondary equipment like protection and control are expected to have 8 to 10 years of service.

Good maintenance comprising of routine maintenance, periodic maintenance overhaul, preventive and failure maintenance help to attain the service life of the equipment nearing to the design values. However, high cost of operations, maintenance and servicing cause negative impacts on reliability and forces the utilities to upgrade/renovate their old substations and there by achieve the minimum overall cost and high reliability.

For the secondary equipment, additionally the constant upgradation of technologies with focus on ease of operations, size reduction, automation, speed of performance, ability to remote monitoring and remote operation influence the utilities to constantly pursue upgrading by replacement before expiry of life.

For both primary and secondary equipments, the capacity expansion, faulty technologies and equipment, non availability of spares drives the utilities to go for retrofitting.

The ever increasing land prices and non-availability of lands on one hand and increasing civil costs on the other hand lead us to new set of choices in technologies.

The main concern of a retrofit is the need to have minimal disruption to the continuity of services. To reach this goal, a comprehensive survey of new technologies has to be done and the cost benefit analysis should be addressed, visa vise safety and speed retrofit work.

Primary Equipment Design for Retrofitting

This section discusses different design criteria for retrofitting the primary equipment. Also various advanced technologies are analyzed and considered through an examples of disconnecting circuit breaker, hybrid GIS switchgear as a potential retrofit options in existing substations.

Primary Equipment Design Criteria

The primary equipments are chosen by common basic criteria such as reliability, flexibility, safety, environmental impact, footprint and cost.

Reliability

Controllability of power transfer, high efficiency and redundancy improvement.

Safety

Limitation of touch and step potential (voltage), risk of fire or explosion, avoidance of unauthorized users or intrusion by continuous surveillance, and seismically qualified equipment.

Environmental Impact

Limitation of electromagnetic and electric field, low level of noise emission, and use of waste recycling.

Flexibility

Plug-and-play design, integrated compact design, low level of maintenance and easier operation.

Footprint

Generally, as small and compact as possible.

Costs

Low cost equipment, minimized life-cycle cost.

Case Study 1

Existing disconnector and its associated earth switch retrofitting with a single combined disconnecting circuit breaker (DCB).

DCB is basically a standard circuit breaker with additional features of a disconnector and is type tested in accordance with both CB and disconnector standards. Model of the DCB is shown in Figure 2. The circuit breaker contacts in open position are thus open disconnector contacts as well. The combined equipment replaces the conventional combination of circuit breaker and separate disconnectors. It permits a simpler and more compact substation layout, with increased availability due to the reduction of maintenance requirements, low failure rate, increased safety and low life cycle cost.

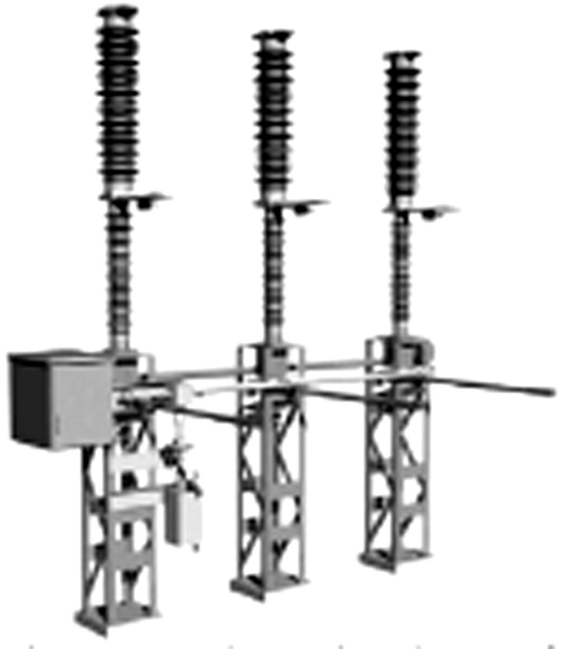

Figure 2 : Disconnecting circuit breaker with one set of moving contacts/poles

As the experience of disconnector has not been satisfactory, it was decided to be retrofitted with highly established SF6 gas type breaker, DCB was chosen as a result of study.

For safety and reliability reasons, there are some special features applied to the design and construction of DCB which are –

• Reliability composite insulation across open gap providing minimal leakage currents and proven long term properties, such as, flash over resistant, aging withstand and low mass.

• The number of sealed joint is minimized to reduce risks of leakage to less than 0.5%.

• SF6 volumes are also minimized, 10 times as much as in live-tank breakers.

• External grounding switch outside the breaking chamber with visible grounded and ungrounded positions provide maximum safety for operating personnel. This switch also gives the visual indication for operation of DCB, which is shown in Figure 3.

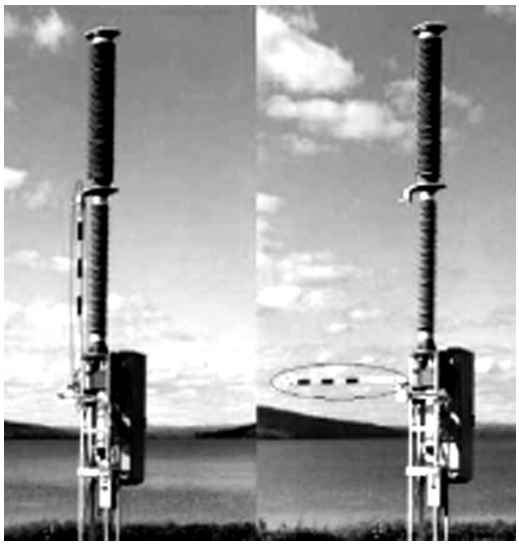

Figure 3 : Operating procedure of DCB-visual indication

Advantages of DCB

• The most significant improvement is that DCB brings the new possibilities for substation design. When designing a sub-station, there are a lot of considerations that have to be taken, namely, load, surrounding power network, power losses, reliability and maintenance for apparatus etc.

• The traditional way of building substation with many busbar systems and DS decreases rather than increases the availability. The consideration of increasing the availability is leading to conclusion to take out all DS out of the substation and only use CBs. However, a disconnection function is still needed for safety reason. The new DCB with the integrated disconnection function is an alternative that can fulfill both of the functions.

• The maintenance interval of DCB is 15 years, like modern CB, but the overall maintenance demand decreases when disconnectors are eliminated. With the combined DCB maintenance interval of 15 years, the use of double bus bar systems is not necessary. If a double bus bar system is still needed, due to very high requirements for service availability, a good solution is to use a double bus bar /double breaker system (the very limited DCB

maintenance only affects one bus bar).

• Another advantage is space saving which is in the range of 20% to 50% less as shown in Figure 4.

Thus, a combined DCB can save cost in all aspects whose statistics may be approximated in comparison with standard CB and DS combination as follows.

Planning work (25%), design work (25%), land acquisition and preparing (30%), project management and time (25%), building costs (30%), outage costs (50%-60%), maintenance costs (50%-60%), the overall life cycle cost (LCC) will be far lower than conventional design.

The environmental effects are the lowest in terms of SF6 usage, metallic and plastic material.

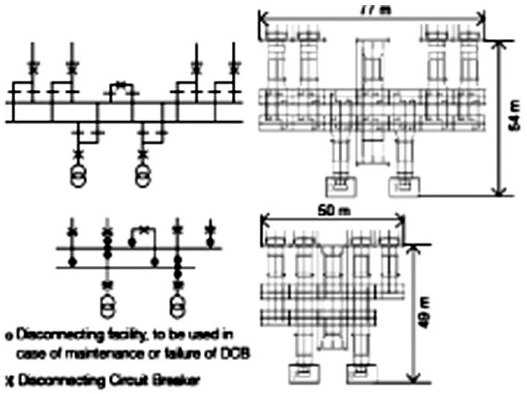

Figure 4 : Space requirement comparison of 145 kV sub-stations (conventional CBs and DS against DCB)

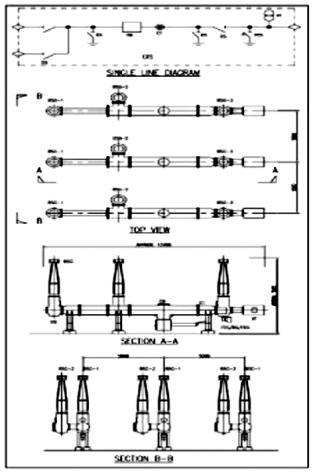

Figure 5 : Typical 400 kV DBB OHL feeder H-GIS

Case Study 2

Conventional AIS switchgear bay retrofitting with hybrid gas insulated switchgear (H-GIS).

To facilitate, upgrade or replace aging AIS switchgear bay, H-GIS is being increasingly applied. The reasons are as outlined below.

H-GIS is a well established type of SF6 switchgear which is compact in size, reliable in operation and economical in cost. H-GIS combines the air insulated bus bar and feeder connection features of GIS and GIS features are adopted for the rest of the equipment to form H-GIS. Compared with AIS, H-GIS greatly saves space and vastly reduces installation and maintenance of equipment in the substation.

The main components of these hybrid substations, namely, circuit breakers, instrument transformers, disconnectors, and grounding switches are based on GIS technology, while busbars and bushings originate in conventional AIS technology. A typical 400 kV double bus bar OHL feeder bay module of H- GIS in various views is shown in Figure 5 for reference. Air insulated bus bars and feeder connections are highly reliable and need minimal maintenance. This results in optimization of cost and space.

Hybrid compact switchgear applications mainly used in the refurbishment, expansion of AIS substations and upgrading of voltage and capacity particularly in cases when such modifications need to be accomplished with the substation in service. Circuit breakers, disconnectors, grounding switches, and instrument transformers housed in gastight enclosures, H-GIS provide the possibility to complete the work in the shortest time and without the need for additional space.

Advantages of H-GIS

• Modular, reliable operation, performance, high degree of intelligence and very little requirement for maintenance.

• AIS bus bar in H-GIS : Economical, reliable and has low maintenance.

All live contacts in SF6, adopting GIS features experience has proven that H-GIS virtually maintenance free. This combines with a high level of reliability to ensure a lower life cycle cost.

Factory pre-assembled and tested that ensures a higher quality of finished bay than if it is assembled under site conditions minimizes installation time on site and reduces the possibility of delay due to adverse site conditions. On line monitoring and diagnostics for local and remote indication is possible.

Substation Modularization

A modular approach to substation design offers cost and time savings during the design and construction phases. The use of standardized components reduces the number of possible variations and hence the risk of design errors. More predictable costs also offer a higher level of confidence in the project estimation process.

Versatility

The hybrid switchgear modules offer a series of modules for HV substations including: single bus bar (SBB); double bus bar (DBB); DCB. It can also be installed as a high voltage bay on a mobile truck for use in emergencies or if work has to be carried out on existing HV bays.

Space Saving and Reduced Civil Works

The hybrid design can save up to 60% ~70% of the space normally required for a conventional AIS substation, while also reducing the need for civil works, such as, foundations, steelwork and cable trenching operations. Space saving is demonstrated through Figures 6 and 7.

Case Study 3

Retrofit works of 275 kV and 132 kV AIS sub-station by eliminating age old 275 kV mesh arrangement.

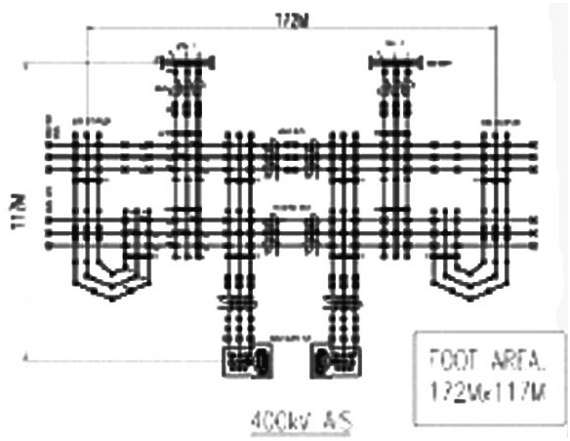

Figure 6 : Conventional 400 kV AIS double bus bar sub-station (typical)

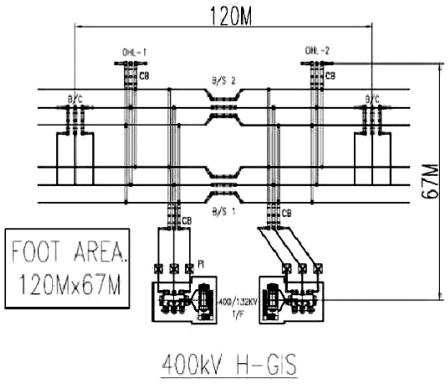

Figure 7 : Conventional 400 kV H-GIS double bus bar sub-station (typical)

Initial Plant Arrangements

A 275 kV, 4 corner mesh AIS sub-station is fed from a 400 kV feeder in LILO arrangement. 400 kV is step down to 275 kV through inter bus transformers and connected to 275 kV mesh sub-station. Mesh sub-station caters the loads at 132 kV and 275 kV through mesh feeder and mesh transformer circuits (Figure 8). For plant initial existing arrangements shown in black colour. Space constraints.

Very minimum disturbances to existing utilities/ customers and maximizing the services availability.

Increased load requirements for distribution elimination of mesh arrangements for better availability and operation conveniences.

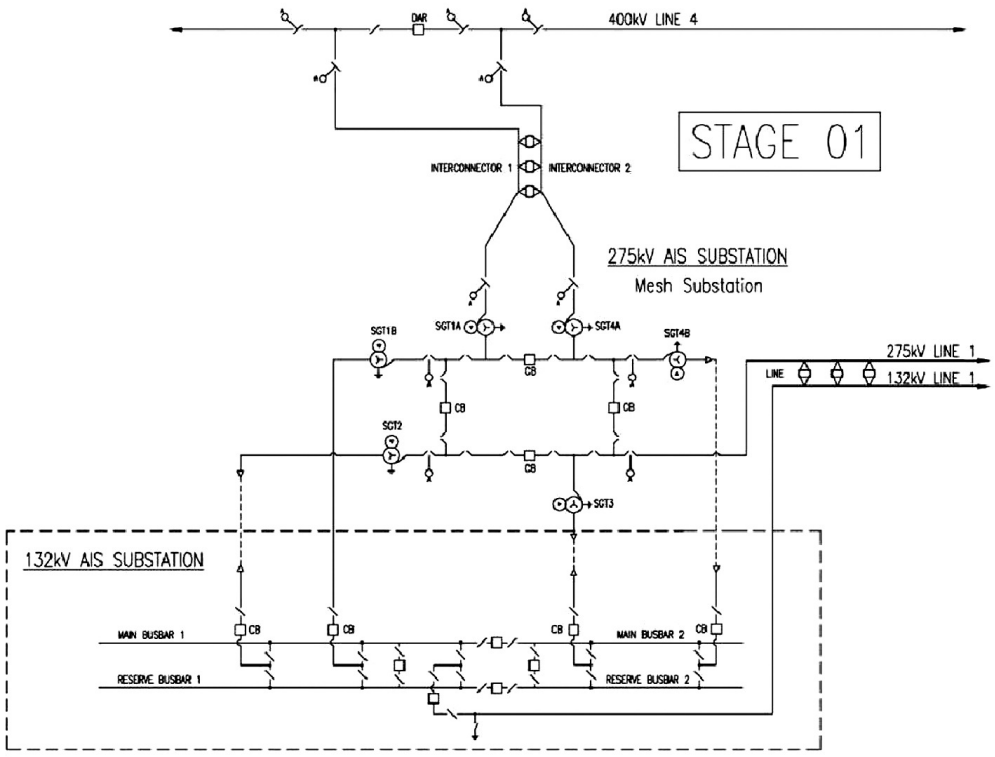

Figure 8 : 275/132 kV sub-station (initial plant arrangements)

Aging of existing 275 kV switchgear and difficulties in maintenance and spares (Figure 8).

Under this project, substation retrofitted by demolishing the mesh arrangement of 275 kV AIS by keeping only MC4 equipments and SGT4A, SGT3 in service and modifying the control and protections accordingly at 275kV. Also in 132 kV side constructed new lines and connected to 275 kV substation and 400kV lines with new SGTs. Final arrangement of the substation is shown in Figure 9.

Planning and Execution

Project was planned to execute in various stages to complete the retrofit works. Total 10 stages covering a span of 4 years were proposed for the completion of the project with very minimal disruption of services by the utilities.

Detailed studies have been made on the existing site drawings of 275 kV and 132 kV sub-stations.

In order to reflect the new equipment details/ information, at first the drawings that need to be modified as per the site drawing, are listed, which is included with circuit diagrams, wiring diagrams, connections diagrams, block diagrams, lay-outs and cable schedules.

The existing drawings were modified by separate green and red colour coding of the drawing by removing and including the details related to new equipment as applicable.

Green colour coded drawing shows the equipment demolished or removed and red colour coded drawing shows the newly installed equipment. The red colour coded equipment drawings will supersede the existing equipment drawing with newer equipment drawing and demolished equipment drawings will be obsolete. All existing drawings affected by the retrofit works and drawings and documents covering the safety and conforming to the work progress were prepared and delivered (Figure 9).

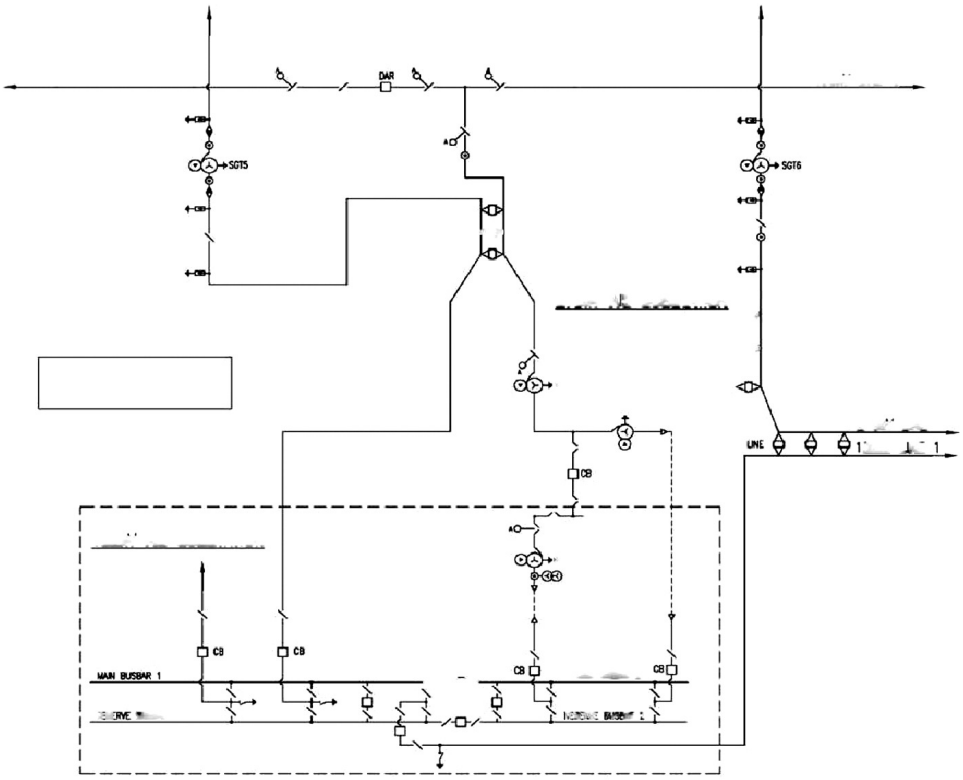

Figure 9 : 275/132 kV sub-station (final plant arrangements)

Secondary Equipment Design for Retrofitting

In this section, some retrofit options on sub-station secondary equipment are discussed. The main functions of the secondary system of the sub-station are categorized into protection, monitoring, communication, backup and emergency controls. The retrofit design for sub-stations may vary since the criteria for upgrades may be different. This section describes different strategies for retrofitting the secondary equipment at a large typical substation.

Needy sections where sub-station secondary equipment retrofit is split into following

Switchyard Monitoring Devices

The main function of the sensors is to measure signals from primary equipment in the sub-station. Original copper-wired analog sensors are replaced by optical fiber-based sensors for monitoring and metering.

Retrofitting of these devices transforms the old sub-stations to modern sub-stations.

Monitoring devices / sensors available is,

- Temperature sensors
- Pressure sensors
- Vibration sensors
- Oil and gas monitoring devices

Besides the protection of the transformers, the monitoring of the operation of transformers is essential as well. Dissolved gas analysis (DGA) monitoring is one of the most valuable diagnostic tools available. On-line and in-line DGA sensors are two new methods for transformer monitoring. Existing substations are mainly using off-line and at-line methods to evaluate the oil condition of the transformer.

Current and Voltage Sensors

Widely used current and voltage transformers are

based on magnetic circuits. This may create series of problems, such as measured signal bandwidth limitation, magnetic saturation, etc.

To overcome these challenges, such as, gas insulated CT, PT, and oil minimum current transformers, magneto-optic current transformer, Optical CT and PT are currently available.

• The most prominent advantages of this kind of technologies are high accuracy, no saturation, reduced size and weight, safe and environmental friendly, higher performance, wide dynamic range, high bandwidth and low maintenance.

Intelligent Electronic Devices (lEDs)

Recent multi-functional intelligent electronic devices (IEDs) provide higher performance, reduction in operating cost, reduction in size, increase in efficiency and improvement in robustness in the existing sub-stations. The main advantages of multi-functional IEDs are that they are fully IEC 61850 compatible, have compact size and offer various functions contained together in one design. New IEDs are complex and offer variety choices of settings and functions.

Some options for retrofitting sub-stations secondary equipment in the areas of IEDs/relays are listed below.

• Multi functional metering and monitoring relay uses a multiplexer that has high speed synchronous communications, bit error correction, data management, and alarms with diagnostic at the same time.

• Multi-functional safety relay combines multiple functions of individual safety relays in a single device. The arrangement of the functions in the diverse variants ensures that the most common applications can be realized with minimum engineering and cost expenditures.

• Transmission line protection relay

• Transformer protection relay

• Bus protection

• Fault recorder

Fiber Optic Cables

The electrical substation environment has many environmental challenges to reliable and secure communications. These challenges involve high voltages, extreme temperatures, high-current faults, electro-magnetic interference and electrostatic discharges. To overcome these challenges and to have a reliable, safe, secure and economical communications, the best option for upgrading the substations is to use fiber optic cables to interconnect all monitoring, control and protection parts. Also, no external power is required for fiber optic transceivers which are designed to work in the harsh sub-station environment. The reliability, performance and weight of this wiring material can affect the entire performance of the sub-station. The other advantages of this technology are higher speed, longer distance of transmitting information, greater immunity to electromagnetic interferences and lower cost.

Wireless Communication

Wireless communication is another option for data transfer from substation switch yard to control house which does not require wire installation in the switch yard. This solution is easy to install and provides compact low cost solution. Data transfer speed is not critical because data are not used in real-time control applications. Considering recordings size and number of units in the switch yard data rate of 115 or 256 kbps should enable relatively fast data transfer.

Because of high level of EMI in sub-stations, output power of transmitters should be higher than power required for normal outdoor application.

Retrofitting Jobs Execution Strategies

Retrofitting jobs are more challenging and their

execution needs detailed site investigations, detailed execution planning, compatibility and the continuity of the substation's operation must be assured during the transition complete knowledge on existing equipments and its technology and new equipments as well, detailed interface engineering before the start of actual execution at site and testing as necessary.

These strategies includes defining detailed project intent documents, developing modular standard solutions and detailed planning in staged manner are discussed in through a case study on retrofitting a bay control and protection schemes.

Case Study 4

Standard Bay Solution for a Control and Protection Scheme to Feeder Circuits

There is a strong demand by utilities all over the world to renovating their existing conventional control, protection and Automation circuits by utilitizing digital multi-functional protective relays.

Usage of these relays along with traditional switches, annunciation panels and panel board meters are growing need for Protection and control scheme retrofits.

A standard bay solution (SBS) for control, protection and monitoring of a feeder bay will encompass the complete functionality required to effectively manage the interface between the sub-station and a circuit element. The solution shall establish a design to facilitate a connection between the bus bars and the circuit, inclusive of all the primary, light current equipment and infrastructure required, to provide a safe and functional connection for the service life of the bay. The bay boundary and interface design incorporates all elements (line, cable and transformer), the bus bars, light current functions, civil infrastructure and core interfaces with the sub-station auxiliary systems.

Considerations for Retrofit

The approach provides for the development of effective and sustainable techniques for replacement activities within the live operational sub-station environment. Hence the following criteria that Utilities set the specifications such that the solution shall ensure and demonstrate:

- Is cost effective throughout the bay life cycle.
- Is safe and simple to maintain.
- Maximizes substation reliability and availability during construction, operation and maintenance.
- Does not fail in a manner that will adversely affect personnel or adjacent circuit integrity.
- Utilizes latest technology with due regard to social and environmental responsibilities.
- Minimizes the introduction of lifetime liability issues.
- Provides a seamless interface with existing and alternative supplier's equipment.
- Provision of full bay availability at the rated levels defined and associated documentation.
- Minimize disturbance to the network and loads.
- Perform in a safe manner (including failure) - maintaining 100% availability of adjacent bays.
- Capable of being maintained in a safe and efficient manner.
- Minimize equipment unreliability.
- Demonstrate reliable and secure automated and remote operation.

The solution shall contain a high level of self-supervision and alarm detectable failure modes.

Design Standardization for Retrofit

The purpose of this design process is to develop a standard solution confirming all specifications, which can be repeatedly used within the network for the purpose of retrofit and ideally any subsequent new connections. The design

conformance will concentrate more on the bay application rather than each component.

Designs ensure that all possible pre-outage work is maximized by installing equipment and cabling and completing site functional testing prior to commencement of the outage and connection following replacement.

Figure 10 shows typical control and protection function arrangement for newly installed protection and control cubicles. Here the green colour code demonstrates the removal of the cubicle and associated protection devices. The red colour code exhibits the new protection functions included as part of SBS retrofit.

Figure 11 Shows typical retrofit arrangement of protection and control cubicles in relay room. (conventional relay panels against new multi-functional relay panels as part of SBS retrofit.

Site Investigations and Retrofitting Execution Plan

The design takes into account of potential restrictions associated with replacement in a live and operational sub-station. Due consideration is given to the lifetime management of the bay such as access to equipment for maintenance and the impact to adjacent bays caused by maintenance or access issues, both during and after construction.

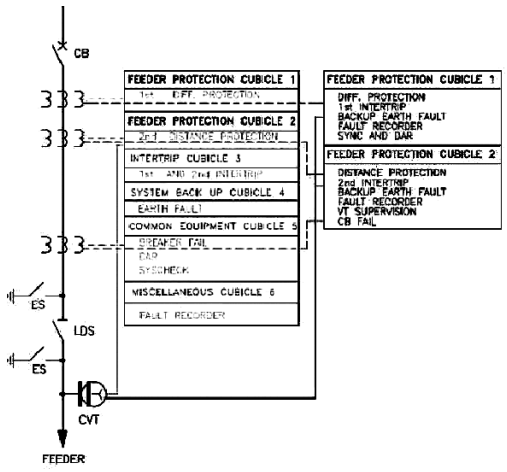

Figure 10 : Typical protection functional key line diagram

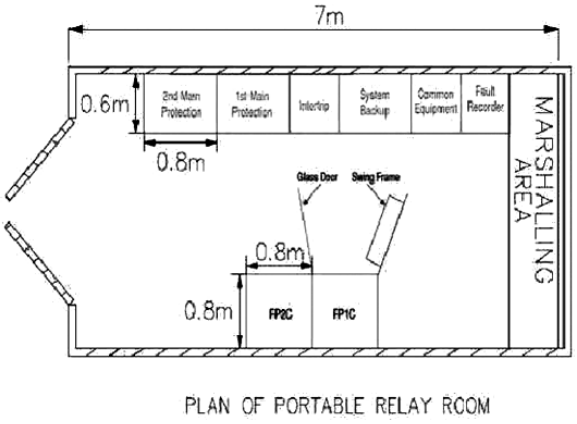

Figure 11 : Plan of portable relay room

Hence detailed site investigations and reporting mechanism was developed prior to take off the project.

Some of the conformities addressed during investigations are:

- identify standard bay footprint size (min and max) for which the whole bay design is valid.
- identify bay volume (m^3 min and max) for which the design is valid.
- define bay centers (for maintenance access).
- expected construction practices (use of cranes near over-sailing conductors).
- acknowledge clearances (electrical and safety).
- identify exceptions to safety rules with program for alternative safety case.
- demolition of the existing bay equipment.

Benefits of Retrofit Design

The benefits of retrofit of the existing sub-stations can be summarized as follows.

- Cost reductions in operation, maintenance and service.
- Prolonged equipment service life
- Higher productivity and availability of assets
- Improving reliability, entire performance and efficiency
- Improved maintainability

- Lower installation time
- Enhanced communications
- Better utilization of data
- New functionality
- Increased cost efficiency, performance and availability of the system

Equipment Aging and Condition Monitoring

Retrofitting activity is closely associated with the ability of understanding the status of aging by continuous monitoring.

Preserving and or enhancing system reliability and reducing operation and maintenance cost are top priorities for electric utilities. Electrical equipment deteriorates (wear out) while in service for a host of causes. The primary reasons include ©Asabhanu Technical Services Ltd.

Sustained heating due to electrical current flow, insulation degradation due to voltage tress, wear and material fatigue of mechanical parts, corrosion from chemicals in the soil, air and a slow but steady deterioration due to the effect of sun, wind, rain, ice and snow.

As system equipment continues to age and gradually deteriorates the probability of service interruption due to component failure increases.

Concept of Life Time

Equipment performs both technical and economic functions in Power systems. There are three different concepts of life time.

Physical Life Time

Equipment starts to operate from new condition to a status in which it can no longer be used in normal operating state and must be retired. Preventive maintenance can prolong its physical life time.

Technical Life Time

A piece of equipment may have to be replaced due to technical reason although it may still be physically used. For example a new technology is developed for a type of equipment and manufacturers no longer produce spare parts.

Economical Life Time

A piece of equipment no longer valuable economically, although it still may be usable physically.

1. When the depreciated cost of equipment reaches zero.

2. When the O and M costs which grow with age, equal to t he depreciated value of equipment.

Optimizing Equipment Life Cycle

Various issues to be considered for the optimizing equipment are:

Condition Monitoring

Some condition monitoring system include infrared inspection, dissolve gas-in- oil analysis, frequency response etc.

Substation equipment can be cost effectively monitored through SCADA systems. Online techniques include alarms, namely, current, temperature and pressure to continuous monitoring of dissolve gas in oil.

Life Extension

Equipment replacement is expensive, resource intensive, and operationally disruptive. For this reason utilities are increasingly looking at life extension strategies as a way to defer replacement. Equipment life extension program is coupled with a condition monitoring program and as the equipment reaches a certain degree of deterioration, life extension options are examined and adopted.

Repair against Replace

Utility practices vary widely and some utilities compare repair verses replace and decide when to replace. Others only replace equipment if it fails or becomes overloaded.

Optimized Life Cycle Management

The ultimate goal of a utility is to provide reliable electricity for the lowest rates.

The policies of utilization, operation, inspection, maintenance-repair, retirement and replacement in an integrated manner aimed at minimizing total levelised cost are vital. Optimized life cycle management requires good data, effective conditions and remaining life analysis and evaluation, sound implementation.

Conclusion

The retrofit design used to upgrade the existing sub-station with minimal disruption to service is discussed. Different technologies are analyzed and considered. These devices may enhance the performance of a substation or can replace its existing equipment. The retrofit designs not only perform the main functions more efficiently but also may introduce some new functionality as well as increasing operation time of sub-station for at least 10 years. This will allow utilities to have time in preparing capital investment for upgrading current aging infrastructure. With new technologies, such as, digital communication system or fiber optic wiring, such devices will have a better performance and synchronism with the whole substation.

Different retrofit scenarios, strategies and options are outlined to retrofit the existing sub-stations to meet some pre-defined requirements.

It is vital to adopt retrof itting work process design to be detailed and prioritized step by step work progress to be determined. Outage time to be minimized and pre-outage work maximized safety and speed are vital.

The following are goals concluded for this approach:

1. Adding new equipments to supplement existing sub-station as well as paving the way for the future replacement of legacy solution.

2. Replacing existing equipment due to performance or age deterioration as well as making it compatible for total future replacement. Balancing the need for open system design and cyber security demands while expanding the best practices and gradually training personnel for new equipment.

References

1. Report on 'The 21st Century Substation Design', Power Systems Engineering Research Center Publication, Arizona State University, September 10-15, 2010.

2. Article on 'General Review on Aging Electrical Distribution Systems and Maintenance Strategies'.

Conversion of 66 kV 'Hyderabad-Nizamsagar Line' for 132 kV Operation

Tayi Krishna Rao

Former Chief Engineer, Transmission Corporation of Andhra Pradesh Limited, Hyderabad, Telengana
E-mail : tayikrishnarao@gmail.com

Introduction

In a fast developing country like ours, addition of power generation capacity and expansion of transmission network are inevitable and need to be planned and implemented. Power system studies are conducted from time to time and EHV transmission lines and EHV sub-stations are planned to meet the system requirements. Retrofitting of age old EHV sub-stations and up gradation of EHV lines and connected EHV sub-stations can also be planned as an alternative option to meet the system requirements instead of planning entirely new lines and sub-stations. With the passage of time, land acquisition for new EHV sub-stations and gaining access to corridors for new EHV transmission lines are getting extremely difficult and expensive too. This apart, the statutory clearances are required for new EHV lines from telephones, railways, airports, high ways and forest department which get delayed due to various reasons. It was in this context that Andhra Pradesh State Electricity Board explored the alternative means to enhance the transmission capability. One such feasible alternative considered by the Board was conversion of existing 66 kV dc line from Hyderabad to Nizamsagar for 132 kV operation. This conversion project was engineered, designed, constructed and commissioned successfully by the Board's engineers. In this paper the technical issues involved and methodology adapted to utilize existing 66 kV d c line for transmission of power at 132kV are discussed.

EHT Transmission Network at Nizamsagaras Existing before Upgradation.

The Nizamsagar Hydro Power Generating Station has two generators each of 5 MW Capacity. These generators are run only for 6 months in a year depending upon availability of water head. The Nizamsagar switch yard was earlier connected to Hyderabad (Erragadda sub-station) by 66 kV dc line. During mid-fifties, power was transmitted from Nizamsagar to Hyderabad. Later Nizam sagar area has become a load centre due to extensive use of pump sets for agricultural purpose. Consequently power is being drawn from Hyderabad. The 33 kV bus at Nizamsagar SS is connected to four 33 kV feeders. In view of steep rise in load growth, the existing 66 kV feeders from Hyderabad to Nizamabad were found absolutely inadequate.

Examination of Existing 66 kV dc Towers

All the vital data related to the original designs of towers could be retrieved from the available documents.

The tower drawings and related technical details were thoroughly examined. The parameters adapted for design of existing 66 kV double circuit towers have been worked out.

Technical Details of Original 66 kV d c Line

The following are the technical details of the original 66 kV d c line before conversion to 132 kV operations.

Length of the line	:	103 km
Normal span	:	280 m

Height of bottom cross-arm of normal suspension tower	:	13.792 m
Height of bottom cross-arm of normal angle tower	:	12.496 m
Vertical spacing between cross-arms of suspension tower	:	3.00 m
Vertical spacing between cross-arms of tension tower	:	2.40 m
Conductor	:	30+7/2.59 mm WOLF ACSR
Ground wire	:	No ground wire
Max sag of conductor at 600 C and still air	:	5.486 m
No. of disc insulators in suspension string	:	4
No. of insulators used in tension string	:	5

It is observed that the original 66 kV dc line though erected as early as mid fifties, the towers and the conductors are in fairly good condition.

Methodology Adapted for Upgradation

• Wolf ACCR conductor already strung on existing 66 kV double circuit line was used after repairs/ replacement of damaged conductor.

• Metal cross arms of suspension towers were replaced by insulator cross-arms. Solid core insulators were used.

• The spacing of insulated cross-arms for suspension towers were calculated to meet the requirements of 132 kV line. The insulated cross arms were fixed to the towers accordingly by providing suitable adapters.

• The conductors were fixed to cross arms using suspension clamps.

• The ground clearance from the bottom cross arm suspension point was found adequate for 132 kV line as existing 66 kV double circuit towers were liberally designed and there was no need to increase the height of towers.

• The metal cross-arms of angle towers were re used.

• The spacing of cross-arms of angle towers were calculated as per the requirement of 132 kV lines. These metal cross-arms were fixed to the angle towers by providing suitable clamps.

• The tension insulators strings were fixed to the towers and conductors clamped. However jumpers were fixed horizontally using solid core insulators so as to get adequate metal parts clearance of jumpers.

• The creep-age distances of string insulators and solid core insulators were found to be 2628 mm and 2850 mm, respectively against 2200 mm required for 132 kV lines.

Changes Made to Operate at 132 kV

The cross arms of the suspension towers were dismantled and insulated cross arms were fixed to the towers. For this purpose long rod insulators and disc insulators are used as shown in the Figure1. Special attachments were provided on the towers to hold the long rod insulators which were again held in the upright position by insulator strings consisting disc insulators.

The total creep-age distances of string is 2628 mm. The total creep-age distance of long rod insulator is 2850 mm. The suspension clamps were fixed to these insulated cross arms as shown in the Figure 1. There is no swing of the conductor.

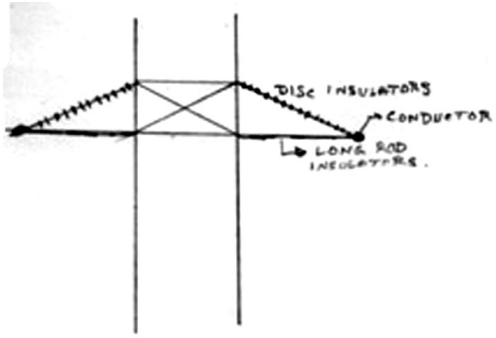

Figure 1 : Arrangement for 132 kV double circuit suspension tower

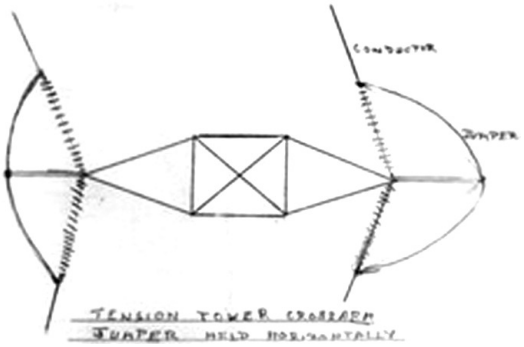

Figure 2 : Crossarm arrangement for 132 kV angle tower

This arrangement facilitated adequate ground clearance as well as metal parts clearances. The picture indicating the above arrangement is given in Figure 3 of Annexure 1.

The cross arms of the angle towers were retained. The tension insulators each consisting of 10 discs were assembled as in the case of conventional towers as shown in the Figure 2. The picture of the above arrangement is given in Figure 4 of Annexure 2.

New 132 kV / 33 kV Sub-Station at Nizamsagar

The new 132kV / 33kV sub-station at Nizamsagar has two 132 kV feeders towards Hyderabad. On 33 kV bus the existing four feeders are retained and two additional 33 kV feeders are also provided.

The 132 kV dc line to Hyderabad (the upgradedbn line) is now connected to the new 132 kV / 33 kV sub-station at Gummadidala and Kowdikpalli by loop in and loop out arrangement. The connected 132 kV line is already fully loaded as the two 132kV circuits are together transmitting over 100 MW. The three 132 kV / 33 kV sub-stations and 132 kV connected dc lines are all working satisfactorily ever since the upgraded 132 kV double circuit line has been commissioned in April 1991.

Performance of Upgraded 132 kV dc Lines

The connected 132 kV dc line was constructed in April 1991. Three 132 kV/33 kV sub-stations were connected to this line subsequently as per priorities. The performance of the line has been satisfactory. The electrical clearances actually obtained and those specified are indicated in Table 1.

Economics of Conversion Project

The estimate cost of a new 132 kV dc line 103 kV long is Rs 580 lakhs as existing in 1991. This estimate cost was exclusive of cost of implementing statutory conditions/clearances. The actual cost of execution of the project including cost of additional materials is Rs 107 lakhs, exclusive of cost of statutory clearance/ implementation.

Statement of Actual Costs Incurred

Insulated cross arms Solid core insulator Attachments to the towers and additional hardware	:	Rs. 67.10 lakhs
Cost of dismantling of conductor, insulators, hardware, fixing of insulated cross arms, solid core insulators, hardware, fixing of clamps and restringing of conductors.	:	Rs. 25.62 lakhs
Payment made to Dept. of Telecommunications for re-engineering of the telecom network.	:	Rs. 36 lakhs
Miscellaneous and Administrative expenses	:	Rs. 14 lakhs
Total actual expenditure *		Rs. 142.72 lakhs

*Total amount is exclusive of credits for the materials replaced / discarded.

Implementation of Up-gradation using HTLS Conductor and SRC Insulators

• High temperature low sag (HTLS) conductors, now available in the market have unique characteristics which can be explored and adapted for up-gradation of EHV transmission lines. For example, up-gradation of 132 kV line for operation at 220 kV may be considered.

Table 1: Clearances provided for the upgraded 132 kV line

Description	Clearance Provided	Std Clearance IS-5613/1976	Remarks
Bottom conductor to ground clearance.			
For suspension tower	7.70 m	6.1 m	Clearance is adequate
For tension tower	6.49 m	6.1 m	Clearance is adequate
Conductor to metal part clearance			
I) Suspension	1.742 m	1.530 m	Clearance is adequate
ii) Tension	2.320 m	1.530 m	Clearance is adequate
Minimum phase to phase vertical clearance Jumpers for angle towers are arranged in the horizontal plane with respect to the cross arms	3.70 m	3.70 m	Clearance is adequate

• Use of HTLS conductor also called 'aluminum conductor composite core' and SRC (silicon rubber composite) insulators can be considered for the up-gradation of EHV transmission lines.

• Maximum sag of HTLS conductor at high temperature, nil wind, 320m span works out about 6 m against 6.6 m of existing 132 kV lines strung with Panther ACSR. The current carrying capacity is about 800 A against 480 A of existing 132 kV lines with Panther ACSR.

• The low sag helps to get necessary ground clearance with minimum modifications to the tower. Vertical spacing of conductors are to be ensured if necessary making modification to the cage of the tower.

• The H.T.L.S conductor only weighs about 70% of Panther ACSR. Thus the vertical load on the tower due to conductor is low.

• The maximum tension in the conductor at 5°C and ¾ the full wind load or at 32°C and full wind is less than 3000 kg where as the tower is designed for maximum conductor tension of about 3800 kgs.

• The coefficient of thermal expansion (a) is very low as the conductor core is made of a composite material with different characteristics.

Table 2 : Parameters for design of 132 kV suspension tower

Description	Parameters Adopted for existing 132kV dc lines (Panther ACSR)		Parameters recommended for conversion to 220 kV operation with HTLS conductor	
	Suspension	Tension	Suspension	Tension
Height of Bottom cross-arm above ground level	14m	12.5m	14m	14 m
Vert. spacing of cross arm	5.2 m	4.0 m	5.1m	Insulated 5.1 m cross- arm
Suspension string length	1.6	1.800 m	Insulatd cross arm	S.R.C insulators
Maximum design tension at 32° and ¾ of full wind	3800 kg	3000 kg		
Tension at maximum temperature still wind	1900 kg	2000 kg		
Maximum sag	6.6 m	6.0 m		
Ground clearance	6.1	7 m		
Current carrying capacity	480 A	800 A plus		
Weight of conductor	976 kg	750 kg		

• The important parameters adapted for design of 132 kV towers with panther ACSR conductor and those to be considered for stringing HTLS conductor for conversion to 220 kV operation are indicated in Table 2.

The following points may be noted from Table 2.

• Body and cage portion of 132 kV suspension tower needs a few modifications. G W peak may need some change to ensure a shield angle of 30°. The horizontal clearance of power conductors have to be checked up and necessary modification has to be made.

• As regards tension tower, the height of bottom cross arm above ground is required to be 14 m against the existing height of 12.5 m the cage portion needs to be lifted by about 2 m. After a review of design calculations, the changes can be implemented by providing necessary reinforcement.

• The horizontal spacing of power conductors at all the three levels of cross arms have to be checked up and necessary clearances are to be provided.

• The additional forces on the angle tower due to increase of tower height have to be checked up vis-à-vis reduction in loads due to lesser tensions and lesser weight of conductors.

Conclusion

The upgradation of 66 kV dc line for 132 kV operation was cost effective and facilitated most efficient utilization of available corridor. This project amply demonstrated that by proper planning of works and timely procurement of materials, it is possible to upgrade the line of about 100 km. long within 3 to 6 months. With the successful conversion of the 66 kV line for 132 kV operation, it is worth while also to consider taking up conversion of 132 kV dc lines for 220 kV operation and conversion of 220 kV lines for 400 kV operation utilizing latest developed materials like HTLS conductor and SRC insulators. This would save the additional corridor, time and money and would facilitate quick realization of benefits of upgraded transmission lines.

Annexure : 1

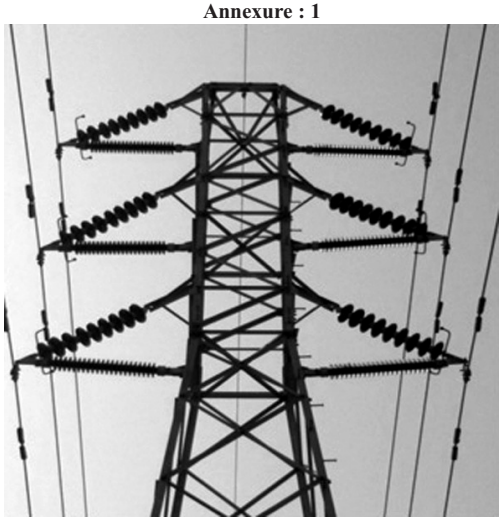

Figure 3 : 132 kV double circuit (converted) suspension tower

Annexure : 2

Figure 4 : Crossarm arrangement for 132 kV angle tower (converted)

Performance Evaluation of 5MW Grid Connected Solar Photovoltaic Power Plant Established in A & N Islands

Abhishek Gupta
Department of Electrical Engineering,
Dr.B.R.Ambedkar Institute of Technology,
Port Blair, Andaman and Nicobar Islands
E-mail : abhishekgspn@gmail.com

Abstract

India is located in the equatorial sun belt of the earth, thereby receiving abundant radiant energy from the sun. The India Meteorological Department (IMD) maintains a nationwide network of radiation stations which measure solar radiation and also the daily duration of sunshine. In most parts of India, clear sunny weather is experienced 250 to 300 days a year. The annual global radiation varies from 1600 kWh/sq m to 2200 kWh/sq m. The equivalent energy potential is about 6,000 million GWh of energy per year. In this paper, the grid connected solar photovoltaic power plant established by Electricity Department, Andaman and Nicobar Islands, is presented, and its performance is evaluated.

Keywords : *Solar photovoltaic; Mobile solar; Rainy climate; Isolated communities; Stand alone*

Introduction

As a part of green initiatives the Electricity Department Andaman and Nicobar Islands (A&N) has installed a commission of 5 MW solar photovoltaic (SPV) power plant in collaboration with National Thermal Power Corporation (NTPC) at Garacharma, Port Blair. The power plant is connected to 33 kV grid supply. Purpose of the project is to generate clean energy without emission of CO_2 and supply to grid. Being Islands the eco system and environment is very sensitive. The power generation emits pollutant gases which is one of the environment air pollution. The power generation in A and N Islands is mainly by diesel power plants. The cost of generation per unit at present is around Rs. 26/- which is very high. As a global policy all the countries in the world are focusing on harvesting energy from renewable sources of energy. The Union Teritory Administration of Andaman Nicobar Islands is also in the line of global policy promoting renewable energy sources like bio-mass, wind and solar power.

The 5 MW solar power plants, Garacharma, has been commissioned nearly one and a half years back to contribute green power in the grid. It is very necessary to examine the performance of any plant from engineering point of view so that necessary improvement and corrections can be made in the system. The findings of the performance in this paper will help the planners of the Islands to rightly choose the renewable energy sources and design hybrid system in efficient way.

Brief Details about the SPV Plant Garacharma

The technical details of 5 MW SPV plant, Garacharma, Andaman and Nicobar Islands has been shown in Table 1.

Construction of Solar Cell

- They are constructed by layering special materials called semiconductors into thin, flat sandwiches.
- These are linked by electrical wires and arranged on a panel of a stiff, non-conducting material, such as, glass. The panel itself is called a module.
- Modules are then interconnected, in series or

parallel, or both, to create an array with the desired peak dc voltage and current.

Working of Solar Cells

- The junction of dissimilar materials (n and p type silicon) creates a voltage.
- Energy from sunlight knocks out electrons, creating a electron and a hole in the junction.
- Connecting both sides to an external circuit causes current to flow.
- In essence, sunlight on a solar cell creates a small battery with voltages typically 0.5 V dc.
- Function 1: Photo generation of charge carriers (electrons and holes) in a light absorbing material.
- Function 2: Separation of the charge carriers to a conductive medium, such as a metal contact or a wire in order to transmit the electricity.

It supplies a voltage and a current to a resistive load (light, battery, motor).

Power = Current × Voltage

Table 1 : Sample module specification

Make		Photon
Technology		Crystalline silicon
Nominal Power Pmax	Watts	235
No. of cells /module	No.s	60
Cell size	p.Sq.	156
Cell efficiency	%	13.5 to 15
Open ckt voltage Voc	Volts	36.3
Short ckt current Isc	Amps	8.42
Voltage at maximum power Vmp	Volts	29.6
Current at maximum power Imp	Amps	8.06
Temperature coefficient voltage Voc	mV/°K	-133.26
Temperature coefficient current Isc	mA/°K	+2.28
Temperature coefficient power	%/°K	-0.48456
NOCT of module	°C	43.8
Module FF	%	0.72 to 0.74
Module dimension		1660 × 990 × 42
Module area	m^2	1.64
No. of modules per structure	Nos	24
Module orientation on str. (LS/Prt)		LS
Bypass diodes	Nos. / Amps	3 / 15
Diode box (sealed / semi tr. / with cover)		
Connecting sleeve / securing sleeve		
Cables within module (size, length, Cu/Al.)		4 sq. mm, 0.9 mtr., 2 nos

Benefits of SPV Power Generation

- Saving environment from green house effects.
- System is eco-friendly.
- Reduce the pollution.
- Reduce the conventional fuel consumption.
- Silent operation.

Annual Month Wise Generation

Annual month wise generation has been tabulated in the Table 2. The same data as bar diagram has been shown in Figure 1. From the bar diagram it is clear that the maximum generation is in the month of March and least generation is in the month of July. If we see the generation in ascending order month wise the trend is as follows:

July-September-June-November-December-October-August-April-February-January-March.

Monthly Peak Generation

The monthly peak generation has been shown as bar diagram in Figure 2. The maximum peak generation of the period was observed on 18th November 2013 and the minimum peak generation was observed on 18th November 2013. The peak generation of most of the month are more than 5 MW the installed capacity. From this it is clear that the SPV Plant is capable of generating power to its maximum capacity.

Table 2 : Annual monthwise power generation

Month	Average Generation, kWh	Total Generation, kWh
August (2013)	19403.45161	601507
September	15551.83333	466555
October	18918.35484	586469
November	18400.63333	552019
December	18823.77419	583537
January (2014)	24283.03226	752774
February	26389.82143	738915
March	27221.63226	843852
April	21796.26667	653888
May	17988.54839	557645
June	18174.56667	545237
July	14058.45161	435812

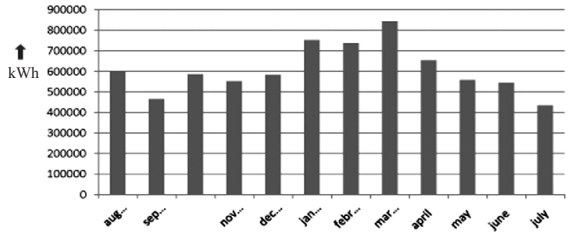

Figure 1 : Monthwise generation from August 2013 to July 2014

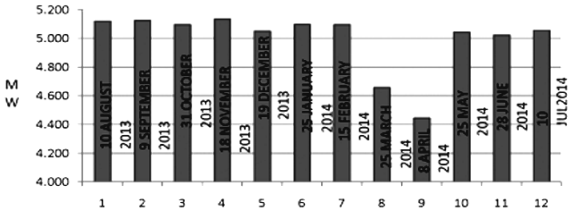

Figure 2 : Bar diagram for monthly maximum peak generation

Net Energy Export

The energy exported during the period from July 2013- August 2014 has been shown as bar diagram in Figure 3. The maximum energy export is during March month where as minimum energy export is during July. Total energy exported during 12th month 7152785 kwh.

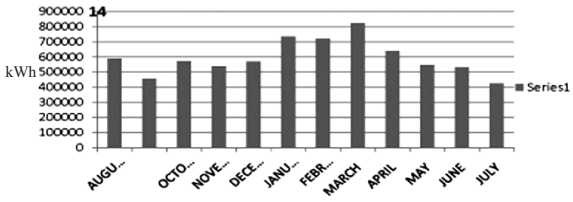

Figure 3 : Net energy export monthwise from August 2013 to July 2014

Special Data for Different Weather Condition

Special data for whole day were taken for a rainy day, a cloudy day and a sunny day for the month of August 2014. The graphs of power generation for these three days have been shown in Figures 4, 5 and 6, respectively. In rainy day generation is less and irregular. In cloudy day the generation is less but variations are less. On a sunny day the generation is more but sudden fall in generation by SPV plant due to clouds affect the stability of diesel power plants running in parallel.

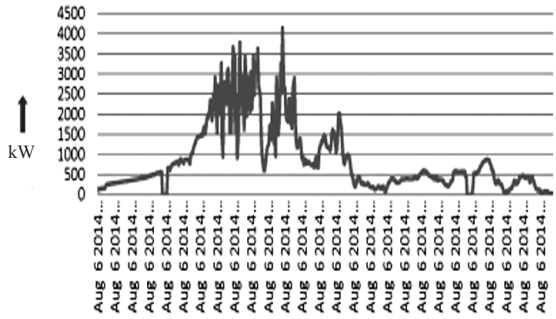

Figure 4 : Load on 6th August from 6-10 am to 3-20 pm

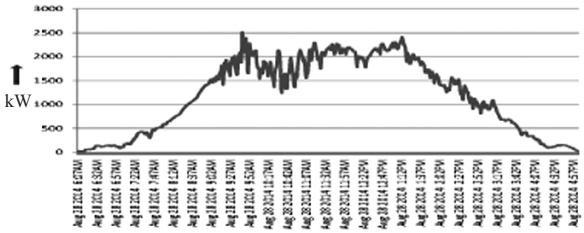

Figure 5 : Load on 28th August from 6-07 am to 4-53 pm

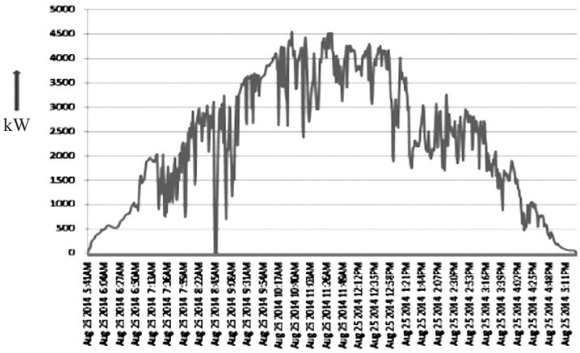

Figure 6 : Load on 25th August 2014 from 5-41 am to 5-21 pm

Monthly Average Irradiance

The monthly average irradiance for the period Aug.2013 to July 2014 for the plant area has been shown in Table 3. The same data has been represented in Figure 7 as bar diagram. From the Figure it is evident that maximum irradiance is in May and minimum is in October.

Monthly Average Insolation

The monthly average insolation for the period August 2013 to July 2014 for the plant area has been shown in Table 4. The same data has been represented in Figure 8 as bar diagram. From the figure it is evident that max. insolation is in November month and minimum is in July.

Table 3 : Monthly average irradiance for the period from August 2013 to July 2014

Month (2013-2014)	Monthly Average Irradiance, w/m^2
August	996.12
September	850.64
October	738.42
November	988.45
December	958.00
January	1034.96
February	1091.03
March	1035.80
April	1076.03
May	1104.87
June	1027.80
July	969.19

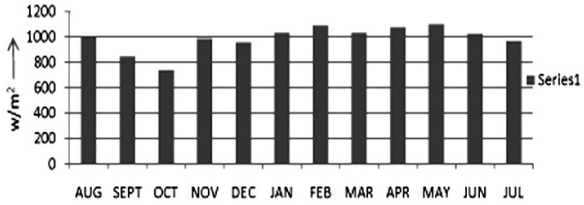

Figure 7 : Monthly average irradiance (2013-2014)

Energy Production and Number of Days in Percentage

The installed capacity of Garacharama SPV Power Plant is 5MW. If the generation curve of a day is seen, practically rated solar power is assumed available for 5 hrs in a day. Hence, for 100% efficiency a 5 MW plant can produce maximum 25000 kWh. The details of generation is tabulated in Table 5.

Table 4 : Monthly average insolation for the period from August 2013 to July 2014

Month (2013-2014)	Monthly Average Insolation, $kWh/m^2/day$
August	4.77
September	3.78
October	3.94
November	35.85
December	5.21
January	5.08
February	5.79
March	6.77
April	5.46
May	4.41
June	4.32
July	3.64

Table 5 : Energy production

Generation (MWH)		No. of days energy produced												Total Days	Days in%
Range	%	Aug	Sept	Oct	Nov	Dec	Jan	Feb	Mar	Apr	May	Jun	Jul		
0-5	0-20	31	30	31	29	28	31	28	31	30	31	30	31	361	98.9
5-10	**20-40**	31	30	30	28	27	31	28	31	30	30	29	28	353	**96.7**
10-15	40-60	30	23	28	27	26	31	28	31	30	29	26	22	331	90.6
15-20	60-80	26	18	25	24	24	28	28	30	27	23	20	13	286	78.3
20-25	**80-100**	13	10	18	16	14	27	27	30	21	16	17	5	214	**58.6**
25+	**100+**	4	1	3	4	8	17	17	24	8	3	3	0	92	**25.2**

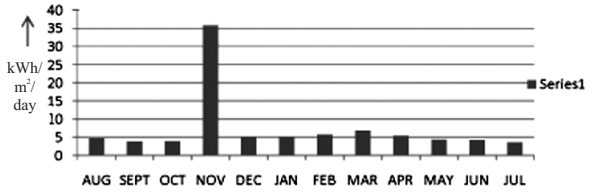

Figure 8 : Monthly average insolation (2013-2014)

From data it is clear that nearly on 25% of the days in an year the plant operates at 100 %. Nearly 58% of the days plant operates at the efficiencies from 80%-100%. Nearly 96% of the days the plant operates below 40% efficiency.

Net Energy Imported

The net energy imported during the period August 13-July 14 is 53416 kWh used as station auxiliary.

Diesel Saving per Annum

Energy exported during one year period = 7152785 Units

Market cost of HSD = Rs 54

SFC of the Govt Power Plant = 0.278 l/unit

Generation unit /l = 3.59 = 3.6

Diesel saved for production of 7152785 units= 1986884.72 =19868851

Cost of the diesel saved/annum in Rs= 1986885×54 = Rs 10,72,91,790

Say Rs. 10,72,92,000 per/annum

Saving as per Actual Cost of Generation

Actual cost of generation per unit= Rs 26.00

Energy exported during one year period = 7152785 units

Total cost of energy produce by SPV Plant in terms of diesel generation = 7152785×26

= Rs18, 59,72,410

Say Rs = 18,60,00,000 per annum

Recovery Time of Plant Cost

The cost of the plant when installed was Rs 12,00,00,000 (12 crore) per MW

Total cost of 5MW Plant at the time of installation = Rs 60,00,00,000

Recovery time as per total cost of energy produce by SPV Plant in terms of diesel generation = 60,00,00,000/ 18,60,00,000 = 3.22 years, say four years. Considering other factors could be 5 years.

Conclusion

In this report be have tried to give an over all view of 5MW power plant. The plant is just nearly one and half year old. It is taken operational data of one year ie, from August 2013 to July 2014.

In the data analysis one has analysed the following parameters:

1. Daily generation for twelve month.
2. Monthly generation.
3. Monthly peak generation.
4. Net energy export.
5. Sample daily generation on rainy, cloudy and sunny day.
6. Monthly average irradiance.
7. Monthly average insolation.
8. Net energy imported.
9. Diesel saving per annum.
10. Saving as per actual cost of generation.
11. Recovery time of plant cost.

From data analysis of power generation of one year duration it is clear that the plant has successfully operated for the whole year and exported 7152785 units from August 2013 to July 2014 to the grid.

If it is seen from saving in diesel point of view the saving in diesels was 1986885 liters for the above mention period.If we see from cost of actual per unit of electrical energy the saving is Rs 15, 02, 10,000 per annum. From above one can say that the power generation by SPV is eco-friendly and cost effective. It will be more popular and acceptable in future as the cost of SPV plants are slashing down.

References

1. Souvik Ganguli and Sunanda Sinha, 'A Study and Estimation of Grid Quality Solar Photovoltaic Power Generation, Potential in Some Districts of West Bengal Patiala, pg 522-528, October 29-30, 2009.

2. A. S. Elhodeiby, H.M.B. Metwally and M.A. Farahat, 'Performance Analysis of 3.6 kW Rooftop Grid Connected Photovoltaic System Egypt, International Conference on Energy Systems and Technologies, Cairo, Egypt, ICEST, March 11-14, 2011.

Land Constraint is Biggest Problem of Conventional SPV Method – Here is a Perfect Solution by the Design and Development of an Innovative 'Solar Power Tree'

S. N. Maity
Technology Innovation Centre,
CSIR-Central Mechanical Engineering Research Institute,
Durgapur, India
E-mail : drsnmaity1959@gmail.com

Abstract

Energy and pollution are the present burning questions. So, there is an impending demand of an alternative green power. Solar, as believed, is the only major alternative in comparison to other sources of available renewable energies. For absorbing the sun solid silicon-crystalline photo-voltaic (SPV) method is the best. SPV panels are laid on structures at tilt angle. SPV is a land consuming system. Scarcity of land is the greatest crisis of the earth. Solar Power Tree is invented for installing PV-modules on a tall pole-like structure with branch- like panels and takes only 1% of land than conventional SPV layout.

Introduction

There is a big hue and cry over energy crisis from all over the world mainly for two reasons, firstly the natural resources are going to be exhausted very soon and the other is whether we should continue with the available natural resources of carbonaceous compound which is posing threat of greenhouse gas effect to human being every day. People are trying over different sources to find out non conventional energies, mainly some sort of renewable source of energy or the green energy like solar power, wind power, tidal power, hydro power etc. Power from sun, as it is thought today, is the only major alternative in comparison to other sources of renewable energies presently being tried to replace the conventional source of fossil fuel like coal, gas, oil etc.

Then how to tap the power of sun to be absorbed for our purpose? There are many ways being devised time to time for absorbing the sun rays coming towards the surface of earth, but most efficient and easily available is the solid silicon crystalline photo voltaic (PV) module form till date. There are other forms like amorphous or thin film etc. But efficient most is the solid crystalline PV cells for direct absorption of sun light. The other methods of sun absorption like reflection, concentration, water heating etc. are the costly and complicated and efficiency is also less compared to PV modules.

One need to erect the PV panels under the sun so that the surface of panel gets the maximum sun of the day being laid at an angle. Today the general method is that hut like inclined structures are made over the land surface to hold the solar panels. Now for an example, the generation of 2 MW power from PV module system requires the land of 10 acres approx. for housing the panels only. But land is going to be the greatest crisis of the earth rather it is already a burning crisis in most of the countries. The cultivable land which is going to be the costliest commodity in the near future, if used for other than agriculture, it will be uncountable loss. Our many national projects are facing the severe problem of acquisition of land. Therefore if land area is used for capturing the solar power it

would never be cost effective and viable for the human society.

Therefore there is a need for devising a method and fabricating a suitable device so that the solar power can be absorbed without occupying much surface area, rather utilizing the minimum amount of land and the electricity must be economically viable.

Here comes the idea of a Solar Power Tree a new invention of installing PV modules on a tall pole like structure with leaf like branches surrounding it following a pattern of spiralling phyllotaxy as found in a natural tree. It would take only 1% of land area in comparison to general PV-housing layout as being practiced at present. As example, it requires 0.2090 m^2 basements for 2.5 kWh PV power, whereas by present general method of housing the PV arrays a land of 20.90 m^2 is necessary for layout. It has so many other advantages to be discussed in this paper.

General Methodology

In our country the solar power generation system are generally being designed by this type of solid crystalline (PV) in different places. One needs to erect the PV panels under the sun so that the surface of panel gets the maximum sun of the day being laid at an angle. The very common application of solar panel is that a poll of small height having one or two panels clamped on its top with a single or couple of lights (stand alone) fixed below to enlighten the roads etc. For more power in kilowatts it is required to have suitable structure over the landed area in an open space to hold the solar panels. Therefore hut like permanent fixed structure are made (Figure 1) to lay the PV panel over them. Now for an example for the generation of 1MW power from PV module system i.e, conventional inclined hut like structures (Figure 2) requires the land surface of 5 acres to 6 acres approximately for housing the panels only. But land is going to be the greatest crisis of the earth rather it is already a burning crisis in most of the

(a) (b)

Figure 1 (a &b) : Conventional SPV solar plants, India

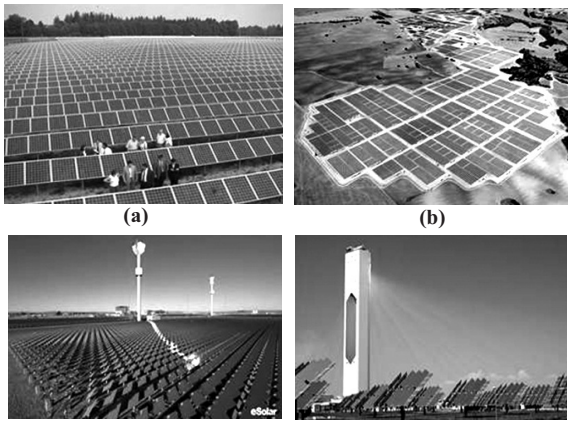

(a) (b)

© (d)

Figure 2 (a,b,c,d) : Conventional solar plants (other countries)

countries. One can find there are news of fights frequently between the farmers and the administration for acquisition of land for any industrial purposes. Again most of the agricultural areas are generally away from the conventional power plants and are in need of electricity. But again if you cover the agricultural land for laying solar panels then how cultivation would be possible? The cultivable land if used for other than agriculture it would be uncountable loss. And thus many national projects are facing the severe problem of acquisition of land. Therefore if vast land is used for capturing the solar power it would never be cost effective and viable for the human society.

Need for New Invention

Therefore there is a need for devising a method and fabricating a suitable device so that the solar power can be absorbed without occupying much surface area or land which is going to be the costliest commodity in the near future. Rather, the device and method should be such that it would be

utilizing the minimum land for maximum solar power absorption by creating maximum solar surface and it was only possible by devising a holding system of PV modules with a vertical pole standing on the ground and holding the PV panels at a height.

Here comes the idea of a device of installing a tall metallic pole of 15.24 m to 21.33 m height founded on a basement of (0.609 × 0.609) m^2 area, which will hold all the required panels on its body like a tree (Figures 2b, 2c, 2d). The surface land therefore is used only a maximum of 0.372 m^2 to 0.464 m^2. Of course, it needs some base foundation for holding the taller pole but most of the foundation work will be below the ground surface.

Land constraint is not only a problem of our country it is a common problem for many countries of the earth.

Uniqueness and Advantages of Solar Power Tree

The uniqueness of this single pole/solar power tree system is that the solar PV modules will be fixed throughout the tall pole following a pattern of spiralling phyllotaxy with due adjustment of load distribution over the pillar for its balancing. At the same the pattern is so maintained that the top panels wouldn't obstruct the bottom ones and each panel of the tree would get the maximum sun in a day time.

Figure 3 : Prototype of solar power tree (tall 9.144 m) capacity 2.5 kWh (max)

The other uniqueness is that all the Solar Panels will be hanging through their connecting stem-system attached with the main trunk (Pole) and may be made flexible in all direction so that they can best avoid the wind pressure due to heavy storm affecting over the main pole/trunk. The leaves (panels) would preferably be spring loaded and the Joints of stems would be flexible. The panels will be naturally facing towards the sun at an angle as required so that they can fix up maximum solar energy in a day time.

The advantages of this system is that it takes about 1% of land area in comparison to general PV housing layout, as example it requires 0.5 m^2 basement for 2.2 kWh PV power (Figure 8) whereas for the same solar power by present general method of housing the PV arrays, a land of 50 m^2 is necessary for layout.

The other advantage is that this system does not require the acquired big landed property at a single place, rather for this type of solar power generation the Road sides, the islands in between wide roads / highways, the boundary walls of paddy lands, the crossings of boundary walls etc. can be used.

Another advantage is that even if the divider walls of paddy land are used for solar power tree plantation, the shadow being created by the panels would not touch the land in most of the cases (as the solar power trees would be very tall) and even if it touches, it will not cover the surrounding field by its penumbra so that growth of plants would be restricted.

The unique advantage is that because of pattern of laying of panels following phylotaxy of natural trees and using the small size panels, the shadows

coming from the panels of upper level do not interfere with the lower panels in most of the daytime. If sometimes they obstruct the lower ones that cover only very small percentage of panel area and for a little while only.

The dust deposition on the panels is a big problem for such type of solar power generation. Generally, as the panels of SPT are placed at higher height they are less subject to dust deposition. Again as the SPT structure is like a pagoda tree and an arrangement of water spraying from the top of the tree could make the panels clean if it works for a few minutes in the morning every day.

There is a big advantage in laying of panels inherited in this device of SPT that all the panels can be laid in east–west direction, unlike the general fixed hut like structure where they are laid in south–north direction in general. An easy method can be devised with this SPT so that all the panels can be tilted around an angle of 45° as to get the maximum sun for whole the day. Instead of sophisticated electro-automated device, a simple mechanical device of pulling a rope can tilt all the panels from east –west to west–east direction to get the maximum sun path in a day quite economically.

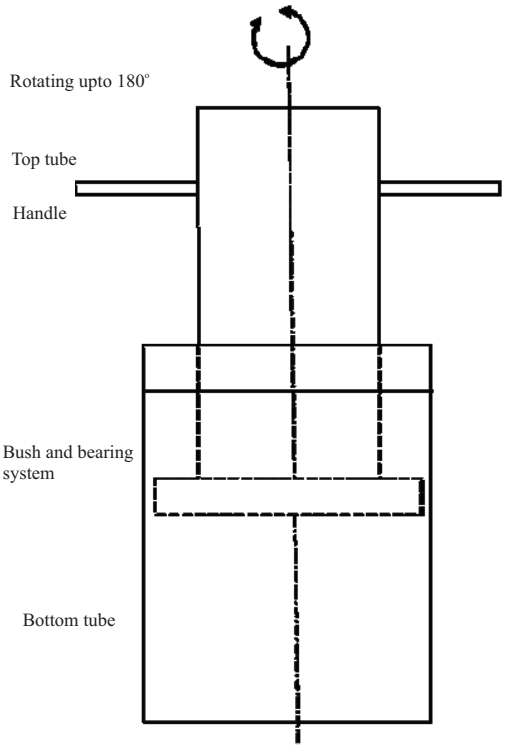

Figure 4 : Swivelling system of solar power tree

Figure 5 : Solar power tree at night

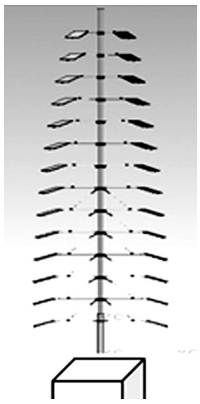

Figure 6 : Proposed SPV for 5 solar power tree kWh

Figure 4 shows the swivelling system of solar power tree. The picture of the solar power tree working at night is shown in Figure 5.

Example

Detailed Technical Specification (Fabrication, Installation and Commissioning of Solar Power Tree)

This is a collection of 26 nos solar PV panels,

which is mounted on a single tall pole with the help of suitable supporting arrangement. Total power generation is 1000 Wh at peak hour on a clear sunny day.

- The arrangement maintains a phyllotaxy pattern.
- The electricity so produced being stored in a battery bank of suitable capacity
- The battery bank being protected from overcharging by Auto Cut-off
- The Battery bank is also attached with alternative charging system from 230V ac power
- A multiple lighting arrangement is provided for spending the accumulated solar energy
- Power supply to the lighting arrangement from battery bank with suitable timer/ manual switch.

Mechanical System

Figure 6 shows the general arrangement of the PV panels, panel supports and the pole. Altogether 26 nos of panels are arranged in a phyllotaxy pattern.

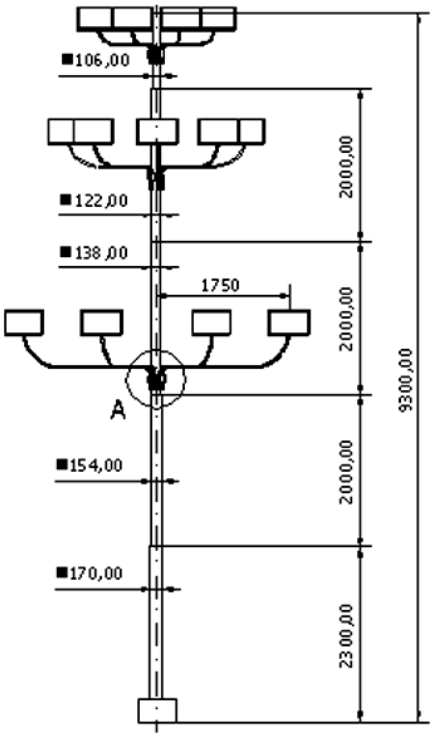

Figure 7 : Assembly to be anchored at the site of erection

The dimensions are tentative and may be deviated if required according to height of the pole. After erection the whole assembly is to be painted to prevent from corrosion.

The whole assembly as shown in Figure 7 is to be anchored and grouted firmly at the site of erection.

Electrical System

The schematic diagram of the electrical system is shown in Figure 8.

Civil Works

The pole and battery bank arrangements are shown in Figure 9 and Figure 10 respectively.

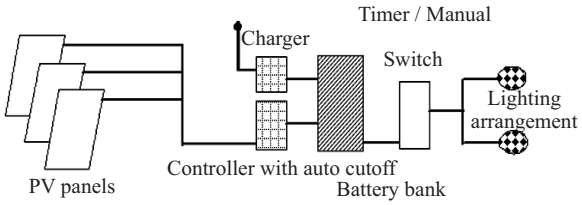

Figure 8 : Schematic diagram of electrical system

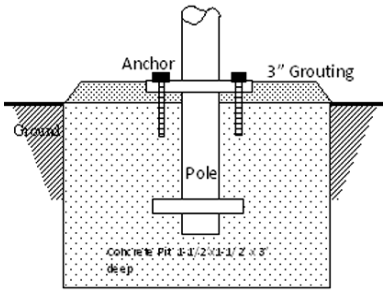

Figure 9 : Foundation of pole

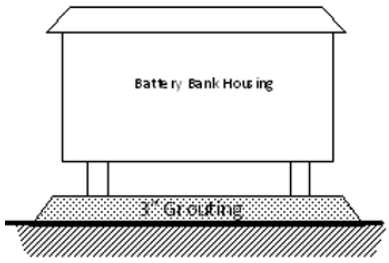

Figure 10 : Foundation of battery bank

Bill of Material

Detailed Description	*Quantity*
Pole with supporting arrangements (Figure 11)	1 no.
Solar PV panel	26 nos

Controller and charging system (Figure 12)	1 set
Additional charging system from 230 V ac electric power line	1 no
Battery bank of suitable capacity	1 set
Weather proof metallic battery housing with grouting at site	1 no
Cut off system for excess power capture	1 no
High efficiency LED light module with mounting and glass covering	2 nos
Timer/manual switching system for lighting	1 no
Concealed weather proof cable routing	1 set
Erection and associated civil work including Anchor, pit and grouting	1 set
Anti-corrosion painting of the total assembly	1 set

Data Collection

Table 1 shows the variation and comparison of controller current between standard 40 W panels fixed with an inclined hut like structure on the ground and similar type panels attached with the solar power tree under the invention at a height.

The graphical plot for the above data set is shown in Figures 13, 14 and 15.

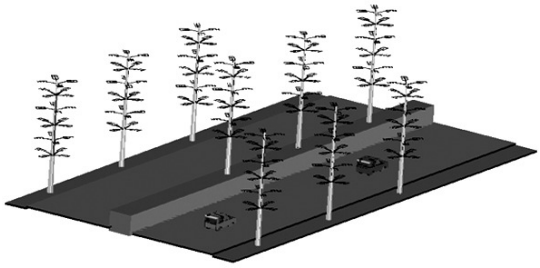

Figure 11 : Proposed plantation of solar power trees on highway sides

Table 1 : Solar data collection

Date	24.07.11		25.07.11		27.07.11	
Panel	Standard Layout	Solar Power Tree	Standard Layout	Solar Power Tree	Standard Layout	Solar Power Tree
Time	A	A	A	A	A	A
11:30 am	4.96	4.4	4	4.70	3.88	4.16
11:45 am	4.26	4.14	3.92	4.47	2.76	4.31
12:00 pm	2.24	3.78	3.92	4.59	2.72	4.12
12:15 pm	2.08	3.5	3.12	3.71	2.8	4.22
12:30 pm	1.84	2.1	3.76	3.57	2.56	3.58
12:45 pm	3.32	3.98	3.76	4.70	2.16	4.45
1:00 pm	3.20	3.3	3.68	3.96	2	3.43
1:15 pm	3.20	3.42	3.92	4.79	1.04	2.92
1:30 pm	2.32	2.94	3.72	3.06	0.8	1.68
2:15 pm	2.96	3.50	3.64	4.16	3.56	3.67
2:30 pm	3.24	4.25	3.6	4.48	3.88	5.20
2:45 pm	3.64	4.36	3.6	4.10	2.4	4.40
3:00 pm	1.88	1.86	3.24	4.15	2.04	4.69
3:15 pm	1.44	2.07	2.88	3.54	2.08	3.78
3:30 pm	1.80	2.56	3.12	2.82	2.56	3.33
3:45 pm	1.20	2.33	2.56	3.36	2.56	3.32
4:00 pm	1.32	2.35	2.48	2.77	2.44	2.94
4:15 pm	1.12	2.27	2.64	3.16	2.42	2.80
4:30 pm	0.68	1.89	1.12	2.32	2.4	2.07
4:45 pm	0.54	1.65	0.8	1.65	2.08	2.33
5:00 pm	0.24	1.05	0.25	1.16	1.22	2.28
5:15 pm	0.20	1.00	0.12	1.04	0.88	2.08
5:30 pm	0.10	0.89	0.11	0.98	0.20	1.40
5:45 pm	0.11	0.88	0.09	0.10	0.22	1.50

Figure 12 : Solar power tree - a tall single trunk with multi-stage branches

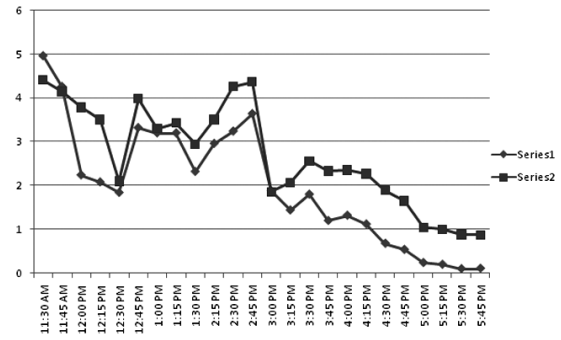

Figure 13 : Graphical presentation : comparison of output current between a panel of conventional low height structure (series 1) and a panel of solar power tree (series 2) at height on 24/07/2011

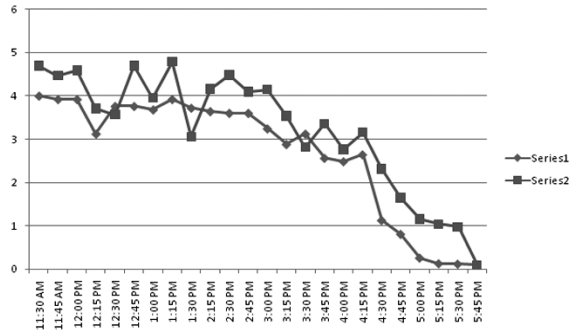

Figure 14 : Graphical presentation : comparison of output current between a panel of conventional low height structure (series1) and by a panel of solar power tree at height (series 2) on 25/07/2011.

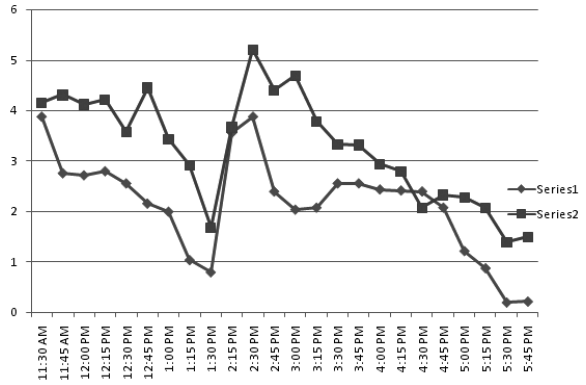

Figure 15 : Graphical presentation : comparison of output current by a panel on ground (series1) and by a panel of solar power tree at height (series 2) on 27/07/2011.

Conclusion

The solar power trees can be planted without any acquisition of vast land exclusively for this purpose in a particular place. They can be installed on the road sides as they consume around 0.371 m^2 of area for a single tree. The village roads and the big boundary walls of paddy lands can provide sufficient space for planting solar power trees that can supply enough power for electrification of villages and irrigation activities. The state and national highways are big sources for Solar Power Tree (SPT) plantations. Two sides of single road high ways and the three sides of double road highways including island in between can be utilised for solar power trees (Figure 11). A simple calculation shows that if the national highway is used for plantation of solar power trees from Kolkata to Asansol which is around 300 km in length it would be possible to produce 110 MW by installing solar power trees of 2 kW capacity through the road sides at a certain interval (say 15m between two trees). This would actually require 660 acres of land for the same power generation at a single place by the existing method of laying out solar panels in a conventional way i.e. over the roofs of low height fixed structures. Hopefully if this new method of SPT plantation is adopted widely it would be possible to produce

sufficient energy and to satisfy the demand of power for the world keeping the best ecological balance and preserving the nature as it is.

References

1. T. Markvart, 'Photovoltaic Solar Energy Conservation', Proceedings of Energy for Europe, Strassbourg, July 7- 14, 2002.

2. P. Baruch, 'A Two Level System as Photovoltaic Solar Cell', Journal of Applied Physics, vol 57, p 1347, 1985.

3. L. L. Bucciarelli, 'The Affect of Day to Day Correlation in Solar Radiation on the Probability of Loss of Power in a Stand-alone Photovoltaic Energy Systems'. Solar Energy, vol 36, p 11, 1986.

Performance Evaluation of Grid Connected DFIG based Wind Energy System under Unbalance Voltage Condition with Dual Sliding Mode Control

K.G.Sharma
Department of Electrical Engineering,
Government Engineering College,
Ajmer, Rajasthan

Kiran Gajrani
GE Utility Electric Supply,
Military Engineering Services,
Delhi Cantonment, New Delhi
E-mail : gajrani.kiran17@gmail.com

Abstract

Wind energy is getting a considerable attention worldwide from the fraternity of the power system engineers as clean and green energy that can help reduce the carbon content and limit dependence on conventional fossil fuels. Doubly fed induction generator (DFIG) is the most commonly used variable speed turbine among the available wind energy conversion systems. Low voltage ride through (LVRT) ensures continuous connectivity of wind farm with the grid and early recovery in case of faults/disturbances. This is possible through proper operation and control. In this paper, sliding mode control (SMC), a variable structure control method is used to dampen the oscillations, arises due to unbalanced grid voltage conditions. The performance is also improved, as it results into symmetrical and sinusoidal grid current injections. The simulations have been carried out on 1.5 MW DFIG based wind turbine systems of MATLAB®/SIMULINK®. The results presented demonstrate that the proposed controlling method is able to dampen the torque, stator power, and currents ripples in comparison with the conventional vector control method.

Introduction

Wind energy is recognized as the most technically competent, economical, and environment friendly option among the available renewable energy sources. The expansion of wind energy sources is constantly increasing across the world to obtain pollution free environment. This growth is assisted by encouraging government guidelines and competitive market players, which leads to continuously increase of installed wind power capacity worldwide [1].

Wind energy is highly intermittent, unstable, and unpredictable in nature, which makes the modern electric grid more distributed, deregulated, dynamic, and complex. This poses new challenges for power system engineers when integrated to conventional electric grid. Stringent grid code and guidelines are developed to overcome the challenges and enforced across the utilities for reliable and stable power system operations. Grid code is nothing but a set of basic rules for operators and wind farm planners. It basically requires meeting the fault ride through (FRT) requirement and to maintain the grid voltage within permissible limits [2]. It emphasizes continuous connectivity of wind farm with the grid and early recovery in case of faults/disturbances. This can be achieved through proper operation and control.

Among the available wind generation technologies, doubly fed induction generator (DFIG) based variable speed wind turbines are accepted worldwide. As, it presents noticeable advantages like the variable speed generation to optimize the turbine speed at low wind speed, the vector control of active and reactive power based on proportional integral (PI) controllers, the reduction of mechanical stress and the use of a power converter with rated power only 25%-30% of total system power.

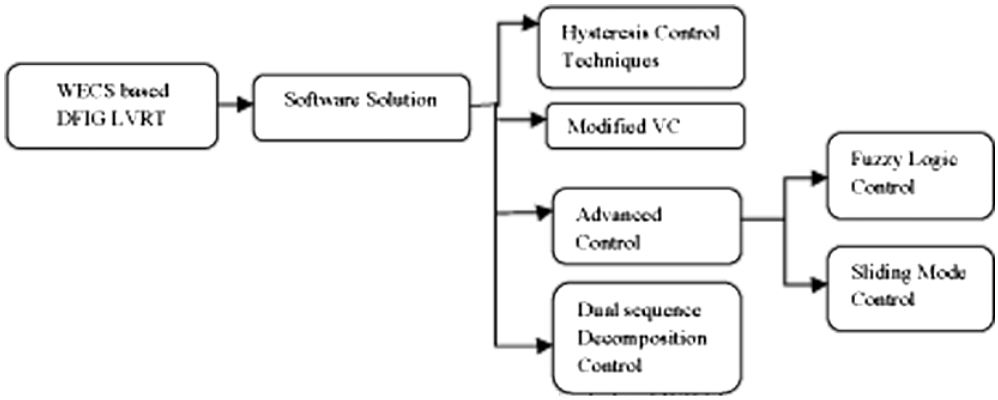

Figure 1 : LVRT controlling methods for DFIG based wind turbine

In DFIG connected wind energy system, a number of control methods based on fuzzy logic are presented under balanced grid voltage conditions [3]. In induction wind generators, unbalanced three-phase stator voltages cause a number of problems, such as over current, unbalanced currents, reactive power pulsations, and stress on the mechanical components from torque pulsations. The paper [4] presents a control strategy for DFIG based wind system, which enhances the speed and reactive power controllers under unbalanced grid voltages.

Under unbalanced grid voltage conditions, the dynamic performance of DFIG is adversely affected due to oscillations. The author [5] proposed a new vector proportional integral (VPI) controller to dampen the oscillations. This author [6] presents direct active and reactive power control of grid-connected DFIG-based wind turbine systems under unbalanced grid voltage condition. The controller reduces the power ripples but simultaneously odd order harmonics are generated, which increases the additional cost of filtering. In this paper, a low cost solution is presented using sliding mode control. This method is a nonlinear control method that alters the dynamics of a nonlinear system by application of a discontinuous control signal that forces the system to slide along a cross-section of the system's normal behaviour.

Overview of Low Voltage Ride through(LVRT) Solutions

In past years, wind turbines were designed to be disconnected from the grid in case of fault conditions, which resulted into uneconomical operation of wind turbines. Recent published research provides many software solutions, as depicted in Figure 1.

DFIG Mathematical Modeling

In recent years, several configurations are used for the dynamic model of DFIG systems, which can be shown in various reference frames, such as, stationary reference frame, or rotating reference frame. In this paper, DFIG is modeled in a rotating reference frame [7] under balanced and unbalanced operation conditions.

Balanced DFIG Model

Using the assumption of linear magnetic circuits, the stator and rotor voltage expressions of the DFIG based wind turbine as shown in Figure 2, under balanced operating condition are written as follows [8] :

$$V_r = \begin{pmatrix} v_{dr} \\ v_{qr} \end{pmatrix} = \begin{pmatrix} R_r i_{dr} + \dfrac{d\phi_{dr}}{dt} - (\omega_s - \omega)\phi_{qr} \\ R_r i_{qr} + \dfrac{d\phi_{qr}}{dt} + (\omega_s - \omega)\phi_{dr} \end{pmatrix} \quad (1)$$

$$V_s = \begin{pmatrix} v_{ds} \\ v_{qs} \end{pmatrix} = \begin{pmatrix} R_s i_{ds} + \dfrac{d\phi_{ds}}{dt} - \omega_s \phi_{qs} \\ R_s i_{qs} + \dfrac{d\phi_{qs}}{dt} + \omega_s \phi_{ds} \end{pmatrix} \quad (2)$$

Where i_{ds}, i_{qs}, i_{dr} and i_{qr} are, respectively, the direct and quadrature stator and rotor currents. R_S and R_r are stator and rotor resistances. ω_s, ω are stator and rotor electrical angular speed. The stator and rotor fluxes can be expressed as :

$$\phi_s = \begin{pmatrix} \phi_{ds} \\ \phi_{qs} \end{pmatrix} = \begin{pmatrix} L_s i_{ds} + M i_{dr} \\ L_s i_{qs} + M i_{qr} \end{pmatrix}$$
$$\phi_r = \begin{pmatrix} \phi_{dr} \\ \phi_{qr} \end{pmatrix} = \begin{pmatrix} L_r i_{dr} + M i_{ds} \\ L_r i_{qr} + M i_{qs} \end{pmatrix} \quad (3)$$

Where L_s, L_r and M are stator, rotor and mutual inductances. The active and reactive powers at the stator are defined as:

$$P_s = v_{ds} i_{ds} + v_{qs} i_{qs};\ Q_s = v_{qs} i_{ds} + v_{ds} i_{qs} \quad (4)$$

The principle of conventional vector control (VC) method consists of orientating the stator flux in such a way that the stator flux vector points into the *d* -axis direction. This approach is realized by setting the quadrature component of the stator flux to the null value:

$$\phi_s = \phi_{ds}; \qquad \phi_{qs} = 0 \quad (5)$$

Using the condition that per phase stator resistance is neglected, and grid system is in steady state that is having a single voltage V_s that leads to stator's constant flux f, the voltages can be easily deduced as:

$$v_{ds} = 0; \qquad v_{qs} = \omega_s \phi_s = V_s \quad (6)$$

The following equations are obtained when replacing the rotor flux eqn. (3) in eqn. (1) and using the above condition in eqn. (6), the rotor voltages become:

$$v_{dr} = \sigma L_r \frac{di_{dr}}{dt} + R_r i_{dr} - \sigma L_r \omega_r i_{qr} + \frac{M d\phi_{ds}}{L_s d_t}$$
$$v_{dr} = \sigma L_r \frac{di_{qr}}{dt} + R_r i_{qr} - \sigma L_r \omega_r i_{dr} + \omega_r \frac{M}{L_s} \phi_s \quad (7)$$

Where V_s which is the stator voltage magnitude is assumed constant, and $\omega_r = \omega_s - \omega = g\omega_s$ is the slip frequency, and g is the slip range and is $\sigma = 1 - \dfrac{M^2}{L_s L_r}$ the leakage coefficient, with regard to eqn.(5), the fluxes are simplified as indicated below:

$$\phi_{ds} = L_s i_{ds} + M i_{dr}$$
$$0 = L_s i_{qs} + M i_{qr} \quad (8)$$

From eqn. (8), the stator currents can be deduced as:

$$i_{ds} = \frac{\phi_{ds} - M i_{dr}}{L_s}$$
$$i_{qs} = -\frac{M}{L_s} i_{qr} \quad (9)$$

By using eqns (4), (6) and (9), the stator active and reactive powers can then be expressed only against these rotor currents as:

$$P_s = -V_s \frac{M}{L_s} i_{qr}$$
$$Q_s = -V_s \frac{M}{L_s} \left(i_{dr} - \frac{\phi_{ds}}{M}\right) \quad (10)$$

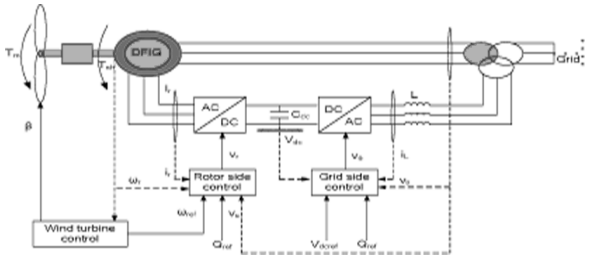

Figure 2: DFIG based wind turbine

Unbalanced DFIG Model

As stated in [9] during unbalanced grid voltage, the DFIG system can be separated into positive, negative and zero sequences. In this paper, two methods are proposed to separate positive and

negative sequences:

- delay inverse component canceling (DICC) method.

- notch filter method.

In the first method, the components in the three phase a, b, c system are transformed into two-phase α, β stationary reference frame. Then, the positive and negative components can be determined by the following expression:

$$\begin{pmatrix} v^{+}_{\alpha s} \\ v^{+}_{\beta s} \\ v^{-}_{\alpha s} \\ v^{-}_{\beta s} \end{pmatrix} = \frac{1}{2}\begin{pmatrix} 1 & 0 & 0 & -1 \\ 0 & 1 & 1 & 0 \\ 1 & 0 & 0 & 1 \\ 0 & 1 & -1 & 0 \end{pmatrix}\begin{pmatrix} v_{\alpha s(t)} \\ v_{\beta s(t)} \\ v_{\alpha s}(t-\frac{T}{4}) \\ v_{\beta s}(t-\frac{T}{4}) \end{pmatrix} \quad (11)$$

The obtained positive and negative sequences from eqn. 11 in stationary reference frame are transformed into positive and negative sequences in rotating reference frame as follows:

$$\begin{pmatrix} v^{+}_{ds} \\ v^{+}_{qs} \\ v^{-}_{ds} \\ v^{-}_{qs} \end{pmatrix} = \frac{1}{2}\begin{pmatrix} \cos(\theta_s) & \sin(\theta_s) \\ -\sin(\theta_s) & \cos(\theta_s) \\ \cos(-\theta_s) & \sin(-\theta_s) \\ -\sin(-\theta_s)\cos(-\theta_s) \end{pmatrix}\begin{pmatrix} v^{+}_{\alpha s} \\ v^{+}_{\beta s} \\ v^{-}_{\alpha s} \\ v^{-}_{\beta s} \end{pmatrix} \quad (12)$$

Figure 3 shows the three phase stator voltage of DFIG wind turbine, in which the unsymmetrical voltage dip is applied between 1.5 s to 1.6 s, as shown in Figure 4. Afterwards, with separation method, the positive and negative sequences of stator voltages in the rotating frame d and q are separated. Assuming the zero sequence component of grid voltage is zero, the unbalanced stator voltages can be written as follows:

$$V_s^{+} = \begin{pmatrix} v^{+}_{ds} \\ v^{+}_{qs} \end{pmatrix} = \begin{pmatrix} R_s i^{+}_{ds} + \dfrac{d\phi^{+}_{ds}}{dt} - \omega_s \phi^{+}_{qs} \\ R_s i^{+}_{qs} + \dfrac{d\phi^{+}_{qs}}{dt} + \omega_s \phi^{+}_{ds} \end{pmatrix} \quad (13)$$

$$V_s^{-} = \begin{pmatrix} v^{-}_{ds} \\ v^{-}_{qs} \end{pmatrix} = \begin{pmatrix} R_s i^{-}_{ds} + \dfrac{d\phi^{-}_{ds}}{dt} + \omega_s \phi^{-}_{qs} \\ R_s i^{-}_{qs} + \dfrac{d\phi^{-}_{qs}}{dt} - \omega_s \phi^{-}_{ds} \end{pmatrix} \quad (14)$$

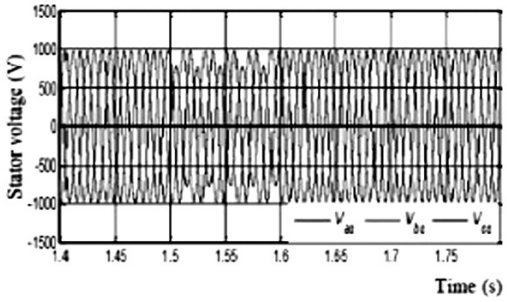

Figure 3 : Three phase grid side stator voltage

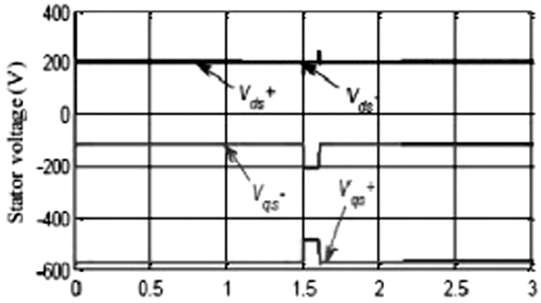

Figure 4 : Positive and negative sequence components of unbalance voltages in dq reference frame

The voltages at the rotor side are:

$$V_r^{+} = \begin{pmatrix} v^{+}_{dr} \\ v^{+}_{qr} \end{pmatrix} = \begin{pmatrix} R_r i^{+}_{dr} + \dfrac{d\phi^{+}_{dr}}{dt} - (\omega_s - \omega)\phi^{+}_{qr} \\ R_r i^{+}_{qr} + \dfrac{d\phi^{+}_{qr}}{dt} + (\omega_s - \omega)\phi^{+}_{dr} \end{pmatrix} \quad (15)$$

$$V_r^{-} = \begin{pmatrix} v^{-}_{dr} \\ v^{-}_{qr} \end{pmatrix} = \begin{pmatrix} R_r i^{-}_{dr} + \dfrac{d\phi^{-}_{dr}}{dt} - (\omega_s + \omega)\phi^{-}_{qr} \\ R_r i^{-}_{qr} + \dfrac{d\phi^{-}_{qr}}{dt} + (\omega_s + \omega)\phi^{-}_{dr} \end{pmatrix} \quad (16)$$

The stator and rotor fluxes are:

$$\begin{pmatrix} \phi^{+}_{ds} \\ \phi^{+}_{qs} \\ \phi^{-}_{ds} \\ \phi^{-}_{qs} \end{pmatrix} = \begin{pmatrix} L_s i^{+}_{ds} + M^{+}_{dr} \\ L_s i^{+}_{qs} + M^{+}_{qr} \\ L_s i^{-}_{ds} + M i^{-}_{dr} \\ L_s i^{-}_{ds} + M i^{+}_{dr} \end{pmatrix} \begin{pmatrix} \phi^{+}_{dr} \\ \phi^{+}_{qr} \\ \phi^{-}_{dr} \\ \phi^{-}_{qr} \end{pmatrix} = \begin{pmatrix} L_r i^{+}_{dr} + M^{+}_{ds} \\ L_r i^{+}_{qr} + M^{+}_{qs} \\ L_r i^{-}_{dr} + M i^{-}_{ds} \\ L_r i^{-}_{dr} + M i^{-}_{ds} \end{pmatrix} \quad (17)$$

Under unbalanced grid, the active and reactive powers as stated in eqn. (4) is decomposed into different pulsating components, which can be rewritten as:

$$\begin{pmatrix} P_s \\ Q_s \\ P_{s\sin 2} \\ Q_{s\cos 2} \end{pmatrix} = \begin{pmatrix} v_{ds}^{+} & v_{qs}^{+} & v_{ds}^{-} & v_{qs}^{-} \\ v_{qs}^{+} & -v_{ds}^{+} & v_{qs}^{-} & -v_{ds}^{-} \\ v_{qs}^{-} & -v_{ds}^{-} & -v_{qs}^{+} & v_{ds}^{+} \\ v_{ds}^{-} & v_{qs}^{-} & v_{ds}^{+} & v_{qs}^{+} \end{pmatrix} \begin{pmatrix} i_{ds}^{+} \\ i_{qs}^{+} \\ i_{ds}^{-} \\ i_{qs}^{-} \end{pmatrix} \quad (18)$$

In order to obtain a constant stator power, the oscillating terms of the active and reactive powers P_{ssin2}, Q_{scos2} in eqn. (18) are neglected, therefore, only the average terms are controlled. By inverting eqn. (18) the stator currents can be calculated as follows :

$$\begin{pmatrix} i_{ds}^{+} \\ i_{qs}^{+} \\ i_{ds}^{-} \\ i_{qs}^{-} \end{pmatrix} = \frac{P_s}{D_1} \begin{pmatrix} v_{ds}^{+} \\ v_{qs}^{+} \\ v_{ds}^{-} \\ v_{qs}^{-} \end{pmatrix} + \frac{Q_s}{D_2} \begin{pmatrix} v_{qs}^{+} \\ -v_{ds}^{+} \\ v_{qs}^{-} \\ -v_{ds}^{-} \end{pmatrix} \quad (19)$$

The positive stator flux is aligned along with the d+ -axis and rotates at the speed of ωs, whereas the d- -axis rotates at an angular speed of $-\omega_s$, with the phase angle to the α-axis being $-\theta_s$.

Therefore, by using eqns. (13) and (14) with stator flux orientation under unbalanced grid, the stator currents are simplified as follows:

$$\begin{pmatrix} i_{ds}^{+} \\ i_{qs}^{+} \\ i_{ds}^{-} \\ i_{qs}^{-} \end{pmatrix} = \frac{1}{L_s} \begin{pmatrix} \phi_{ds}^{+} \\ 0 \\ \phi_{ds}^{-} \\ 0 \end{pmatrix} - \frac{M}{L_s} \begin{pmatrix} i_{dr}^{+} \\ i_{qr}^{+} \\ i_{dr}^{-} \\ i_{qr}^{-} \end{pmatrix} \quad (20)$$

Combining eqn. (20) with eqn. (19), the rotor currents are written as follows:

$$\begin{pmatrix} i_{dr}^{+} \\ i_{qr}^{+} \\ i_{dr}^{-} \\ i_{qr}^{-} \end{pmatrix} = -\frac{L_s}{M}\frac{P_s}{D_1} \begin{pmatrix} v_{ds}^{+} \\ v_{qs}^{+} \\ -v_{ds}^{-} \\ -v_{ds}^{-} \end{pmatrix} - \frac{L_s}{M}\frac{Q_s}{D_2} \begin{pmatrix} v_{qs}^{+} \\ -v_{ds}^{+} \\ v_{qs}^{-} \\ -v_{ds}^{-} \end{pmatrix} + M \begin{pmatrix} \phi_{ds}^{+} \\ 0 \\ \phi_{ds}^{-} \\ 0 \end{pmatrix} \quad (21)$$

Sliding Mode Control

The details of the conventional SMC have been presented in [10], the sliding mode control (SMC) strategy with unbalanced DFIG model is considered in this paper. According to the SMC theory, the errors of direct and quadrate rotor currents are chosen as sliding surface:

$$\begin{aligned} S_1\left(i_{dr}^{+}\right) &= i_{dr}^{+*} - i_{dr}^{+} \\ S_2\left(i_{qr}^{+}\right) &= i_{qr}^{+*} - i_{qr}^{+} \\ S_3\left(i_{dr}^{-}\right) &= i_{dr}^{-*} - i_{dr}^{-} \\ S_4\left(i_{qr}^{-}\right) &= i_{qr}^{-*} - i_{qr}^{-} \end{aligned} \quad (22)$$

$$\frac{d}{dt}S = F + DV_r \quad (23)$$

When the trajectories of rotor current converge towards sliding surface:

$$\frac{d}{dt}S = 0 \quad (24)$$

The following equation is obtained by replacing the rotor flux of eqn. (17) in eqn. (15), eqn. (16) and combining with eqn. (23) and eqn. (24) :

$$F = \begin{pmatrix} F_1 \\ F_2 \\ F_3 \\ F_4 \end{pmatrix} =$$

$$\begin{bmatrix} i_{dr}^{+*} + \frac{R_r}{\sigma L_r} i_{dr}^{+} - \omega_r i_{qr}^{+} + \frac{M}{\sigma L_r L_s} v_{ds} \\ \frac{R_r}{\sigma L_r} i_{qr}^{+} + i_{qr}^{+*} + \omega_r i_{dr}^{+} + \frac{M}{\sigma L_r L_s} v_{qs}^{+} - \frac{M}{\sigma L_r L_s} \phi_{sd}^{+} (\omega_s - \omega_r) \\ i_{dr}^{-*} + \frac{R_r}{\sigma L_r} i_{dr}^{-} - \omega_r i_{qr}^{-} + \frac{M}{\sigma L_r L_s} v_{ds}^{-} \\ i_{qr}^{-*} + \frac{R_r}{\sigma L_r} i_{qr}^{-} + \omega_r i_{dr}^{-} + \frac{M}{\sigma L_r L_s} v_{qs}^{-} - \frac{M}{\sigma L_r L_s} \phi_{sd}^{-} (\omega_s + \omega_r) \end{bmatrix} \quad (25)$$

$$D = \frac{1}{\sigma L_r} \begin{bmatrix} 1 & 0 & 0 & 0 \\ 0 & 1 & 0 & 0 \\ 0 & 0 & 1 & 0 \\ 0 & 0 & 0 & 1 \end{bmatrix} \quad (26)$$

$$V_r = -D^{-1} \begin{bmatrix} F_1 + K_1 sat(S_1) \\ F_2 + K_2 sat(S2) \\ F_3 + K_3 sat(S_3) \\ F_4 + K_4 sat(S_4) \end{bmatrix} \quad (27)$$

Where K_1, K_2, K_3, K_4 are positive control gains and

$$sat(S_1) = 1, \; S_i > \lambda_i$$
$$S_i / \lambda_i \quad |S_i| \le \lambda_i \quad (28)$$
$$-1, \quad S_i < -\lambda_i$$

Where is the width boundary layer and indicates 1, 2, 3 or 4.

Many PWM techniques for three-level inverters have been studied in many paper. In this paper, the PWM technique is applied with two bipolar carriers, half period of phase $V_{car\ 1}$, $V_{car\ 2}$. This technique is characterized by three parameters: the modulation index (MI), the modulation rate *r* and V_k^* is the three-phase voltage, k = 0 to 3. Two steps of this VSI control algorithm for the arm k are as follows: This first step consists of determining the intermediate signals:

-if $V_K^* \ge V_{car,1}$ then $V_{k0} = V_c/2$

-if $V_K^* < V_{car,1}$ then $V_{k1} = 0$

-if $V_K^* \ge V_{car,2}$ then $V_{k0} = V_c/2$

-if $V_K^* < V_{car,2}$ then $V_{k1} = -V_c/2$ (29)

The second step consists of determining the main signal:

$$V_k = V_{k0} + V_{k1} \quad (30)$$

Then, the gate control of the sitch T_{ks} is:

-if $V_k = V_c/2$, then $(F_{k1}, F_{k2}) = (0, 1)$

-if $V_k = -V_c/2$, then $(F_{k1}, F_{k2}) = (0, 0)$ (31)

-if $V_k = 0$, then $(F_{k1}, F_{k2}) = (1, 1)$

Simulation Results

The generator is tested under single line to ground fault condition on phase 'a'; at 1.5 s an unbalanced voltage drop of 20 % is created for a time of 0.5 s as shown in Figure 3. In this paper, all the physical quantities are expressed in per unit values and the quantities of the rotor are referred to the stator side. The switching frequency of converter is 1 KHz; the nominal dc voltage of converter is 2000 V. The phase locked loop (PLL) estimates the frequency, the grid voltage magnitude and the stator angle. Wind speed varies from 11 m/s to 10 m/s. To examine the validity of the proposed SMC scheme, these results are compared with the conventional single SMC method published in [11].

Figure 5 (a), (b), Figure 6 (a), (b), Figure 7 (a), (b) and Figure 8 (a), (b), show that, during grid voltage unbalance, if conventional control is applied, the active and reactive powers contain important oscillations, due to the nature of the second harmonic at twice the grid frequency (100 Hz) with magnitude of 0.78 pu. Whereas, by using the proposed control method, these oscillations are dramatically reduced.

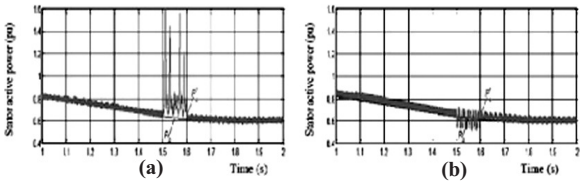

Figure 5: Stator active power: (a) conventional single SMC, (b) proposed dual SMC

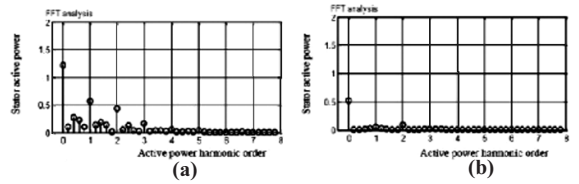

Figure 6 : Harmonic spectra of the stator active power: (a) conventional single SMC, (b) proposed dual SMC

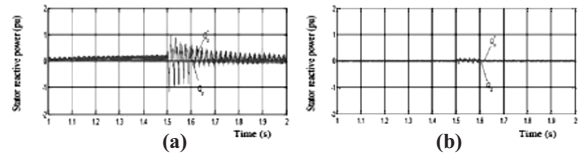

Figure 7 : Stator reactive power : (a) conventional single SMC, (b) proposed dual SMC

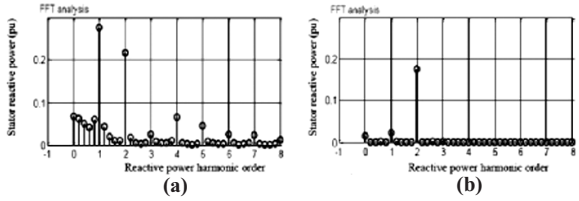

Figure 8: Harmonic spectra of the stator reactive power : (a) conventional single SMC, (b) proposed dual SMC

Conclusion

In this paper, an improved control strategy for DFIG based wind turbine under unbalanced grid voltage is presented. The dynamic behaviour of DFIG by the proposed control algorithm proved to be suitable by a set of simulation tests using the Matlab®/ Simulink® environment. The results obtained show that with the conventional single SMC scheme, the magnitude of the second harmonic oscillations can become high, intolerable and may lead to electrical and mechanical failures. After removing the voltage unbalance, in the conventional control method small oscillations appear in the powers and currents waveforms. On the contrary, when the proposed dual SMC scheme is used these power oscillations are effectively damped to a reasonable level.

References

1. K. G. Sharma, A. Bhargava, and K. Gajrani, 'Small Signal Stability of DFIG Connected Power System and Identification of Oscillatory Modes using Prony Analysis', International Review of Electrical Engineering, vol. 9, no. 5, October 2014.

2. I. Erlich, H. Wrede, and C. Feltes, 'Dynamic Behavior of DFIG Wind Turbines during Grid Faults,' Proc. of IEEE Power Conversion Conference, Naagoya, pp. 1195-1200, April 2007.

3. K. D. E. Kerrouche, A. Mezouar, L. Boumediene and K. Belgacem, 'Modeling and Optimum Power Control based DFIG Wind Energy Conversion System,' International Review of Electrical Engineering, vol. 9, no. 1, February 2014.

4. T. K. A. Brekken and N. Mohan, 'Control of a Doubly Fed Induction Wind Generator under Unbalanced Grid Voltage Conditions,' IEEE Transactions on Energy Conversion, vol. 22, no.1, pp. 129 – 135, March 2007.

5. F. Mwasilu, J. J. Justo, K. -S. Ro and J. -W. Jung, 'Improvement of Dynamic Performance of Doubly Fed Induction Generator based Wind Turbine Power System under an Unbalanced Grid Voltage Condition,' IET Renewable Power Generation, vol. 6, no.6, pp. 424 – 434, November 2012.

6. J. Hu, H. Nian, B. Hu and Y. He, 'Direct Active and Reactive Power Regulation of DFIG using Sliding Mode Control Approach,' IEEE Transactions on Energy Conversion, vol. 25, no.4, pp. 1028–1039, June 2010.

7. G. Abad, M. A. Rodriguez, G. Iwanski and J. Poza, 'Direct Power Control of Doubly-fed Induction Generator based Wind Turbines under Unbalanced Grid Voltage,' IEEE Transactions on Power Electronics, vol. 25, no. 2, pp. 442-452, August 2009.

8. C. O. Omeje, D. B. Nandi and C. I. Odeh, 'Theory and Modeling of a 150 kW Doubly-fed Induction Machine with Bidirectional Multi-level Converters Control SVPWM Technique,' Arabian Journal of Science and Engineering, vol. 39, pp. 6339-6349, 2014.

9. L. Xu and Y. Wang, 'Dynamic Modeling and Control of DFIG based Wind Turbines under Unbalanced Network Conditions,' IEEE Transactions on Power Systems, vol. 22, no. 1, pp. 314-323, February 2007.

10. A. Mezouar, M. K. Fellah and S. Hadjeri, 'Adaptive Sliding Mode Observer for Induction Motor using Two-time-scale Approach,' Electric Power Systems Research, vol. 77, no. 5, pp. 604-618, April 2007.

11. K. Kerrouche, A. Mezouar and L. Boumediene, 'A Simple and Efficient Maximized Power Control of DFIG Variable Speed Wind Turbine,' Proc. 3rd IEEE International Conference on Systems and Control, Algeria, pp. 894- 906, 2013.

A Simulation Study of Four Configurations of Brushless Doubly-Fed Reluctance Machine

S. S. Kunte M. P. Bhawalkar N. Gopalakrishnan Y. P. Nerkar G. A. Vaidya

Department of Electrical Engineering
Pune Vidyarthi Griha's College of Engineering and Technology, Pune, Maharashtra
E-mail : soumitra.kunte21@gmail.com, mandar_bhawalkar@yahoo.co.in

Abstract

The Brushless Doubly Fed Reluctance Machine (BDFRM) is basically a modified synchronous reluctance machine and its operation is similar to doubly fed induction machine. In recent years it is gaining more importance as it is robust, more efficient and allows use of fractional rating power converter. These benefits and unusual pole combinations motivated researchers to do detailed investigation with reference to variable speed applications including generating action. Performance of this machine is greatly dependent on design and modulation of interaction between stator windings through rotor which is decided mainly by saliency of rotor. Design issues and their impact on machine performance are addressed here. In this paper, a time stepping two-dimensional finite element method is used for modelling and analysis of BDFRM. Finite element machine model is used for studying the performance of machine with different stator and rotor configurations. Performance of BDFRM with different stator and rotor configuration are analyzed using time stepped finite element analysis. This approach is used to examine the capabilities and behavior of BDFRM at various conditions. A prototype type developed for 2-4-6 is tested for validation of the facts.

Keywords : *Rotor saliency; Reluctance rotor; Axially laminated rotor; Flux barriers*

Introduction

The Brushless doubly fed reluctance machine is an attractive alternative for conventional controllable machines for wind power generation due to the absence of brushes as well as rotor winding with the consequence of elimination of rotor copper losses and partial converter rating [1,2, 3]. Over last few years considerable work is carried out in the area of design or transformation of reluctance machine into BDFRM [4, 5, 6]. Conceptual and theoretical analysis, comparison with other counter parts are reported [7, 8]. The control strategies applied for BDFRM are covered extensively by different research workers [9, 10, 11]. With the use of increased automation and enhanced complexity, many field applications demand variable speed operation with efficient, reliable, simple and cost effective solution. BDFRM is still considered as a new machine and under development and investigative phases. In spite of continuous development activities being carried out, a few research papers are available on design, performance optimization and behaviour of machine. Performance of BDFRM with different configurations such as radially laminated rotor, ducted rotor and axially laminated rotor with different poles on rotor and in stator windings is studied extensively and presented in this paper.

Reluctance Machine

The reluctance machines were developed before 70s and used for some low torque constant speed applications. Torque developed by machine was based on variation of reluctance produced by the salient rotor construction. The characteristic features such as simple construction, maintenance free operation and flat torque speed characteristics have retained the interest of developers and users regardless of overall inferior performance of this machine [12]. Efforts were put in for improving performance of plain reluctance machine [12].

Gradual development in this direction leads to the fabrication of switched reluctance machine. Further development took place leading to design and fabrication of axially laminated rotors or BDFRM.

It is observed that performance of plain reluctance machine is greatly affected by saliency ratio. It is the ratio of direct axis inductance to quadrature axis inductance. Higher the saliency ratio, better is the performance. Plain reluctance machine has the maximum saliency ratio in the range of 2 to 3. The saliency ratio can be improved by modifying rotor structure so as to align mutual flux in the direction of direct axis. The ideal value of saliency ratio is about 15. These modified machines is popularly known as line start synchronous reluctance machines. These machines are having flat torque speed characteristics. For variable speed operation, power electronics converter having rating equal to kW capacity of machine is necessary. It increases the overall cost of setup. Another version of the machine catering needs of variable speed applications is the switched reluctance machine where number of stator and rotor poles are different. Invariably rotor is of conventional reluctance type having more number of poles than that of number of poles for stator winding. The advantage of this machine is simpler power electronics interface and associated cost reduction. However limitations as described earlier are still valid. It is therefore necessary to amend older machine into a new one. One of such relatively new type of reluctance machine has two windings on stator and a modified rotor geometry. This is brushless doubly fed reluctance machine capable of overcoming many short comings of reluctance machine. This extremely interesting machine is discussed in next section.

Brushless Doubly Fed Reluctance Machine

The classical BDFRM has two stator windings wound for different number of poles. Windings are distributed and may be full pitched or short pitched. One winding is wound for p number of poles and other is wound for q number of poles. The rotor has salient poles without any winding on the rotor. The rotor laminations are stacked radially such that saliency is created. The number of rotor poles (Pr) is given by eqn. (1)

$$P_r = \left(\frac{p+q}{2} \right) \tag{1}$$

The schematic representation of BDFRM is shown in Figure 1. It is seen that one of the winding wound for p number of poles which is connected to nearby grid and excited by normal power frequency supply called as power or primary winding. Other winding wound for q poles is excited by either a dc source or by a variable frequency variable voltage supply derived from the grid or from any separate source. The interaction of two magnetic fields produced by stator currents produces electromagnetic torque in the machine.

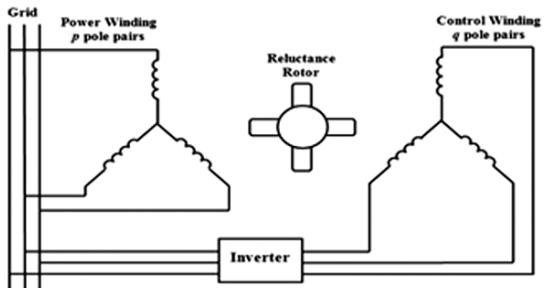

Figure 1 : Schematic representation of BDFRM

Working of BDFRM

The salient rotor of BDFRM modulates the interaction between two sets of stator winding currents. Operation of machine depends on this mutual interaction. The angular speed of rotor ωr is given by eqn. (2) where power winding angular frequency is ωp and that of control winding is ωc.

$$\omega_r = \left(\frac{\omega_p + \omega_c}{P_r} \right) \tag{2}$$

If power winding frequency remains constant, operation of machine is decided by the control winding frequency. With known rotor poles and keeping the power winding frequency constant, control winding frequency can be selected to achieve variable speed operation of rotor. Depending on the magnitude of ωc; there can be three modes of operation. In Mode 1 ($\omega_c < 0$), machine operates below synchronous speed. In Mode 2 ($\omega_c = 0$), control winding is excited by dc supply resulting in synchronous (rated) speed. In Mode 3 ($\omega_c > 0$), where machine runs at super synchronous speed.

Design and Modelling of BDFRM

Design of BDFRM is complex as there are two independent stator windings placed in the same slot. Rotor has no winding. Ampere turn (MMF) requirement of machine need to be fulfilled by stator. Current magnitude is also large and therefore area of cross-section of conductors used for stator winding is also large. Selection of current density is one of the most important factors. Dual excitation and different pole combination results in flux concentration in certain sections of machine. It causes machine to work with moderate saturation and puts limits on air gap flux density; which is another important design parameter. Other design considerations are base speed, electro-magnetic torque, ampere conductor loading, slot dimensions etc. It is necessary to take into account different economic and operational parameters into account for design of BDFRM.

Performance of reluctance machine depends on various parameters such as saliency ratio, selection of number of poles for stator and rotor, winding layout, choice between power and control winding and control strategy. Out of above mentioned parameters saliency ratio, correct selection of number of poles for stator and rotor and winding layout are design related issues. Saliency ratio is related to rotor design. Selection of number of poles for stator and rotor decides the coupling between magnetic fields. Winding layout can be single or double winding type. In this paper results obtained with two separate winding for stator windings are presented. Keeping the winding layout same which is two separate winding type; machine is analyzed for different pole combinations of stator and rotor configurations.

Saliency Ratio

Saliency ratio (L_d/L_q) is one of the important factors associated with performance of reluctance machine. Performance parameters such as torque, power factor, efficiency depend on saliency ratio. Performance of machine is better with increased saliency ratio. Figure 2 clearly indicate improvement in power factor with saliency ratio. Please refer eqn. 3. It is seen that power factor improves with increase in saliency ratio. Please refer eqn. 4. Electromagnetic torque also increases with increase in saliency ratio.

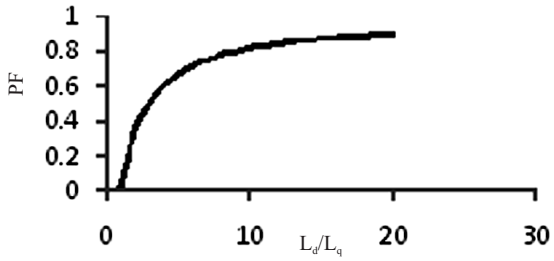

Figure 2 : Effect of saliency ratio on power factor

$$PF_{\max} = \frac{\left(1 - L_d / L_q\right)}{\left(1 + L_d / L_q\right)} \quad (3)$$

$$T_e = \frac{3}{2}(p+q)\left(\lambda_{dc} i_{qc} - \lambda_{qc} i_{dc}\right) \quad (4)$$

where L_d and L_q represent direct and quadrature axis inductances respectively, λ_{dc} and λ_{qc} represent direct and quadrature axis flux linkages due to control winding current, i_{qc} and i_{dc} represent quadrature and direct axis control winding currents.

Ducted rotor, single barrier type rotor, multiple barrier type rotor and axially laminated type rotor are shown in Figure 3. Plain reluctance rotor is shown in Figure 3 (a). Ducted rotors are shown in Figure 3(b) and Figure 3(c), respectively. Axially laminated (ASA) rotor is shown in Figure 3 (b). In barrier type rotors number of barriers and shape of barriers determines the saliency level. Salient type rotor has the lowest saliency ratio and axially laminated rotor has the highest saliency ratio. Construction cost for axially laminated rotor is significantly large.

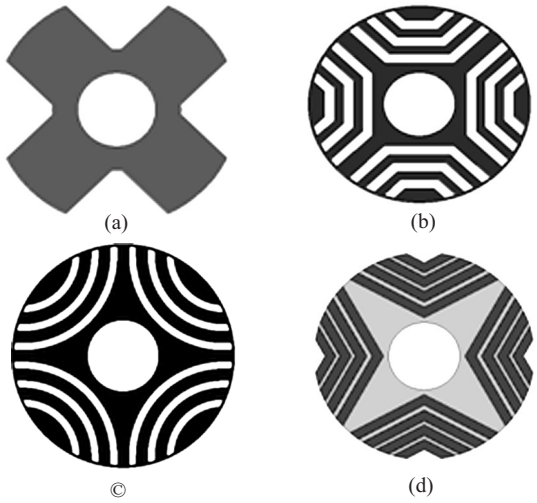

Figure 3 : Different rotor configurations

Pole Combinations

Stator windings are designed for different number of poles. Number of rotor poles are decided using mathematical relation shown in eqn. (1). Actual number of poles for stator and rotor of these motors is decided on the basis of requirement of coupling factor. Coupling factor is related to self and mutual interaction of magnetic flux produced by each winding. Coupling factor should be 1 for ideal machine. But it generally in the range of 0.75 to 0.9 due to leakage flux in machine. In BDFRM value of coupling factor depends on different pole combinations [13]. In some combinations combined flux in some portion is aiding while in other combinations it is subtractive due to cross-coupling [14]. There may be problems in calculating coupling factor accurately due to different pole numbers or even odd number of poles on rotor. Varied geometry and composition of different materials increase non-liberalities and computational complexities. It is observed that the machine with closest pole combination has better coupling factor [13]. Odd number of poles may be selected on rotor however odd number of poles has poor acceptability in general. In this paper major emphasis is done with even number of poles of stator and rotor. Commonly used configurations are 2-4-6 and 4-6-8.

Mathematical Modeling of BDFRM

Performance of a well-developed machine can be obtained by simulation under steady state and transient conditions using phase coordinate model. This model is used for obtaining performance characteristics of BDFRM. Concept of multiple reference frame used for BDFRM is introduced in Figure 4.

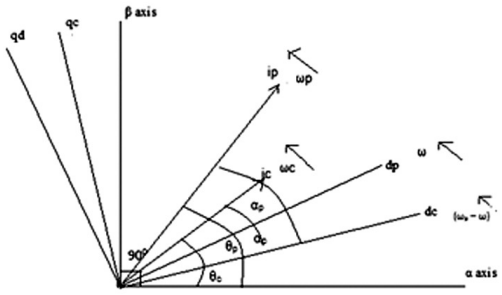

Figure 4 : Multiple reference frame for BDFRM

There are two synchronously rotating reference frames one for power winding and another for control winding. q axis leads the d axis. Frame of power winding leads to control winding frame. Please refer eqn.5 and eqn.6. Concepts of phasor coordinates are introduced using these equations.

$$\begin{bmatrix} V_R \\ V_Y \\ V_B \end{bmatrix} = R_p \begin{bmatrix} i_R \\ i_Y \\ i_B \end{bmatrix} + \frac{d}{dt}\left(\lambda_{RYB}\right) \qquad (5)$$

$$\begin{bmatrix} V_r \\ V_y \\ V_b \end{bmatrix} = R_c \begin{bmatrix} i_r \\ i_y \\ i_b \end{bmatrix} + \frac{d}{dt}\left(\lambda_{ryb}\right) \quad (6)$$

where, λ_{RYB} and λ_{ryb} are given by eqns (7) and (8). $[L_{RYB}]$ and $[L_{ryb}]$ are self-inductances for power and control winding respectively and $[L_{RYBryb}]$ indicates mutual inductance of machine.

$$\lambda_{RYB} = \begin{bmatrix} L_{RR} & L_{RY} & L_{RB} \\ L_{YR} & L_{YY} & L_{YB} \\ L_{BR} & L_{BY} & L_{BB} \end{bmatrix} \begin{bmatrix} i_R \\ i_Y \\ i_B \end{bmatrix} + \begin{bmatrix} L_{Rr} & L_{Ry} & L_{Rb} \\ L_{Yr} & L_{Yy} & L_{Yb} \\ L_{Br} & L_{By} & L_{Bb} \end{bmatrix} \begin{bmatrix} i_r \\ i_y \\ i_b \end{bmatrix} \quad (7)$$

$$\lambda_{ryb} = \begin{bmatrix} L_{rr} & L_{ry} & L_{rb} \\ L_{yr} & L_{yy} & L_{yb} \\ L_{br} & L_{by} & L_{bb} \end{bmatrix} \begin{bmatrix} i_r \\ i_y \\ i_b \end{bmatrix} + \begin{bmatrix} L_{Rr} & L_{Ry} & L_{Rb} \\ L_{Yr} & L_{Yy} & L_{Yb} \\ L_{Br} & L_{By} & L_{Bb} \end{bmatrix} \begin{bmatrix} i_R \\ i_Y \\ i_B \end{bmatrix} \quad (8)$$

Speed equation is given by eqn. (9). *Te* is electromagnetic torque developed by the machine and T_l is the load torque and *J* be the moment of inertia of the machine.

$$J\frac{d}{dt}\left(\omega_{rm}\right) = T_e - T_i \quad (9)$$

Finite Element Analysis

Finite element method is very popular due to its capability to solve non-linear problems. Electrical machines are complex geometries, Boundary conditions and material specifications affect the performance of rotating machine. Higher order non-linear partial differential equations which only can be solved by FEA.

ANSYS Maxwell 16.02 platform is used to develop a finite element model of BDFRM. A 2kW machine is designed for two different pole combinations with different rotor constructions. First combination is 2/6/4 in which 2 and 6 pole windings are embedded in stator; and rotor has 4 poles on it. Likewise the second combination is 4/8/6 with 6 pole rotor; and 4 and 8 pole windings in stator. Machine with above mentioned pole configurations are simulated separately with salient type rotor and axially laminated rotor. Finite element models of BDFRM are shown in Figure 5(a) and Figure 5(b).

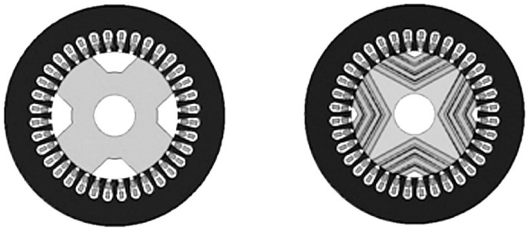

Figure 5 (a) : 2/6/4 combination with salient and axially laminated rotor

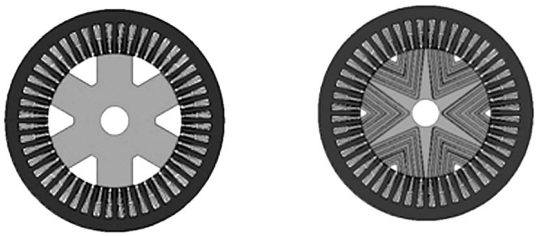

Figure 5 (b) : 4/8/6 combination with salient and axially laminated rotor

BDFRM models are simulated with limited time step finite element analysis with backward Euler Time Integration Method. Assumption for FEM study was that higher number of poles are considered for power winding and lower number of poles are considered for control winding.

Results and Discussions

Winding Currents

Currents drawn by power winding of BDFRM for different configurations mentioned earlier are shown in Figures 6 (a-d)

Power winding currents in 2-4-6 configuration are unbalanced and distorted. Comparatively 4-6-8

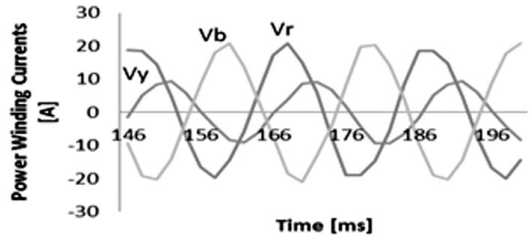

Figure 6(a) : Power winding current for 2-4-6 combinbation with salient rotor

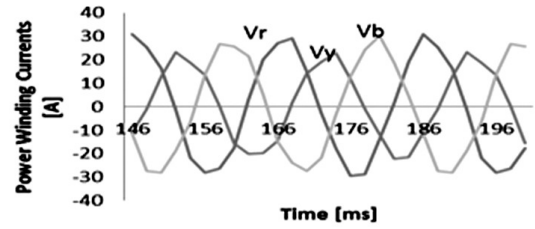

Figure 6(b) : Power winding current for 2-4-6 combinbation with axial rotor

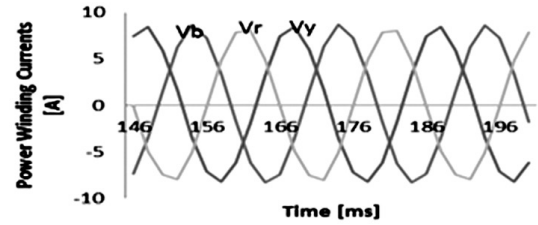

Figure 6(c) : Power winding current for 4-6-8 combinbation with salient rotor.

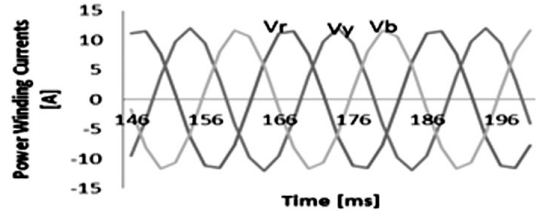

Figure 6(d) : Power winding current for 4-6-8 combinbation with axial rotor

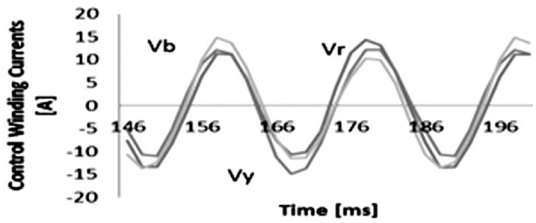

Figure 7(a) : Control winding current for 2-4-6 combinbation with salient rotor

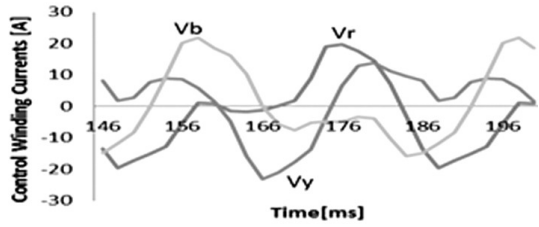

Figure 7(b) : Control winding current for 2-4-6 combinbation with axial rotor

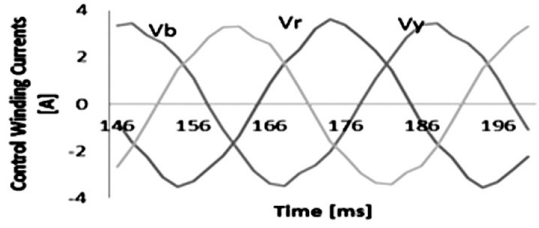

Figure 7(c) : Control winding current for 4-6-8 combinbation with salient rotor

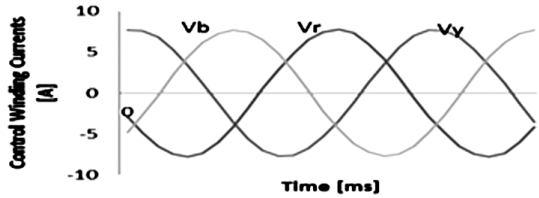

Figure 7(d) : Control winding current for 4-6-8 combinbation with axial rotor

combinations have balanced and fairly sinusoidal current waveforms. Also magnitude of current required to produce torque is also relatively lower in 4-6-8 configuration if compared with magnitude of current with 2-4-6 configuration. Coupling factor of 4-6-8 configuration is better.

Currents drawn by control winding for 4-6-8 combinations are shown in Figure 7 (a-d). These currents are perfectly balanced and sinusoidal as against current waveforms obtained with 2-4-6 combination. Magnitude of torque produced in BDFRM depends on frequency and magnitude of applied voltage of control winding [1]. Still rotor modulation plays major role defining the waveshape of current flowing through control winding. Due to poor coupling and poor modulation, 2-4-6 configuration with salient rotor has unbalanced current waveshape.

Flux and Flux Density Plots

The distribution of flux inside the BDFRM and associated flux density values can be obtained from simulation studies. Figures 8 (a-d) and

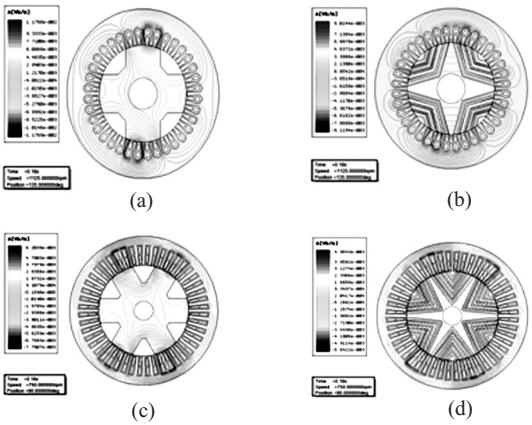

Figure 8 : Flux distribution in BDFRM

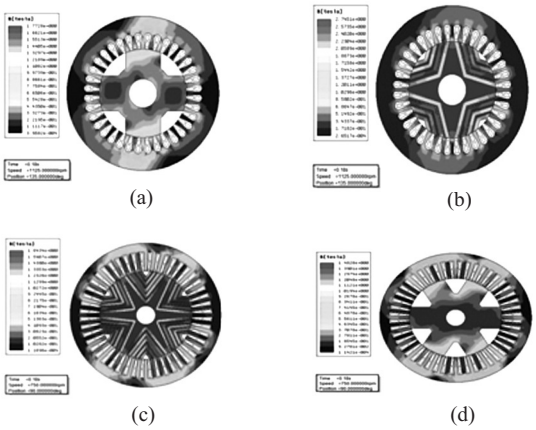

Figure 9 : Flux density distribution in BDFRM

Figures 9 (a-d) show flux plot for different combinations mentioned above. The axial rotor has better flux distribution avoiding saturation as against conventional rotor configuration. Maximum flux density in stator teeth portion is around 1.77 T for conventional rotor used with 2-4-6 combination.

Torque Production

Torque developed by BDFRM is obtained when power winding is excited by 50 Hz mains and control winding is excited by variable frequency variable voltage supply. Waveforms of torque developed are shown in Figure 10 (a-b) for 2-4-6 winding configuration, with salient rotor and axially laminated rotor. Machine is designed for 750 rpm. Simulation study is carried out for 4-6-8 winding combination at 500 rpm. Figure 10 (c-d) represents torque waveforms for 4-6-8 pole combinations. It is noticed that 2-4-6 pole combinations produces pulsating torque. The pulsations are reduced with 4-6-8 combination with axially laminated rotor. Comparative study of different pole configuration of BDFRM and corresponding values of average torque and ripple current is presented in Table 1.

Table 1 : Torque produced by different configurations of BDFRM

Configuration	Average Torque, Nm	Ripple Content, %
2-4-6 Salient	4.95	131.12
2-4-6 Axial	9.83	82.86
4-6-8 Salient	9.19	64.11
4-6-8 Axial	15.51	36.47

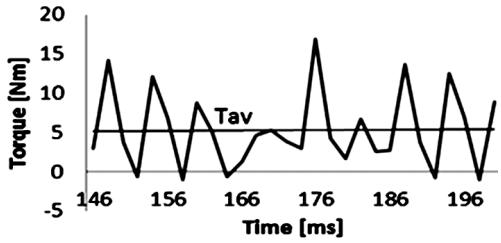

Figure 10(a) : 2-4-6 Configuration with salient rotor

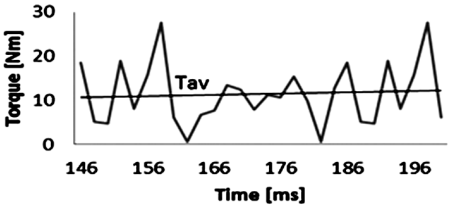

Figure 10(b) : 2-4-6 Configuration with axially laminated rotor

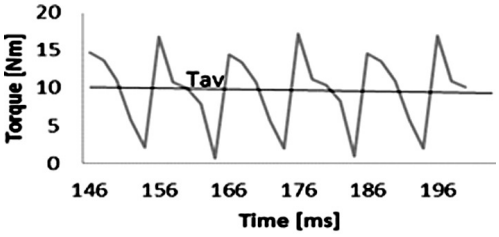

Figure 10 (c) : 4-6-8 Configuration with salient rotor

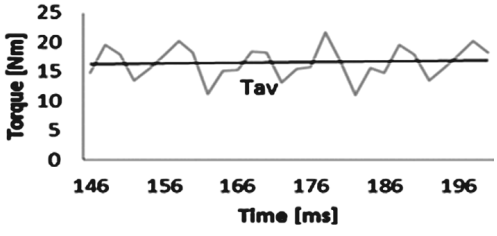

Figure 10(d) : 4-6-8 Configuration with axially laminated rotor

Figure 10 (a-b-c-d) show nature of torque produced by each configuration of BDFRM during same interval. Average value of torque and corresponding percentage ripple developed are summarized in Table 1.

It is noticed that BDFRM with 4-6-8 pole combination and with axial rotor has the highest torque production with less percentage ripples. This is due to better coupling factor and higher saliency ratio.

Rotor Surface Forces

Unbalanced magnetic pool is one of the major operational constraints of BDFRM. Magnitude of unbalanced magnetic pool depends on magnetic flux density and length of air gap, Analysis carried out for various cases is presented in Figure 11(a-b). It is noticed that the unbalanced magnetic pool is the minimum for 4-6-8 pole combination and with axial rotor combination.

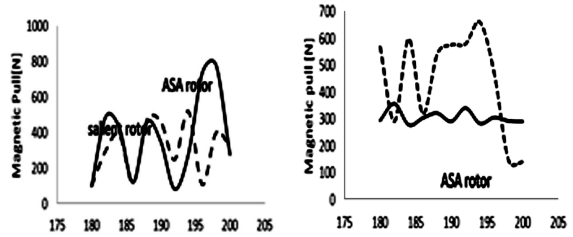

(a) (b)

Figure 11 : Unbalanced magnetic pulls develed in BDFRM magnetic flux lines a) 2-4-6 combination and b) 4-6-8 combination (dotted line salient rotor and continuous line ASA rotor)

Experimental Results and Discussions

A 2-4-6 poles configuration BDFRM is fabricated having salient pole rotor structure. The peculiarity of this machine is that it has a single winding embedded in stator slots catering need of two windings. The arrangement of winding is as shown in Figure 12(a) which is arranged in 36 slots. The coil groups of winding are arranged such that regrouping of terminals form 2 and 6 poles simultaneously. Figure 12(b) shows photographs of fabricated BDFRM. The fabricated machine has been tested for different conditions such as,

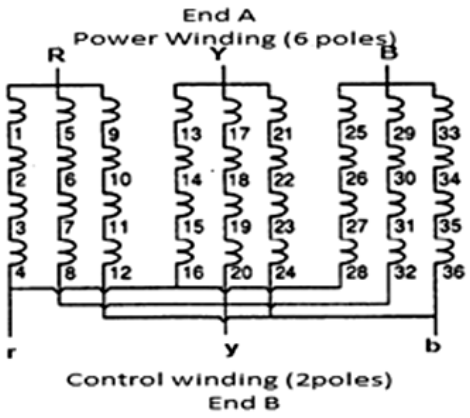

Figure 12(a) : Winding arrangement of 2-4-6 poles BDFRM

Figure 12(b) : Fabricated rotor and stator assembly of BDFRM

excitation at power frequency is given from 6 pole side followed by BDFRM is supplied from both power and control sides.

The voltage(blue) and current(yellow) waveforms captured during testing working at certain operating condition with power winding is excited with 50 Hz supply is shown in Figure 13. It can be observed that voltage and current waveforms are fairly sinusoidal and the operating power factor is about 0.8 lagging which is fairly agree the design value.

For variable speed operation variable frequency variable voltage excitation is given to control winding. By variation of control winding frequency change in speed is obtained and the variation in speed with change in control winding excitation frequency is shown in Figure 14.

The current drawn by both winding during variable speed operation is shown in Figure 15 which shows distortions in current wave forms due to modulation of airgap flux density mutual coupling between two windings.

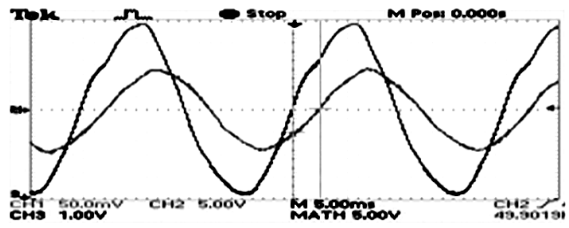

Figure 13 : Power winding voltage and current waveforms

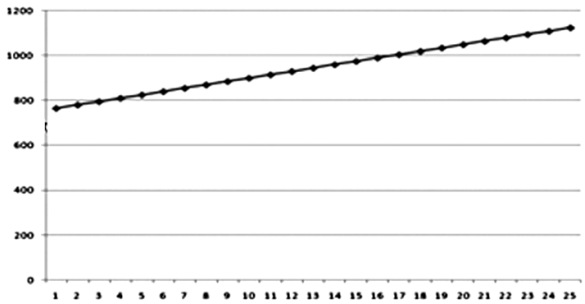

Figure 14 : Variation of speed of BDFRM with change in excitation frequency

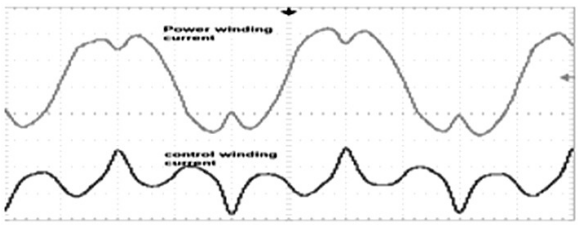

Figure 15 : Current drawn by BDFRM under dual excitation

The tests results presented here are sample ones. The results of detailed investigations will be presented as a separate paper. It is observed that the fabricated BDFRM is working reasonably well however torque pulsation and noise are issues to be addressed.

Conclusions

• A few of the finite element models developed for BDFRM are presented. Simulation results are comparable with those presented in open literature.

• It is observed that simplest design configuration is 2-4-6 salient rotor but it suffers from severe torque pulsations along with distorted currents. Situation is better with axial rotors.

• 4-6-8 combination shows improved results for both the combinations but results with axial rotor are remarkable.

• To validate the actual design, a 2 kW prototype machine is designed and fabricated with 2-4-6 poles combination. From the sample test results presented, it can be seen that it is working satisfactory. However needs certain modifications for effecting improvements.

Acknowledgement

Work carried out here is a part of Board of College and University Department, Savitribai Phule Pune University (BCUD), Pune funded research project. Authors are thankful to BCUD for providing support for this project.

References

1. L. Xu, F. Liang and T. A. Lipo, 'Transient Model of a Doubly Excited Reluctance Motor,' IEEE Transactions on Energy Conversion, vol. 6, no. 1, pp 126-133, March 1991.

2. F. Liang, L. Xu and T. A. Lipo, 'd-q Analysis of a Variable Speed Doubly ac Excited Reluctance Motor,' Research Report 90-16, pp 849-855, 1990.

3. R. Betz and M. Jovanovic, 'Brushless Doubly Fed Reluctance Machine – a Tutorial.'

4. A. Knight, R. Betz and D. Dorrell, 'Issues with the Design of Brushless Doubly Fed Reluctance Machines : Unbalanced Magnetic Pull, Skew and Iron Losses,' IEEE International Conference on Electrical Machines and Drives, pp 663-668, 2011.

5. Y. Liao, L. Xu and Li Zhen, 'Design of a Doubly Fed Reluctance Motor for Adjustable Speed Drive,' IEEE Transactions on Industry Applications, vol. 32, no. 5, September/October 1996.

6. B. Chalmers and L. Musaba, 'Design and Field Weakening Performance of a Synchronous Reluctance Motor with Axially Laminated Rotor,' IEEE Transactions on Industry Applications, vol. 34, no. 5, September 1998.

7. R. Betz and M. Jovanovic, 'Theoretical Analysis of Control Properties for Brushless Doubly Fed Reluctance Machine,' IEEE Transactions on Energy Conversion, vol.17, no.1. September 2002.

8. R. Betz and M. Jovanovic, 'The Brushless Doubly Fed Reluctance Machine and the Synchronous Reluctance Machine – a Comparison,' IEEE Transactions on Industry Applications, vol. 36, no. 4, July/August 2000.

9. H. Chaal and M. Jovanovic, 'Power Control of Brushless Doubly Fed Reluctance Drive and Generator Systems,' Journal of Science Direct, Renewable Energy, vol 37, pp 419-425, 2012.

10. M. Jovanovic, 'Control of Brushless Doubly Fed Reluctance Motor,' IEEE ISIE 2005, pp 1667-1672, June 2005.

11. S. Ademi, M. Jovnaovic and M. Hasan, 'Control of Brushless Doubly-Fed Reluctance Generators for Wind Energy Conversion Systems,' IEEE Transactions on Energy Conversion.

12. I. Boldea, 'Reluctance Synchronous Machines and Drives,' Oxford Science Publications, 1996.

13. A. Knight, R. Betz and D. Dorrell, 'Design and Analysis of Brushless Doubly Fed Reluctance Machines,' IEEE Transactions on Industry Applications, vol. 49, no.1, January/February 2013.

14. N. Bianchi, 'Electrical Machine Analysis using Finite Elements,' CRC Press, 2015.

Design and Development of a Laboratory Model of Unified Power Flow Controller

Meera Murali **V. N. Pande**
Department of Electrical Engineering
College of Engineering Pune, Maharashtra
E-mail:mm.elec@coep.ac.in; vnp.elec@coep.ac.in

N.Gopalakrishnan
Department of Electrical Engineering
PVG's College of Engineering, Pune
ngkraji1969@gmail.com

Abstract

Unified Power Flow Controller (UPFC) is a Flexible AC Transmission Systems (FACTS) device that can control active and reactive power flow on the transmission line and the bus voltage. Considerable research has been done in the development of various controllers for this device and most of the controller design has been verified through simulation only. In order to understand how to effectively incorporate FACTS devices into existing Power Systems a hardware prototype is necessary in addition to simulation studies. This paper presents the development of various components of the UPFC laboratory model. In this study, the authors have investigated and analyzed the effect of the system for a step change of dc voltage and PCC bus voltage. In order to illustrate the effectiveness of the control algorithm, simulation and experimental studies have been conducted using the MATLAB/SIMULINK and dSPACE DS1104 data acquisition board. The results of the study show a closer agreement between simulation and experimentation.

Keywords : *FACTS; UPFC; Transmission line; Voltage source converter; Laboratory model*

Introduction

FACTS devices hold considerable promise in the form of power system controllers of the new generation. The UPFC is the second generation of the FACTS devices that is able to provide series and shunt compensations in transmission systems [1]. Considerable research work has been done on developing various control strategies of different FACTS controllers mostly through simulation [2].But there is a general lack of experimental verification of many of the proposed controllers under practical conditions. A hardware prototype for verification is quite necessary in addition to simulation studies as the simulation results are unable to replicate the real operational conditions. A few researchers [3-5] have attempted to build the model of UPFC in order to meet this purpose. The information about the laboratory model available in open literature is of low rating only. Hence, a high rating laboratory model (about 10 kVA) will be fully capable of capturing the depth and breadth of large scale dynamics of actual system [3]. The experimental results so obtained will provide valuable data to evaluate different models, test newly proposed algorithms, compare results obtained using different algorithms, and analyse the dynamic performance. Experimental results will provide the basis with which to predict the device performance in actual power system operational conditions. In short the module can be used to study the power system performance in steady state, transient state and post transient steady state conditions. The experimental set-up of UPFC Lab Model consists of following parts :

a) Transmission line.
b) UPFC module.
c) dSPACE 1104.
d) Loads.
e) Sending end and receiving end cubicles.
f) Phase shifting transformer.

Transmission Line Model

Since the publication of a paper on Unified Power

Flow Controller (UPFC) by Gyugyi [6] there is a widespread interest in FACTS controllers as seen by the papers published in open literature [6-13]. A close study of papers [2-3], [14-18] reveal that modeling and parameter selection of transmission line needs to be elaborated in detail. The study of FACTS controllers could have been enhanced by the use of a scaled down model of an existing over head transmission line which will also help the students to understand the behaviour of practical transmission line systems under steady state and transient conditions in both simulation and experimental studies. This lacuna is addressed by fabricating a laboratory model of an existing true line developed on the method of per unit systems widely used in power system literature. It is shown that the performance of the model with that of the true line under steady state and transient conditions can be obtained with good accuracy.

A scaled down model of 620 MVA, 275 kV, 3 ϕ, 50 Hz, 300 km long line, whose parameters are given in [19] is developed. The mutual inductances between the three phases, skin effect and the influence of ground wire are neglected. The highlights of this developed model are :

a) The X/R ratio of the model is kept same as that of the true line.

b) The model is made of six π sections. Each π section will represent a 50 km line.

c) As the current carrying capacity of the model is 20 A it can be used in dynamic studies with good accuracy.

d) The model is flexible i.e it can be arranged to represent a short line, medium line or long line by connecting the requisite number of π sections.

e) While designing and building the hardware, proper care has been taken to see that the complete model is not too bulky but at the same time it is able to emulate the performance of the true line.

The specifications of true line [19] along with those of scaled down model are given in Table 1. The transmission line is fabricated in modules of 50 km. The π section of the model is shown in Figure 1. Based on the information given in [3], [14] the accuracy is taken to be around 0.25% and frequency of interest for harmonics is limited to 600 Hz [16]. This has led to choice of number of π sections of the line to be six. This choice has made the model economical and minimised the error due to numerical calculations.

Table 1 ; Specifications of the transmission line and scaled down model at the rate of 50Hz.

Description	Actual System	Scaled Down System	Value, p.u
Base power	206.667 MVA	3.333 kVA	1.0
Base voltage	158.771 kV	254.034 V	1.0
Base impedance	121.9758 Ω	19.36 Ω	1.0
Power rating	620 MVA	10 kVA	3.0
Voltage rating	275 kV	440 V	1.732
Frequency	50 Hz	50 Hz	1.0
Resistance	0.0345 Ω/km	0.0052 Ω/km	2.7874×10^{-4}
Inductive reactance	0.323 Ω/km	0.0513	2.6×10^{-3}
Shunt admittance	9.52 μS/km	59.696 μS/km	1.16×10^{-3}
Series inductance	0.001 H/km	0.16319 mH/km	8.276×10^{-6}
Shunt capacitance	30.303 nF/km	190.12 nF/km	3.69×10^{-6}

Testing

The testing of the model is carried out in two stages:

A) Hardware testing and

B) Simulation Studies.

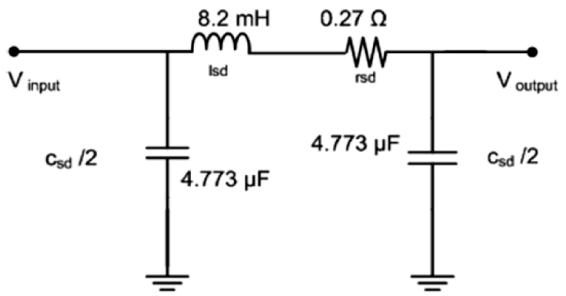

Figure 1 : 50 km model of transmission line (single phase is only shown)

Hardware Testing

The first part of the hardware testing was to measure the inductance and the ESR of the inductor. The ESR value of the inductor came out to be 0.27 Ω and hence it was concluded that there is no need to use the additional resistors. Next part of the testing was to ensure the values of inductance and resistance with respect to current remain constant in the working range of 5 A to 20 A. Once these were confirmed the next part of the testing was to determine the charging current and to verify the bilateral property of the transmission line. The results obtained were the same and the charging current was found to be 1.12 A. Each of the six-π sections fabricated has the required values within a tolerance limit of ± 1 %.

Simulation

A comparison of the performance results of the scaled down model with the true transmission line is necessary under different conditions as detailed below to know whether the transmission line model is able to emulate the true line. For this purpose a simulation study was conducted in MATLAB to determine the following :

i) Steady state values of voltages and currents.

ii) Impedance against frequency characteristic to determine the occurrence of poles and zeros.

iii) Transient and energizing voltage response at the receiving end.

Table 2 : Magnitude of voltages and currents in true line and scaled down model

Name	True Line	Scaled Down Transmission Line
Voltage, V	258541.96	415.38
Voltage, pu	0.944	0.944
Angle, deg	-0.940	-1.03
Current, A	705.71	7.13
Current, pu	0.5429	0.54427
Angle, deg	89.35	89.25
Travelling Time, ms	1.65	1.67
Poles, Hz	[151;444;704;918]	[149;436;695;907]
Zeros, Hz	[2;301;580;819]	[2;297;572;805]

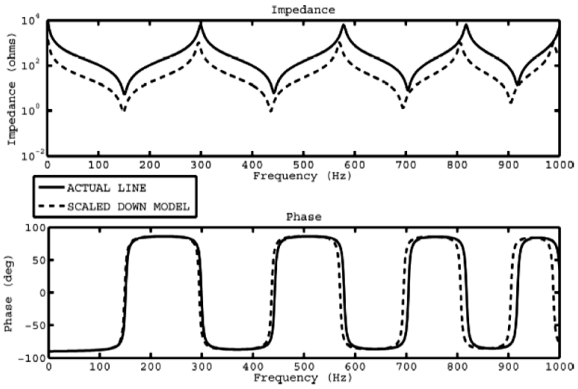

Figure 2 : Impedance against frequency response

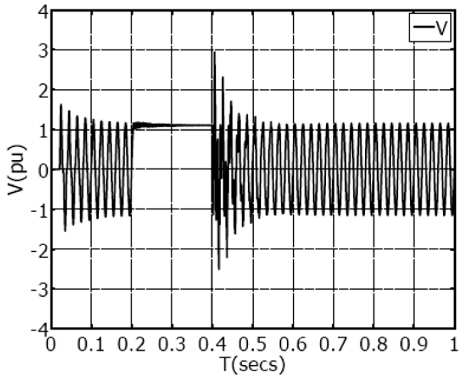

Figure 3a : Transient response of scaled down model

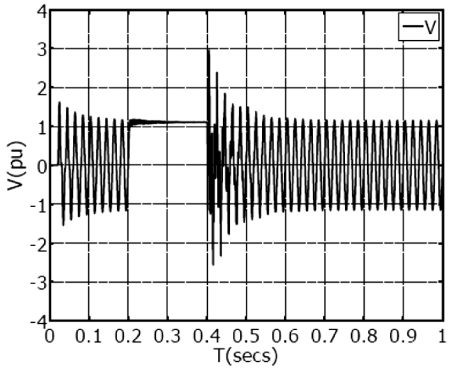

Figure 3b : Transient response of true line

The results are given in Table 2, and shown in Figure 2 and Figure 3, respectively.

UPFC Module

The single line diagram of the experimental setup along with the UPFC module is shown in Figure 4. It consists of four circuit breakers CB1, CB2, CB3 and CB4 that can be used to connect or disconnect manually different FACTS devices like STATCOM, SSSC and UPFC from the test system to

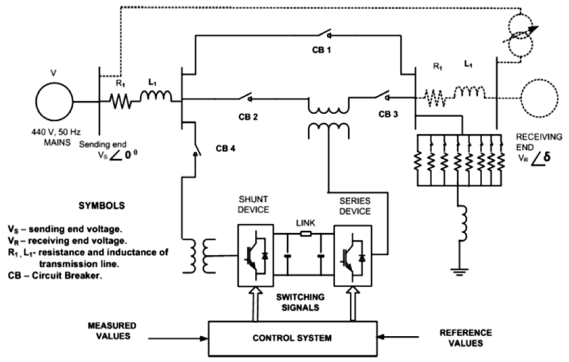

Figure 4 : Single line diagram of experimental set-up

demonstrate the action of these FACTS devices. Depending upon the status of the Cb's performance of various FACTS devices are investigated as given below in Table 3.

Hardware Description

Figure 5 shows the front panel and Figure 6 shows the front view of the UPFC module. The hardware of the UPFC module consists of various components which are described below :

Shunt Transformer

The 3 phase, 10 kVA transformer has its windings wound on a core made of CRGO stampings. It has a primary, secondary and tertiary winding and each phase is identical and rated at 254 V (rms). All the terminals of the windings are brought to the front panel of the module for ease of connection. The windings can be connected in star/delta/zigzag as per requirement.

Table 3 : Status of circuit breakers and links in experimental set-up

CB's Open	Link	CB's Closed	FACTS Device	Remarks
CB2,CB3	OPEN	CB1,CB4	STAT COM	Steady state
CB1,CB4	OPEN	CB2,CB3	SSSC	Steady state
CB1	CLOSED	CB2,CB3, CB4	UPFC	Steady state
CB2,CB3	OPEN	CB1,CB4	STATCOM	Dynamic state
CB1,CB4	OPEN	CB2,CB3	SSSC	Dynamic state
CB1 OPENED SUDDENLY	CLOSED	CB2,CB3, CB4	UPFC	Dynamic state

UPFC Inverters

The UPFC module consists of two 6 pulse inverters. Inverter Bridge I is connected to the ac system through shunt transformer with turns ratio of 1:1. While Converter Bridge II is connected to SSSC through a booster transformer of 10:1 turns ratio. The dc side of shunt inverter is connected to two 10000 μF, 1000 V dc capacitors which are connected in series, while the series side of the inverter is connected to two 3300 μF, 1000 V dc capacitors which in turn are connected in series. A HRC fuse connects the positive sides of the dc capacitors. The midpoint of the shunt capacitors is connected through a metallic link to that of series side capacitors. By opening the metallic links either inverter I or inverter II can be brought into operation.

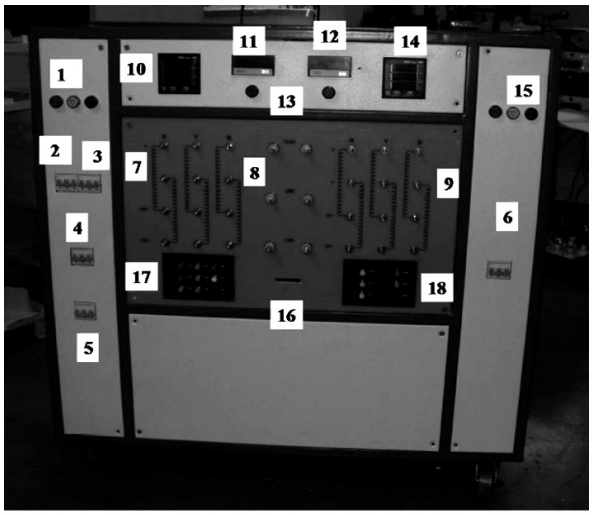

No.1 - Indicators for the 3-φ supply at the sending end.
No.2 to 6 – MCB's 1,2,3,4,5.
No. 7 – shunt transformer terminals for SY side connection.
No. 8 – dc link capacitor connection terminals.
No. 9 – series transformer connection terminals.
No. 10 – Power analyser for sending end.
No. 11 – dc voltmeter.
No.12 – dc ammeter.
No. 13 - Indicators for dc.
No. 14 – Power analyser for receiving end.
No. 15 – Indicators for 3- φ mains.
No. 16 – Slot for dSPACE interconnections.
No. 17 – Connections for CT's 4,5,6,7,8 and 9 input side (sending end) and connections for PT's R,Y,B for input side (sending end).
No. 18 - Connections for CT's 10, 11 and 12 for output side (receiving end)and connections for PT's R,Y,B for output side (receiving end).

Figure 5 : Front panel of UPFC module

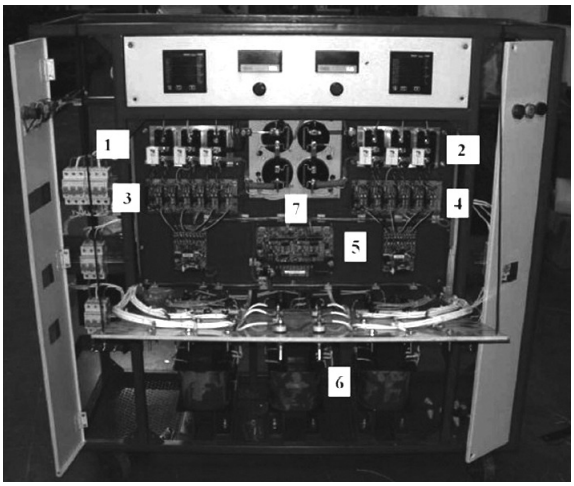

No.1 - IGBT's of Shunt side

No.2 - IGBT's of Series side.

No.3 - Driver Circuit for shunt side IGBT's.

No.4 - Driver Circuit for series side IGBT's.

No.5 - Control Card for interfacing with dSPACE

No. 6 - Shunt transformers.

N0. 7 - DC Capacitors.

Figure 6 : Front view of UPFC module

Choice of Switching Devices

The switching devices used in the UPFC module must have self commutating capability. Power semiconductors which have self commutating capability include GTO thyristor, MOS controlled thyristor (MCT), static induction thyristor(SIT) and insulated gate bipolar-junction transistor (IGBT) [20-21]. The IGBT is extensively used in low and medium applications because of following advantages :

1) Availability of IGBT's of rating up to 1200 A, 4.5 kV.

2) Low on state losses even at high voltage rating.

3) High switching frequency.

4) Simple and low power gate driver requirements.

5) Possibility of Snubberless operation is possible.

Hence, IGBT's 100 A, 1200 V (Mitsubishi IGBT Modules CM 100DY-24NF have been chosen to

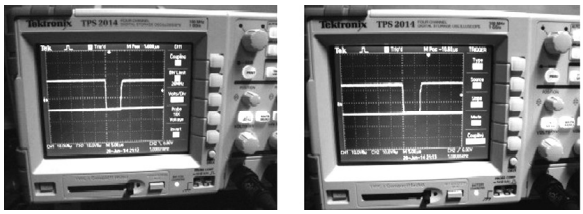

Figure 7: Dead band verification (rise time and fall time)

build the inverters of the laboratory UPFC module. The inverters are operated at 440 V (line to line). Proper snubber circuits are designed and used so as to reduce the electrical stresses on the IGBT switches. Over current protection is also provided. Short circuits across the inverter dc side should be avoided, ie, two switches on the same leg should not be turned on at the same time. This is achieved by designing proper dead-band time. The dead band time that is set is based on the IGBT characteristics. The dead band verification is illustrated in Figure 7.

Driver Card with Protective Circuit and dSPACE Connections

A 12V, 5 A SMPS power supply with isolation gives the necessary power to the driver card for generating the trigger pulses for the IGBT's of Inverters I and II as per the commands received from dSPACE board. Whenever the line current exceeds 25 A or whenever there is a short circuit a protective signal is generated in the driver card shutting down the equipment (Figure 8).

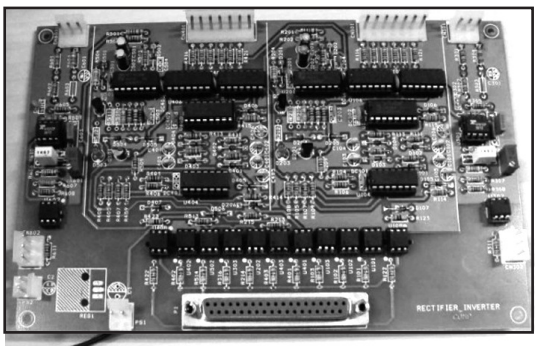

Figure 8 : Interfacing card

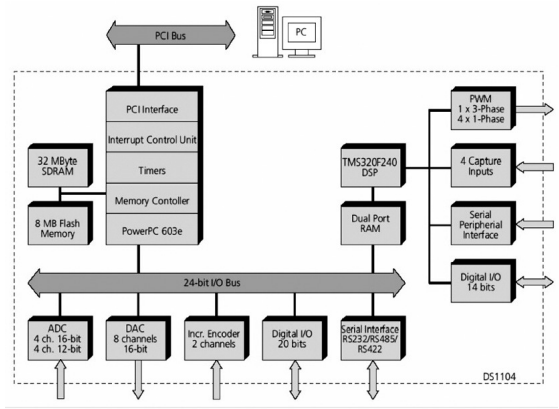

Figure 9 : Functional units of the dSPACE DS1104 PPC controller board

The dSPACE DS1104 Data Acquisition and DSP Board

The host computer is interfaced with the experimental UPFC module through the control desk (CD) software with dSPACE DS1104 PPC controller. The signals like currents, voltages and dc voltages are sensed using current transformers and voltage transducers. The dSPACE Ds1104 R&D controller board [22] is a hardware that upgrades a PC to a powerful development system for rapid control prototyping. It is a single board system based on the 250 MHZ Motorola Power PC 603e processor (PPC). The PPC controller board has the following main parts which are shown in Figure 9.

i)I/O Units

This is set of on-board peripherals. It includes 8 D/A channels, 4 ADC inputs of 16 bit, 8 channels of analog output which are 16 bit, 20 bits of digital I/O ports and a serial interface.

ii) DSP Sub-system

The DSP subsystem is based on Texas Instruments (TI) TMS320F240 DSP. It has three-phase PWM outputs plus 4 single PWM outputs. The resistive load for the UPFC module is of a special design and it is possible to incorporate the dynamic condition by suddenly changing the impedance of the load from the three phases at the same instant

Figure 10 a : Resistive load front view

Figure 10 b : Inductive load

by either switching ON or OFF the MCB's as required.

Loads

The rating of the load is 4kW per phase. Each phase has 8 resistors 50 each connected in parallel and shown in Figure 10a. The variable inductive load 3 phase, 440V, 20 A. is shown in Figure 10b.

Cubicles

To minimise the connections of the UPFC module with other hardware components, two cubicles one for sending end and another for receiving end are designed and fabricated. These cubicles are shown in Figure 11a to Figure 11b. Connectors are provided for connecting the transmission line models, Variac, UPFC module, rectifier and phase shifting transformer. A microprocessor based delta

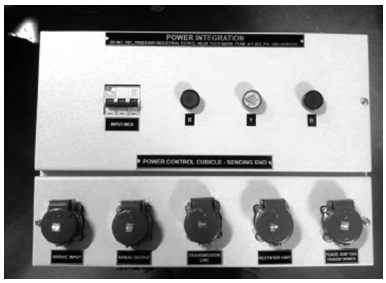

Figure 11a : Sending end

Figure 11 b : Receiving end

measurement is implemented in the receiving end cubicle to measure the phase difference between the sending end and receiving end voltages and display the delta. A phase sequence relay with control circuit is built in each module for monitoring the phase sequence.

Phase Shifting Transformer

The purpose of the phase shifting transformer (PST) is to introduce a phase difference between the sending end and receiving end voltages of the transmission line for power flow. The design of PST was a challenging task, as 3 phase, 440 V, 20 A, 50 Hz, on load tap changer with δ variation from 0° to 40° is not readily available in the market. The PST was constructed as a two core symmetrical PST with one main transformer the primary and secondary are star connected of which taps are

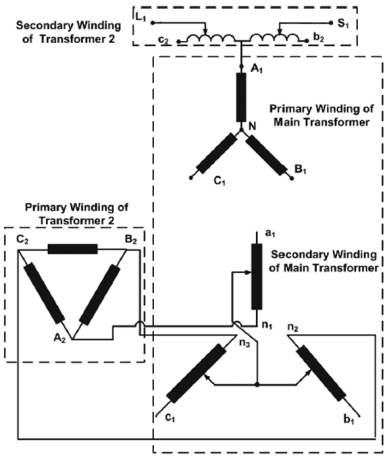

Figure 12 a : Circuit diagram of PST (phase-A secondary only is shown)

Figure 12 b : Front view of PST developed

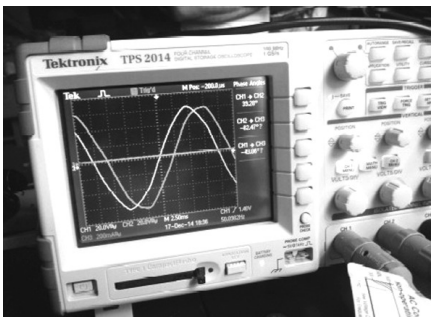

Figure 12 c : Maximum angle of δ

Table 4 : Different values of δ calculated

Calculated δ, deg	Experimental δ, deg
5	7.21
10	12.22
15	16.91
20	21.49
25	26.29
30	32.43
35	36.23
40	39.28

provided on the secondary side. The series transformer consists of a primary transformer which is delta connected and secondary has centre tapped windings for each phase and centre tap is connected to the primary of the main transformer as shown in Figure 12a.

Simulation and Experimental Results

The overall experimental setup of UPFC module and its accessories is shown in Figure 13. The parameters of the UPFC laboratory model such as resistance and leakage inductance of shunt and series transformers are obtained experimentally and are given in the Table 5.

Using these parameters a mathematical model of UPFC is developed in MATLAB SIMULINK. A simulation study to observe the response of the

Table 5 : Parameters of UPFC model

Parameters	Symbol	Values
Frequency	f	50 Hz
Angular frequency	ω	314 rad/sec
RMS line to line voltage	V_s	260V
Transmission line	R_s	0.27Ω
	L_s	8.2 mH
DC link capacitor	C_{dc}	6650 μF
Shunt transformer	R_{sh}	1.55 Ω
	L_{sh}	2.59 mH
Series transformer	R_{se}	23.8 Ω
	L_{se}	62 mH
Load Parameters	R_{lf}	25 Ω
	L_{lf}	24.61 mH

system is carried out for 25 sec for step response in the dc reference voltages and load bus reference voltage.

Scenario I : Change in dc Link Voltage (v_{dcref})

After the system reaches steady state at t = 1.5 sec a step disturbance is given wherein the dc voltage reference value (v_{dcref}) is changed from 480 V to 460 V. Similarly a step disturbance is introduced at t = 6 sec where vdcref is changed from 460 V to 480 V in simulation. In the hardware setup, the dc link voltage has to be kept higher because of voltage drop in the transformer impedance, cables and contact resistances etc. A step disturbance is introduced from 520 V to 500 V in hardware at t = 1.5 sec; and another disturbance occurs at t = 6 secs when the dc reference value vdcref is restored to its original value of 520 V from 500 V. The simulation and hardware results are shown in Figure 14a to Figure 14b respectively. In both the cases the dc link voltage can be seen to follow closely the change in the dc reference value and settle down to the set value quickly.

Figure 13 : Experimental setup of UPFC lab model

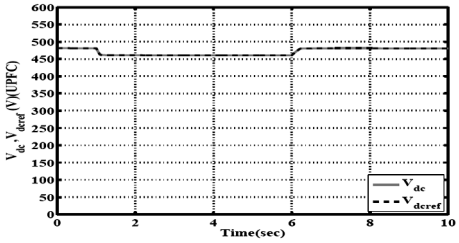

Figure 14a : V_{dc} and V_{dcref} (simulation)

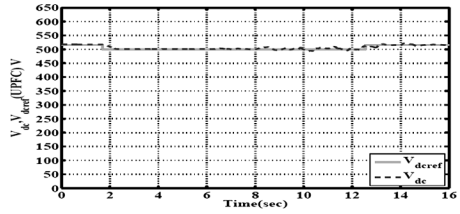

Figure 14b : V_{dc} and V_{dcref} (hardware)

Scenario II : Change in Load Bus Voltage (v_2)

At t = 15 sec a step disturbance is given wherein the voltage reference value (v_2) is changed by 6 V. Due to the limitations of the hardware this voltage can be changed only by ± 5% of the supply voltage. At t =20 sec the voltage is reduced by 6V in simulation.

Similar disturbances are introduced in the hardware at t =16.95 sec and t =20.95 sec respectively. From the waveforms-simulated waveforms (Figure 15a and Figure 15c) and hardware waveforms (Figure 15b and Figure 15d) it is seen the results fairly agree.

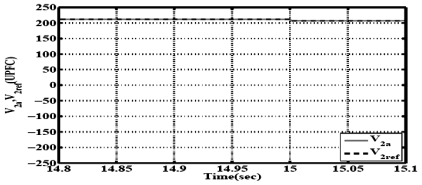

Figure 15a : V_{2ref} and V_{2act} (1st disturbance simulation)

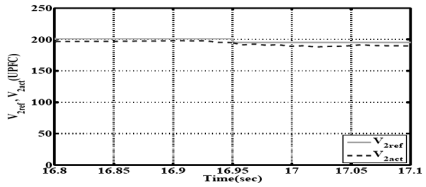

Figure 15b : V_{2ref} and V_{2act} (1st disturbance hardware)

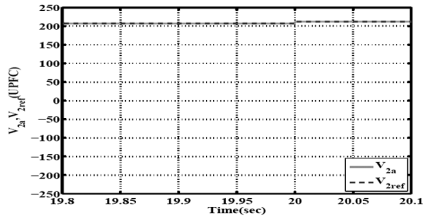

Figure 15c : V_{2ref} and V_{2act} (2nd disturbance simulation)

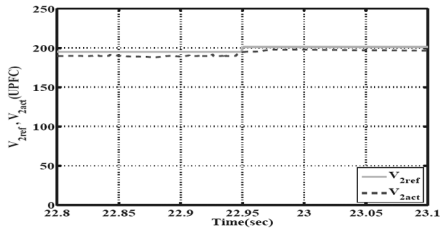

Figure 15d : V_{2ref} and V_{2act} (2nd disturbance hardware)

Conclusion

This paper has presented in brief the design aspects and development of the experimental setup of the UPFC laboratory model. The description of the state- of- the- art. DSP dSPACE DS1104 and its integration with the UPFC module are also explained. The PI based controller developed for the module isexperimentally verified using the laboratory model. This laboratory model will provide an excellent platform to design new novel controllers and validate them experimentally emulating practical conditions in the power systems.

Acknowledgment

The financial assistance from the Department of Science and Technology, Government of India, under the FAST TRACK SCHEME for young scientists, because of which the work reported in this paper was possible is gratefully acknowledged. The financial support received from Alumni Association of College of Engineering Pune, Maharashtra (COEP) and the assistance received from the Department of Electrical Engineering, COEP in terms of equipments is also duly acknowledged.

References

1. M.E.A.Farrag and G.A.Purtus, 'Design of an Adaptive Neuro-fuzzy Inference Control System for the Unified Power Flow Controller', IEEE Transactions on Power Delivery, vol. 27, pp. 53-61, January 2012.

2. K.A.Corzine and M.L.Crow, 'Power Engineering Laboratory Facilities at the University of Missouri-Rolla,' IEEE Transactions on Power Systems, vol. 2, pp. 1187-1191, 2005.

3. L.Dong, M.L.Crow, Z.Yang and L.C.Shen, 'A Reconfigurable FACTS System for University Laboratories, IEEE Transactions on Power Systems, vol.19, pp.120-128, February 2004.

4. K.Wang, M.L.Crow and Y.Cheng, 'Development of a FACTS Real Time Hardware in the Loop Simulation,' 39th North American Power Symposium, NAPS'07, pp. 118 – 123, September 2007.

5. T.Aihong and C.Shijie, 'UPFC Control Algorithm and Implementation Scheme in Laboratory,' IEEE Conference and Exhibition on Transmission and Distribution, pp. 1-6, 2005.

6. L.Gyugyi, 'Unified Power Flow Control Concept for Flexible ac Transmission Systems,' IEE Proceedings-C, vol. 139, pp. 323-331, July 1992.

7. L.Gyugyi, T.R.Riedman, A.Edris,C.D.Schauder, D.R.Torgeson, S.L.Williams, 'The Unifiifed Power Flow Controller : A New Approach to Power Transmission Control", in IEEE Transactions on Power Delivery, vol.10, pp. 1085-1095, April 1995.

8. I.Papic, P.Zunko, D.Povh and M.Weinhold, 'Basic Control of Unified Power Controller,' IEEE Transactions on Power Electronics, vol. 12. pp.1734-1739, November 1997.

9. M.Toufanm and U.D.Annakkage, 'Simulation of the Unified Power Flow Controller Performance using PSCAD/EMTDC,' Electric Power Systems Research, vol. 46, pp. 67-75, July 1998.

10. T.Makombe and N.Jenkins, 'Investigation of a Unified Power Flow Controller,' IEE Proceedings-Generation, Transmission and Distribution, vol. 46, pp. 400-408, July 1999.

11. C.T.Chang and Y.Y.Hsu, 'Design of UPFC Controllers and Supplementary Damping Controller for Power Transmission Control and Stability Enchancement of Longitudinal Power System,' IEE Proceedings – Generation, Transmission and Distribution, vol. 149, pp. 463-471, July 2002.

12. D.J.Won, I.Y. Chung and S.I.Moon, 'Determination of Equivalent Impedance of UPFC Voltage Source Model drom the Dynamic Responses of UPFC Switching Level Model,' Electrical Power and Energy Systems, vol. 25, pp. 463-470, July 2003.

13. I.Papic and A.M.Gole, 'Frequency Response Characteristics of the Unified Power Flow Controller,' IEEE Transactions on Power Delivery, vol. 18, pp. 1394-1402, October 2003.

14. H.Fujita, Y.Wanatabe and H.Akagi, 'Control and Analysis of Unified Power Flow Controller,' IEEE Transactions on Power Electronics, vol. 14, pp. 1021-1027, November 1999.

15. H.Fujita, Y.Wanatabe and H.Akagi, 'Dynamic Performance of a Unified Power Flow Controller for Stabilizing ac Transmission Systems,' Power Electronics Specialists Conference Proceedings, vol. 1, pp. 1348-1354, October 1998.

16. H.Fujita, Y.Wanatabe and H.Akagi, 'Transient Analysis of Unified Power Flow Controller and its Application to Design of dc Capacitor,' IEEE Transactions on Power Electronics, vol. 16, pp. 735-740.

17. S.Paul, S.K.Base and R.Mondal, 'A Microcontroller Controlled Static Var Compensator for Power Systems Laboratory Experiments,' IEEE Transactions of Power Systems, vol.7, pp.370-376, February 1992.

18. R.Jayabharati, M.R.Sindhu, N.Devarajan and T.N.P.N Ambiar, 'Development of a Laboratory Model of Hybrid Static Var Compensator,' IEEE Conference Publications.

19. B.M.Weedy and B.J.Cory, Electric Power Systems. 4th Edition, John Wiley and Sons (Asia) Pvt. Ltd., Singapore, 2002.

20. N.Mohan, T.M.Undel and W.P. Robins, 'Power Electronics : Converters, Applications and Design,' John Wiley and Sons Pvt. Ltd.

21. M.H.Rashid, 'Power Electronics : Circuits, Devices and Applications,' Pearson Education Pvt. Ltd.

22. dSPACE-DS1104, R&D Controller Board. dSPACE GmbH.

Innovative Solutions for Decentralized Distributed Generation (DDG)

P. P. Gupta I. K. Tiwari M. Jadhav A. Rajoba S. V. Lobo

Tata Power Company Limited, Mumbai, Maharashtra

E-mail:prashant.gupta@tatapower.com; Indresh.tiwari@tatapower.com; sydneylobo@tatapower.com

Abstract

With the advent of industrialization, the need of the hour is to strike a critical balance between man and nature which can be struck by efficient engineering and by adopting cost effective, innovative as well as environment friendly technologies. Tata Power (one of India's largest private utility company), has been a pioneer in advocating sustainable development. The business model of Tata Power has sustainability as one of its pillars and community development has always been on the forefront of Tata Power's projects. The projects which are highlighted in this abstract focus on decentralized distributed generation development in the field of solar, hydro, gasification and bio gas generation.

Keywords : *Sustainability; Innovation; Decentralized distributed generation; Solar; Hydro kinetic turbine; Biomass gasification; Bio-gas; Telecom tower*

Abbreviations

ac : alternating current

dc : direct current

DDG : decentralized distributed generation

DG : diesel genset

Ip67 :internal protection class

kWp : kilowatt at peak capacity

LPG : liquefied petroleum gas

MPPT : maximum power point tracking

PLF : plant load factor

PV : photovoltaic

TPCL : Tata Power Company Limited

4G : fourth generation services from telecom companies

Introduction

United Nations report [1] defines sustainable development as development that meets the needs of the present without compromising the ability of the future generations to meet their own needs. This involves conserving the environment and at the same time bringing about overall development of the society. This critical balance between man and nature can be struck by efficient engineering and by adopting cost effective, innovative as well as environment friendly technologies. Tata Power (India's largest private power company, has been a pioneer in advocating sustainable development. The business model of Tata Power has sustainability as one of its pillars and community development has always been on the forefront of Tata Power's projects. Some of the initiatives taken by the clean tech projects department at Tata Power in the clean energy development and in the community development areas are described in this paper.

Tata Power Initiatives

Under the current centralized generation paradigm, electricity is mainly produced at large generation facilities, such as, large thermal power plants, solar parks, wind parks or hydro plants. The electricity is then shipped through a vast network of transmission lines and distribution grids to the end consumers. This also leads to lot of

losses and the final electricity reaching the end consumer is only some fraction of what is generated. There is a recent quest for energy efficiency and reliability and reduction in green house gas emissions which lead to explore possibilities to alter the current generation paradigm and increase its overall performances. Decentralized distributed generation which means generating close to the point of use helps in mitigating most of the problems highlighted above and also helps in providing an increase in energy efficiency by reducing transmission and distribution losses. This paper focuses on decentralized distributed generation and the various innovations which have been implemented by Tata Power and which are proving to be a successful model for replication in the decentralized distributed generation space.

Hydro

Tata Power has three hydel power plants (in MW range) generating electricity by using the hydro energy. In this process, it also has water in its tail races which flows at velocities ranging between 1 m/s to 3 m/s. In its endeavor for adopting innovative technologies as well as for making best use of the resource available, Tata Power has installed a 10 KW hydro kinetic turbine in the tail race of its hydro power station at Bhira. The uniqueness of this turbine is that it can generate electricity if water streams have velocities ranging between 0.75 m/s to 4.2 m/s and at water depths exceeding 2.5 m. This pilot has run consistently for the last 18 months and has given encouraging results. Tata Power has assisted the technology provider (M/S Casmir Group) to indigenize the turbine (generator stator winding including lamination punching and power evacuation–10 kW variable ac-dc-50 Hz, 415 V, 3 phase ac) and bring the cost down further making power affordable for the inhabitants living around such river / streams. Figure 1 describes the setup used to evacuate

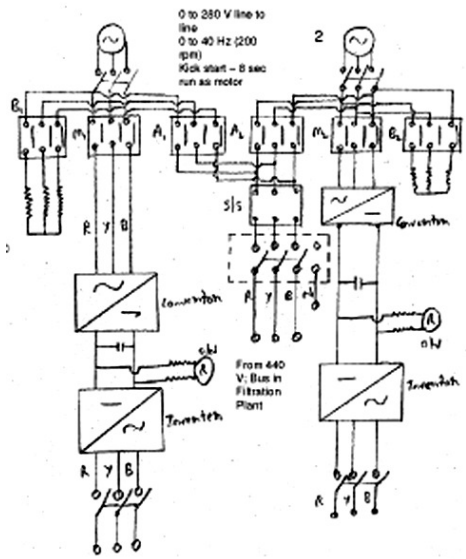

Figure 1 : Development work on power evacuation system

power using simple three phase bridge rectifier, storage capacitor and solar inverter with MPPT to extract maximum power.

The activities conducted include improving the efficiency of the existing inverter by selection of more efficient components as well as providing an ideal test bed during the development and refinement phase. Figure 2 gives a snapshot of the installation at the tail race in Bhira.

Efforts are also ongoing to fine tune the commercially available matrix inverter with the turbines.

This project will also aim to provide electricity to the areas along the river streams wherein the above

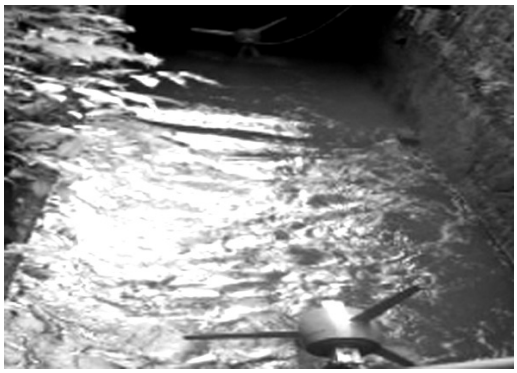

Figure 2 : Snapshot of the installation in the tailrace at Bhira, Maharashtra

technical parameters are satisfied. Tata Power has developed this decentralized distributed Generation solution that can be deployed in tailraces of existing hydro power plants, rivers and canals. This way small cluster of decentralized distributed generation can be developed along water bodies. This technology is also suitable for extracting power from ocean currents since the blades are bi directional and the material used is compatible for harsher conditions encountered in sea. The technology is also scalable as many such turbines can be installed to cater to a larger population / cluster of villages along the tail races, rivers and canals.

Solar

Tata Power has successfully commissioned three solutions in the solar space. Features of the same are described below:

Single Axis Tracker

The strategic location of India makes it a great source of solar power. In its endeavor to promote renewable power production, Tata Power has commissioned a solar system at an institute in Lonavala, a hill station between Mumbai and Pune in Maharashtra, India. This system has a capacity of 69.12 kWp (288 PV modules of 240 W each with single axis tracking) and is providing a plant load factor (PLF) of 17% based on site having solar irradiance of 500 W/m^2 to 750 W/m^2. This irradiance is generally low and not very ideal for solar PV installation leading to low PLF in such areas. In order to boost PLF, Tata Power installed a single axis east west tracker which tracks the movement of the sun and tilts the angle of the solar panels by 10 every 4 minutes. This feature has increased the PLF by 15% as compared to a fixed tilted system. The system was installed and has been generating exceeding expectations.

Figure 3 gives an illustration of the solar installation at the institute in Lonavala. The tariff

Figure 3 : Snapshot of the installation at the institute in Lonavala

structure is such that the customer is saving on his electricity bill and thereby also paying off the investment in the solar plant quickly. This is a successful model for DDG in areas which have moderate to high solar irradiation. The system is engineered in house in such a way that it can be scaled up to a size of a MW sized plant as well as installed on a rooftop at kW scale, thus taking care of the scalability and replicability aspects.

Floating Solar

It is well known that land is a precious commodity and solar projects require lot of land. Typical estimate is 4.2 MW to 4.4 acres/MW. Land availability as well as affordability are therefore two stumbling blocks for any solar based power plant. To address this issue, Tata Power has designed an in house floating system with techno commercially optimal materials which can support solar modules and float them on water bodies. This allows solar based PV installations to be located on water bodies and thereby not compete for precious land. A demo of 30.6 kWp capacity has already been installed in the hydro

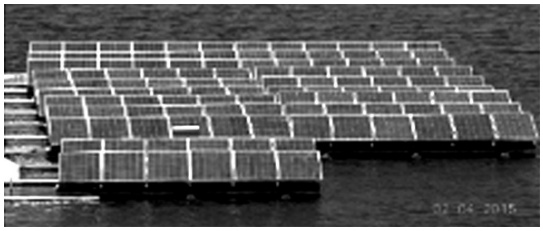

Figure 4 : Snapshot of the 30.6 kWp installation at Walvhan anchoring system designed for floating the system on water body

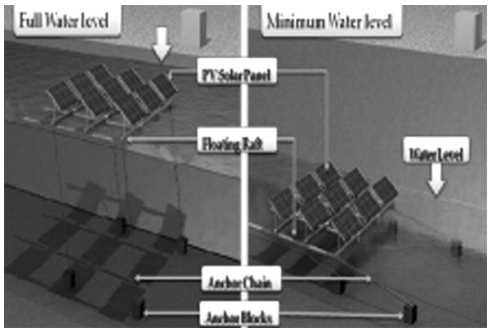

Figure 5 : Illustration of the unique anchoring system

area at Walvhan and is working successfully for the past five months. Figure 4 gives a snapshot of the installation and Figure 5 gives an illustration of the unique anchoring system.

The salient features of the system are illustrated below:

- The system is grid connected. Can withstand wind speeds up to 150 km/hr.
- Solar modules are PID free, light in weight, have positive tolerance of power and are splash proof.
- In house power evacuation system wherein cables are floated on water thereby avoiding need of submarine cables.
- Plant has generated a total of 9429 kWh till 26/8/2015.
- String inverter placed on the raft itself.
- Anchoring system which allows only vertical movement depending upon the level of the water body but does not allow any lateral movement. Also a reel in reel out arrangement to anchor the position is designed. This is especially helpful during monsoon when high waves tend to be created owing to windy conditions.
- Earth leakage protection and graded surge protection provided. A walkway provided in passage of string combiner box.
- No harmful effects to local flora and fauna as certified by a National Environmental Institute.
- Entire design as well as integration and installation done in house.
- The terminal box of the solar module is conforming to Ip67.
- Reduction in evaporation loss of water due to high ambient temperatures in summer.
- Expected increased yield in performance of modules due to passive cooling when compared with land based systems.
- Engineering done in such a way that the entire system can be scaled up to a MW capacity depending upon the lake area available.
- Entire system is scalable and replicable and we are in talks with interested parties for the solution to be deployed in other water bodies.

This system being in house is also cost effective and makes the overall solar power cost affordable, sustainable and competitive with land based systems. This system will be utilized as part of solar systems to be installed on still water bodies as a DDG solution which will ensure electricity supply to inhabitants across still water bodies.

Back up Supply for Telecom Tower

Tata Power has also demonstrated a solar solution for telecom towers at one of the telecom tower location in the senior camp site next to our hydro power plant at Bhira. The solution installed has a capacity of 3.75 kWp and has been catering to the electricity requirements of the double BTS site since 1/4/2015. Figure 6 gives a snapshot of the installation of the system.

Figure 6 : Snapshot of the installation over the porta cabin at the senior camp site in Bhira (about 100 km from Pune)

The salient features of the system are described below:

• In house design of the structure on which solar modules are installed. As can be seen from the installation, the installation is on top of the portacabin (which houses the power management system) thereby not competing for any land.

• Makes use of solar modules under the thin film category thereby generating even in dim lights / shadow. This is particularly advantageous as the tower shadow will fall on the modules thereby hampering generation in case of polycrystalline based PV modules.

• Since telecom towers have to ensure 100% availability, they need uninterrupted power. In areas, wherein grid availability is less, telecom towers utilize diesel gensets as back up power source. This solution will be reducing dependence on the diesel gensets thereby resulting in savings in diesel related expenditure to telecom tower operators as well as help in curbing release of green house gases.

• In house optimization of the power management system resulting in enhanced life of existing battery (temperature compensated charging cycle introduced and check on voltage difference within battery bank). This value addition has been tested at the demo site with considerable success.

• The power conditioning unit in the current set-up is capable of accepting input from four different sources (solar, wind, Grid, diesel genset all simultaneously) and can also accord priority to the input source which should be consumed by the telecom tower power electronics first. It also offers the role of a SMPS and thus can replace even a SMPS in existing telecom sites. It can be easily retrofitted in existing telecom sites and has an efficiency of 95%.

• Overall generation so far (data till 25/7/2015) indicates solar system has supplied 32.9% in April, 38.8% in May, 18.62% in June and 17.93% in July of the total electricity requirement by the telecom tower site. Further add on can be incorporated as per site requirement. This scheme is cost effective as long as the power generated is equal to /less than that of DG capacity.

Replication of this solution at other tower locations will help in utilizing renewable energy and minimize utilization of diesel in diesel gensets which are used currently for back up power requirements in telecom towers. The solution currently is in use for a single tenant site but can be scaled to cover the double and triple tenant sites also. This solution can also be scaled to the soon to be launched 4G services across the country.

Gasification

Tata Power has commissioned a 14 kW biomass based gasification system in our colony in Trombay. Tata Power has also developed in house a 8 kW to 14 kW gas engine through Tata Motors in collaboration with Indian Institute of Science. This system takes in the biomass (twigs, fallen tree branches from streets, coconut shells, etc.) and produces producer gas which is then used to light up the street lights in the colony. The system is run in the evening to cater to the street light requirements. Figure 7 gives a snapshot of the installation in our premises in Trombay colony.

It is also widely know that the kind of biomass varies across various geographies. It therefore makes sense to devise a system which can accept

Figure 7 : Snapshot of the installation of 14 kW gasifier at Trombay colony

any form of biomass thus providing some kind of fuel flexibility. Tata Power is developing an in-house gasification system which shall be able to accept any form of biomass in thousands of villages across India requiring 10 kW to 20 kW of power. The gas produced is used to run a gas engine which then generates electricity. This multi fuel capable system is likely to be commissioned shortly and shall be a demo unit to be put up in Tata Power's hydro areas.

The results from the demo unit will be used to optimize the system which can be replicated as a DDG solution across villages in India.

Waste to Energy

All over India, lot of solid waste is generated which ends up in the dump yards. This is not only a health nuisance but also a social stigma. This waste is accumulating in the dump yards and soon the dump yards will run out of space to accommodate fresh waste produced on a daily basis across India. To address this issue, Tata Power has used the age old technology of a '*gobar* gas plant' and further modified it to take in food and canteen waste for energy generation. The generated gas is being utilized for cooking purposes, thereby saving on liquefied petroleum gas (LPG). This plant is running at our hydro plant in Khopoli wherein residential food and canteen waste is used to produce bio gas daily to be used as cooking fuel in the canteen. As a measure of performance, 20 kg of food waste generates roughly 1 Nm^3 of bio-gas. As it turns out, substituting the cooking fuel with the gas generated from the bio gas plant is more economic than generating power from this resource. As of now, the entire cooking is being done on bio-gas and has substituted LPG in the area. This is a successful model which can very well be replicated in areas where kitchen waste is available.

Tata Power has also installed on similar lines a 2 TPD bio-gas plant in one of its thermal stations in Mumbai wherein the waste from the canteen is fed to an anaerobic digestor (underground pit) and bio gas is collected in a floating dome on top of the pit. This gas is then used to run the cooking stoves in the canteen in place of LPG based cylinders. As of now this system has run for four years and has reduced the dependency on LPG by half at the power station. The standalone bio-gas solution can be easily replicated in areas wherein food waste is produced in plenty such as agricultural yards, cdf abbatoirs, food plazas, malls as well as gated communities and municipal corporations. The solution also helps in reducing the amount of waste going into the landfill thereby saving on precious land as well as improving the overall hygiene and standard of living.

Going forward, Tata Power is developing solutions wherein efficient utilization of plastic waste and food waste shall be demonstrated at a food mall on the national highway. This solution shall provide oil and bio-gas as by products which shall help in solving the solid waste problem as well as create value added products.

Conclusion

All in all, it can be seen that being a responsible corporate citizen we are devising models which can sustain on their own thereby creating a win win situation for all stakeholders involved. These solutions are not only contributing in reducing dependence on conventional fuels for basic energy needs but also reducing green house gas emissions thereby helping in conserving the environment. The initiatives also have a revenue stream thereby making the overall models sustainable. The focus is therefore to implement more such solutions in the decentralized space so as to achieve the objective of spreading invisible goodness as well as be sustainable.

Reference

1. WCED, http://www.un.org/documents/ga/res/42/ares42-187.htm.

Real Time Monitoring and Fault Detection System for Solar PV Field

Sumon Dey **G. S. Ayyappan** **Kota Srinivas**
CSIR-Central Scientific Instruments Organization,
Chennai, Tamil Nadu, India
E-mail : sumondey0305@gmail.com

Abstract

With increasing installations of solar farms, monitoring and detection of faults in PV plants has gained ample importance for the healthy and optimum functioning of the plants. DC side of PV system involves common faults such as line-line short circuit, open circuit and mismatches due to shading and degradation in PV arrays which lead to damage of good modules and even fire hazards. A system was devised that can alert the plant owner in case of any fault in the system and efficiently specify the reason of failure and location of fault. An algorithm was formulated and tested for 1 kW simulated PV farm to detect and locate faults depending on analysis of the parameters which are monitored continuously. The validity of the fault simulations was verified using an experimental 450 W solar farm set up. The algorithm successfully detected, specified and located faults on the practical set up. The developed monitoring system can be easily implemented in real time and can be used as a reliable tool for fault diagnosis in PV systems.

Keywords : *Data analysis; dc side; Fault detection; Fault location*

Introduction

The need for alternatives to fossil fuel based energy generation sources and growing concern for global environment has resulted in burgeon of solar photo voltaic installations. The total installed capacity in India as on April 2015 is 3.74 GW according to Central Electrical Authority (CEA) [1]. Photovoltaic systems are basically designed to trap the solar energy directly and convert it to electricity. In order to generate the maximum possible energy, the entire system design needs to be proper.

Though manufacturers specify the life of the PV modules to be 25 years, the fact that PV systems are exposed to environmental conditions, brings various disturbances in the system. The faults in the DC side include grounding issues, line to line fault, open circuit fault, mismatch between the power generating units, partial shading of the panels and so on. Such faults may occur due to contact failure, corrosion of wire, hail impact, moisture, etc as stated by Bazzi et al.[2]. Two years monitoring study of 27 PV systems by S. K. Firth [3] showed an annual fault occurrence rate in the range of 1.1% to 11.7%. Since the system consists of interconnected PV modules, failure of just one module may lead to severe output power reduction. 7 fire emergency scenarios originating from solar installations have been reported [4]. These mishaps were due to faulty insulation material, short circuit in combiner box, electrical arcing between PV modules and so on. PV faults and subsequent fire-hazards on April 5, 2009, in Bakersfield, California, and April 16, 2011, in Mount Holly, North Carolina due to ground fault and line-line fault provide clear evidence of lack of

knowledge among PV system manufacturers and installers about different PV faults [4].

Finding fault and locating it, can help in faster recovery of fault. It has direct benefit of reduced power loss during the fault period. Secondly, early detection of fault would result in a reduced risk of accidents like fire hazards which may affect both personnel and installed equipments. Due to the large size of the PV plants it is very difficult for personnel to locate the fault. Therefore, fault locating algorithm would result in less labour requirement for the equivalent amount of monitoring. In the long run, it would lead to more cost-effective installations and improve sustainability of PV systems.

Several fault detection procedures have been proposed and experimented in literature partially or completely fulfilling the objective of fault finding and locating. Due to the ease in collecting these electrical parameters, most of the present fault detection techniques are based on electrical equivalent model of solar panel rather than techniques like visual and thermal imaging. A Chouder and S Silvestre proposed monitoring systems based on power loss approximation [5]. Some fault detection systems are based on high frequency reaction measurement and time domain reflectometry, where a high frequency noise is fed into the system and the reflected signal is analysed to find the fault [6],[7],[8]. Such method of fault detection involves huge cost and complexity. Zhao et al [9] proposed a decision tree-based diagnostic method for photovoltaic cells. Fault location finding had not been achieved by this algorithm. Tadj et al [10] proposed a GISTEL model to diagnose the PV array based on fuzzy logic based satellite image. In order to increase the accuracy in fault diagnosis, intelligent machine learning algorithms have been used [11], [12],[13]. These algorithms had been successful in diagnosing the line to line fault type. In another work artificial neural network had been used to estimate the voltage of individual modules [14]. Here fault location could be found. But the algorithm when applied to huge field becomes too complicated. In 2013, outlier rules had been used to detect faults in solar PV system [15]. The faults like line-line faults with and without fault impedance, open-circuit faults, degradation faults and partial shadings had been detected by this method. But this method did not state the user the reason of the fault. Further the panel level fault location was not done by this method.

The goal was to develop a system that could analyze the data received from the solar field and specify and locate the fault in the system. For this purpose, it was important to study the effect of the various faults on different parameters of the PV system. Hence a MATLAB Simulink model of PV farm was constructed and faults were simulated to understand their effects. Further for diagnosing the fault, an algorithm was developed that could detect and locate the faults accurately. It was then implemented in hardware and tested in a small PV farm.

Simulation and Study of Effect of Faults

Performance of a PV system is basically interdependent. The weakest link in the system which is the poorest performing module limits the power generating capability of the entire system. So in order to devise a fault detection system it was necessary to understand how the system parameters are affected by faults. The effect of various kinds of faults on the PV system had been studied by simulating the faults in MATLAB simulink environment. The effect of faults on the I-V characteristics and the maximum power point (MPP) was analyzed. In these simulation studies it was considered that fault in PV array are the only source of fault. Since fault current settles in negligible time, the effect of transients was not considered in this study. Therefore, the focus in

this study is on the system state before fault (pre-fault condition) and state after the fault (post fault condition).

The P-V and I-V characteristics of solar cell were plotted using the MATLAB Simulink tool by varying the load connected to it [16]. To study the effect of faults on the working of panel, the 10 W solar panels were connected in 5 × 4 configuration to form a 200W solar array. Bypass diodes were connected with each solar panel. Blocking diodes were also connected in each string to prevent the flow of negative current through the panels. As per NEC requirement, the negative bus of the system was grounded.

Line-Line Fault

In a PV system, line-line fault mainly occurs when there is a short circuit of PV modules or interconnection of cables of different potential. Insulation failures of cables caused due to animals chewing the cable insulation, short circuit in DC junction box are some of the major reasons for this fault. Different line-line fault conditions were simulated by shorting the panels as shown Figure 1a. The effect of faults on PV curve is shown in Figure 1b. It is seen that short circuit of 1 panel causes a power reduction up to 16%. String current reduces to zero when the operating voltage is greater than open circuit voltage of string.

Open Circuit Fault

An open-circuit fault is caused by an accidental disconnection of a normal current-carrying conductor. This is a common failure that may occur in the solar field. Open circuit may be due to cell cracking. Fatigue due to cyclic stress and wind loading may also cause disconnection of the wiring which may lead such failure. Such faults may lead to high voltage wires left open and hence risk of shocks. Different open circuit fault conditions were simulated as shown in Figure 2a. The effect of faults on PV curve is shown in Figure 2b. It is seen that one open circuit leads to power reduction which is proportional to the amount of field open circuited.

Mismatch Fault

Mismatch in PV module is said to occur when electrical parameters of one or more panels are significantly changed from the others. Since solar panels are dependent on the irradiance and temperature, variation in irradiance and temperature among the interconnected cells also leads to mismatch faults. They are the most common compared to that of line-line and open circuit fault. Further, they often lead to irreversible damage of PV modules and hence contributing to greater power loss. Conventional protection devices cannot detect these faults as they do not cause high fault current. These faults can be divided into two groups, permanent and temporary. Temporary mismatch may be due to shading or dust accumulation which can cause huge power reduction up to 50%. Permanent mismatch could be due to hot spot formation, PN junction degradation or anti-reflective coating deterioration. Degradation of just 1 panel could lead to a reduction of power by 3%-5%.

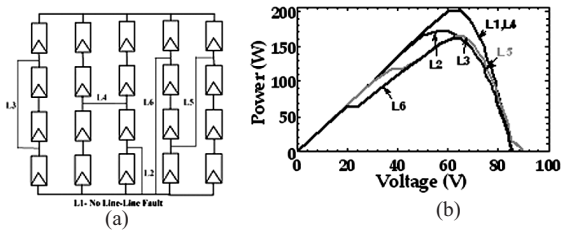

(a) (b)

Figure 1 : Line-line fault (a) different faults created, (b) PV curves under faulty conditions

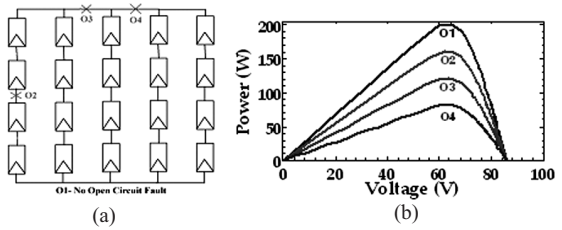

(a) (b)

Figure 2 : Open circuit fault (a) different faults created, (b) PV curves under faulty conditions

From the simulation study it can be concluded that plant performance varies non linearly which the amount of fault created. Fault in a particular panel may affect the entire system. Moreover the problem of fault finding becomes difficult as the plant operates at the same operating point under different fault conditions.

Fault Detection – The Proposed Algorithm

Fault detection can be accurately done only by analysing the variations in the voltage and current of individual panels under different faulty conditions. For this purpose the string currents and panel voltages at maximum power point was collected. Therefore, for a 2×5 solar field, the data collected were irradiance (I_r), temperature (T), currents in each string (I_{si}= current in string I) voltage across 10 panels (V_{pij}= voltage accross panel j in string I) and the entire system voltage (V_{meas}), current (I_{meas}) and power (P_{meas}) at maximum power point. A 1 kW solar field was simulated under different faulty conditions and the results were stored in a database to observe the trends of panel voltages and string current. The algorithm was then formulated for detecting and finding fault as shown in Figure. Taking irradiance and temperature data, estimated value of power was found using a MATLAB model of the actual solar plant. This value is then compared with the actual power being produced are compared to find if there is a fault. Further string currents and panel voltages are compared to find the reason and location of fault. The flowchart for the algorithm is shown in Figure 3.

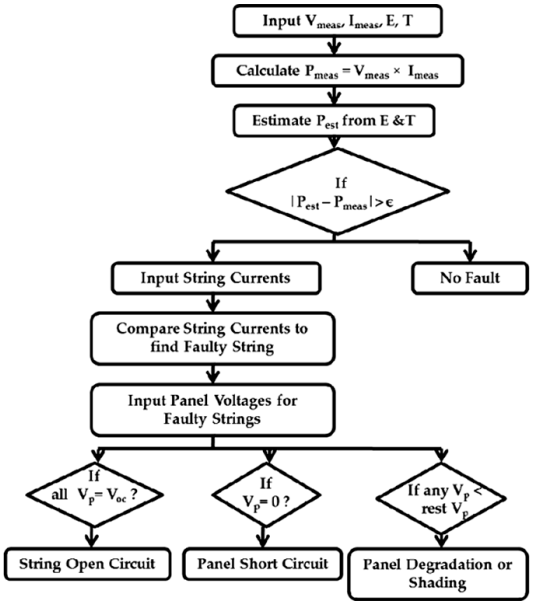

Figure 3 : Flow chart for fault detection algorithm

Validation of Algorithm

The algorithm was then implemented in MATLAB. To validate the algorithm, a graphical user interface was created in MATLAB with the help of GUIDE [17]. The graphical user interface demonstrates the working of the algorithm in a simulation environment. It contained controls that allow the user to simulate different faults in the system. The data collected is then analysed to find the type and location of the fault.

The results from the simulation showed that under any faulty condition, the algorithm was able to detect the fault type and location. The algorithm was tested for 70 different fault conditions. The conditions in which productivity of plant reduced more than 50% were not taken into consideration. All the 70 fault conditions could be detected and located properly by the algorithm. Though this algorithm takes in more number of inputs, a fault detection accuracy of 100% was obtained using this algorithm. Moreover there is no training required for this algorithm.

Hardware Implementation

Though the simulation results showed that the algorithm was able to detect fault under any faulty situation, it was implemented in real time to prove its feasibility. This is because the real time scenario differs a lot from the simulated environment. The simulated system was considered to be ideal with all the panels behaving exactly in a similar way to change in irradiation and temperature. But in the

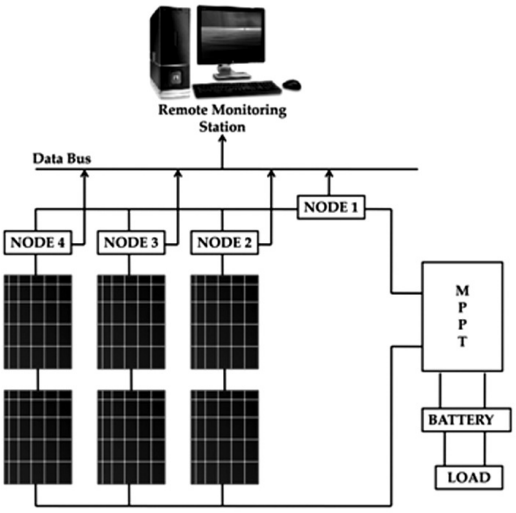

Figure 4 : Block diagram for the hardware implementation

Table 1 : Component details for hardware set-up

Equipment	Type	Detailed Parameters
PV module	Polycrystalline	At STC : V_{oc} = 21.5 V, I_{sc} = 4.8 A, V_{mp} = 17.2 V, I_{mp} = 4.36 A, P_{mp} = 75 W
Entire PV array	2 × 3 Module configuration	At STC: V_{sysmp} = 34.4 V, I_{sysmp} = 13.08 A, P_{sysmp} = 450W
Maximum power point tracker	MPPT 100/30	System voltage = 12/24 V, Max. PV voltage = 95 V, Min. PV voltage = 17/34 V, Max. PV Input power = 450W@12 V
Battery	Lead acid	Capacity: 100 Ah, Voltage = 12 V
Load	Resistive bulb (1 × 8 configuration)	Wattage of each bulb = 35 W, Load voltage = 12 V

real time case, though the panels have similar rating, there exists slight variation in the characteristics of the panels. Moreover accurate data collection for the purpose of analysis also poses a problem in real time. So it was essential to build a hardware model of the system so that the algorithm could be established as an efficient method to locate faults in solar PV system. A 450 W solar array was constructed for test purpose. The field consisted of 75 W solar panels connected in 2 × 3 configuration. The panels were connected to a maximum power point tracker to match the load with the panel output. The MPPT output is connected to a 100Ah battery which is further connected to resistive bulb load of 280W. The complete block diagram of the system built is shown in Figure 4.

The data collection nodes were constructed which consisted of resistive voltage divider to sense the voltage of each panel, current sensor ACS712 to measure the string currents, irradiance sensor which measures the short circuit current of a reference cell to calculate the irradiance level and temperature sensor LM35. The sensors collect data and transmit to the central remote monitoring station through RS485 communication. At the central monitoring station, a front end was created using C# in Visual Basic 2010 platform which is interfaced with MATLAB to continuously monitor the working of the PV system. The details of the PV Components used in the experimental set up are shown in Table 1.

Results and Discussion

The remote PV monitoring system was developed and deployed in Room No F62 CSIR–CSIO, Chennai to validate the working of the algorithm. The data collection nodes were assembled behind the first panel of each string. Figure 5 shows a 450 W solar array, formed by 2 × 3 configuration of 75W solar panels, connected to a 12 V, 100 Ah lead acid battery which is connected to 280 W resistive bulb loads. The nodes were powered by a 12 V, 7Ah

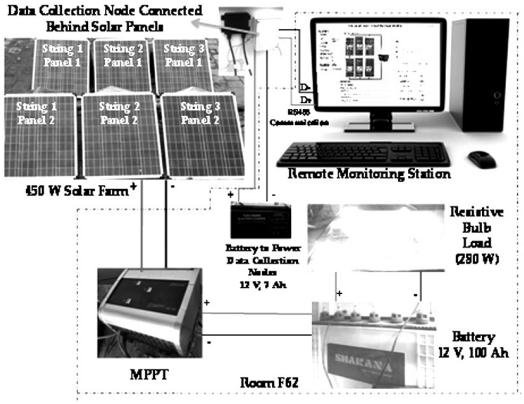

Figure 5 : Installed fault detection system

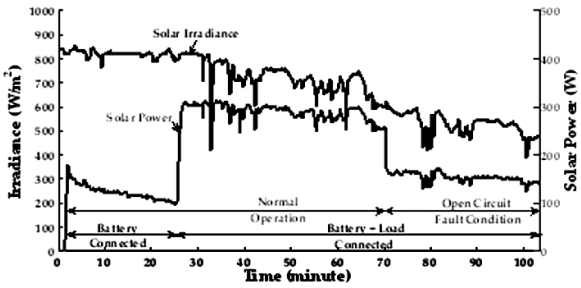

Figure 6 : Effect of open circuit on power production

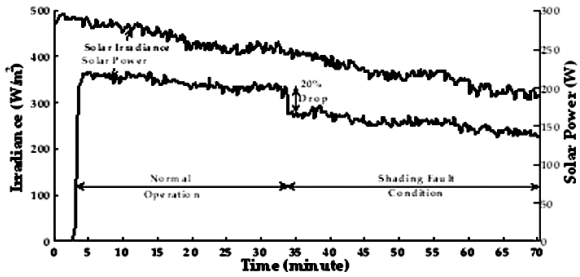

Figure 7 : Effect of mismatch (shading) on power production

battery placed in room F62. The Rs485 transmission lines (Data+ and Data-) are connected to the RS485 converter, which is connected to the serial port of PC where the front end is developed in Visual Basic. Figure 5 shows the complete arrangement.

Effect of Faults on PV System on Real Time

Open circuit fault was created by open circuiting string 2. Since the panels are connected in 2×3 configuration, open circuiting 1 string caused 33% fault in the system. The power drawn from the solar and irradiance is shown in Figure 6. Similarly mismatch fault was created in the PV system by partially shading panel one of string two at t = 33 minute. It can be seen from Figure 7 that there is a sudden in the power drawn from solar panel due to shading of just one panel. The drop in power production is 14% due to shading. The effect of faults on the power curve of the system is found to match the simulation results.

Working of the Remote Monitoring Station

Front end is designed for the fault detection system. The front view displays the power curve

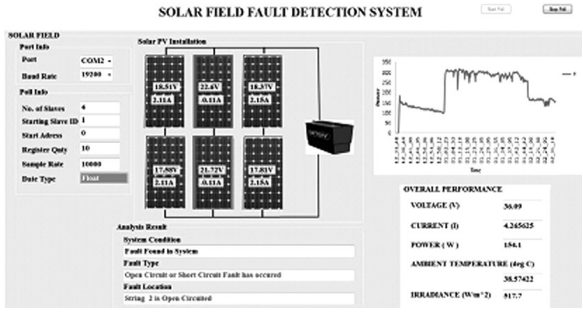

Figure 8 : Front end view showing open circuit fault

and the values of voltage and current from each panel. The Visual Basic application developed calls the MATLAB function to analyze the data received and displays the received results.

Figure 8 shows the front end display when there is an open circuit fault in the system. It is seen that the algorithm is able to find and locate the fault in the system. The open circuited string 2 is highlighted by the program to notify the user the location of the faulty panel. The analysis result panel shows the fault type and location. Similarly in case of other faults also the algorithm was able to find and display the fault location on the front end.

Scalability of the Algorithm

The algorithm was tested on a simulated 20 kW solar farm made up of 9 × 9 arrangement of 250 W solar panels. 76 different instances of mismatch, short circuit fault and open circuit fault (36 short circuit, 36 mismatch, 4 open circuit) were created and the algorithm was tested. The occurrence of a failure was detected in all the cases while 68 faults could be located. Thereby giving a detection accuracy of 100% and locating accuracy of 89.47%. In this calculation, it was considered that all fault conditions are equi-probable. The algorithm was not able to locate the fault in the system only when all the strings were equally faulty. As we know, occurrence of such fault is less probable, the accuracy can be higher than 89.47 %. Therefore, to scale up the algorithm to any given field, number of modules in series and parallel, open circuit voltage and short circuit current of

each panel can be used to develop the modified algorithm.

Feasibility of the Developed Hardware

For the fault detection system that has been constructed, 3 data collection nodes are used. The data collection nodes are powered from a 12 V battery. Each data collection node takes 0.05A current for its operation. The total power consumption by the fault detection system is $12 \times 0.05 \times 3 = 1.8$ W. So the power consumed by the fault detection unit for the 450 W plant is just 0.4% of its total capacity. Similar calculation for a 1 MW plant showed that the power consumption of the monitoring unit is only 0.03% of the plant capacity.

Conclusion

Faults in the dc side tend to bring down the productivity of the entire plant. The effect of common types of solar PV faults like line-line, open circuit, degradation and partial shading was shown in simulation as well as demonstrated for a real time 450 W PV array. A fault detection algorithm was devised and tested to give an accuracy of 100% and locating accuracy of 89.47% was obtained for such system.

Although the algorithm is based on PV module level measurement, the algorithm can be easily implemented any PV installation with minor modifications. The main advantages of the devised monitoring system are cost effective, flexible and potential for implementation in PV farms. The monitoring station can be made wireless in future to increase the ease of installation. More advanced algorithm can be developed that could take in less number of inputs to provide the same results. The simultaneous occurrence of faults can be dealt with using a combination of artificial intelligence and data analysis.

References

1. All India Installed Capacity (in MW) of Power Stations from Central Electrical Authority. [Online]. Available: www.cea.nic.in

2. A. M. Bazzi, K. A. Kim, B. B. Johnson, P. T Krein and Dominguez-Gracia, 'Fault Impacts on Solar Power Unit Reliability,' 26th IEEE Conference-Applied Power Electronics (APEC), pp. 1223-1231, 2011.

3. S. K. Firth, K. J Lomas and S. J. Rees, 'A Simple Model of PV System Performance and Its Use in Fault Detection,' Solar Energy, vol. 84, pp. 624-635, 2010.

4. B. Brooks, 'The Bakersfield Fire : A Lesson in Ground Fault Protection,' Solar Pro Mag., pp. 62-70, 2011.

5. A. Chouder and S. Silvestre, 'Automatic Supervision and Fault Detection of PV Systems based on Power Losses Analysis,' Energy Conversion and Management, vol. 51, pp. 1929-1937, 2010.

6. M. K. Alam, F. Khan, J. Johnson and J. Flicker, 'PV Ground-fault Detection using Spread Spectrum Time Domain Reflectometry (SSTDR),' IEEE Conference-Energy Conversion Congress and Exposition (ECCE), pp. 1015-1020, 2013.

7. M. K. Alam, F. Khan, J. Johnson and J. Flicker, 'PV Arc-fault Detection using Spread Spectrum Time Domain Reflectometry (SSTDR),' IEEE Conference-Energy Conversion Congress and Exposition (ECCE), pp. 3294-3300, 2014.

8. T. Takashima, Yamaguchi Junji and Ishida Masayoshi, 'Fault Detection by Signal Response in PV Module Strings,' 33rd IEEE Photovoltaic Specialists Conference (PVSC '08), pp. 1- 5, 2008.

9. Y. Zhao, L. Yang, B. Lehman, J.-F. de Palma, J. Mosesian and R. Lyons, 'Decision Tree-based Fault Detection and Classification in Solar Photovoltaic Arrays,' Proceedings of the 27th Annual IEEE Applied Power Electronics Conference and Exposition (APEC'12), pp. 93–99, 2012

10. M. Tadj, K. Benmouiza, A. Cheknane and S. Silvestre, 'Improving the Performance of PV Systems by Faults Detection using GISTEL Approach', Energy Conversion and Management, vol.80, pp. 298–304, 2014.

11. Kuei Hsiang Chao, Sheng-Han Ho and Meng-Hui Wang, 'Modeling and Fault Diagnosis of a Photovoltaic System,' Electric Power Systems Research, vol. 78, no. 1, pp. 97–105, 2008.

12. Kuei-Hsiang Chao, Pi-Yun Chen, Meng-Hui Wang and Chao-Ting Chen, 'An Intelligent Fault Detection Method of a Photovoltaic Module Array using Wireless Sensor Networks,' International Journal of Distributed Sensor Networks, Article ID 540147, 2014.

13. Kuo-Nan Yu, Her-Terng Yau and Jian-Yu Li, 'Chaotic Extension Neural Network based Fault Diagnosis Method for Solar Photovoltaic Systems,' Mathematical Problems in Engineering, vol. 2014, Article ID. 280520, 2014.

14. S. Syafaruddin, E. Karatepe and T. Hiyama, 'Controlling of Artificial Neural Network for Fault Diagnosis of Photovoltaic Array,' 16th International Conference-Intelligent System Application to Power Systems (ISAP), pp. 1- 6, 2011.

15. Ye Zhao, Brad Lehman, Roy Ball, Jerry Mosesin and Jean-Francois de Palma, 'Outlier Detection Rules for Fault Detection in Solar Photovoltaic Arrays,' 28th IEEE Applied Power Electronics Conference and Exposition - APEC, 2013.

16. Simulink.[Online]. www.in.mathworks.com/help/simulink/

17. GUI Building.[online]:www.in.mathworks.com/help/matlab/gui-development.html.

Electrical Engineering Division Board (2015-2016)

Mr S B Dubey, FIE
Chairman

Dr S K Calla, FIE
Member

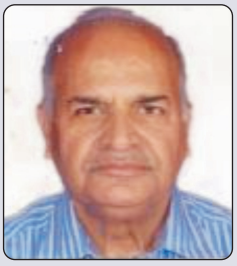

Mr V L Malhotra, FIE
Member

Mr R Ponbadi, FIE
Member

Mr G C Dutta, FIE
Member

Mr A S Satish , FIE
Member

Mr L N Tiwari, FIE
Member

Mr Umasankar J, MIE
Member

ISBN : 978-81-932567-2-5

The Institution of Engineers (India)
8 Gokhale Road, Kolkata 700 020
Phone : +91 (033) 2223-8311/14/15/16, 2223-8333/34
Fax : +91 (033) 2223-8345
Website : http://www.ieindia.org
e-mail : technical@ieindia.org
iei.technical@gmail.com